UNIVERZITA PALACKÉHO V OLOMOUCI
PŘÍRODOVĚDECKÁ FAKULTA
Katedra organické chemie

Solid-Phase Synthesis of Aryl Squaramides Using Liebeskind-Srogl Cross-Coupling

Studentská vědecká soutěž O cenu děkana 2025

Autor práce: Mgr. Jan CHASÁK
Studijní program: Organická a bioorganická chemie
Ročník: 3. (Ph.D.)
Vedoucí práce: doc RNDr. Lucie BRULÍKOVÁ, Ph.D.
Pracoviště: Katedra organické chemie

Solid-Phase Synthesis of Aryl Squaramides Using Liebeskind-Srogl Cross-Coupling

Jan Chasák,[a] Lucie Brulíková[a,]*

[a]*Department of Organic Chemistry, Faculty of Science, Palacký University, 17. listopadu 12, 77146, Olomouc, Czech Republic*

The corresponding author's email address: lucie.brulikova@upol.cz

Abstract

We present a method for the synthesis of aryl-substituted squaramides through the Liebeskind-Srogl cross-coupling reaction performed on solid support. This approach offers a unique application of cross-coupling reaction, allowing for the rapid and efficient production of a diverse range of substituted analogs within a combinatorial framework. Through our technique, we successfully synthesized derivatives that were previously unattainable. Additionally, the optimized conditions have been effectively applied in a scale-up reaction. The derivatives show potential for the treatment of drug-resistant tuberculosis.

Graphical abstract

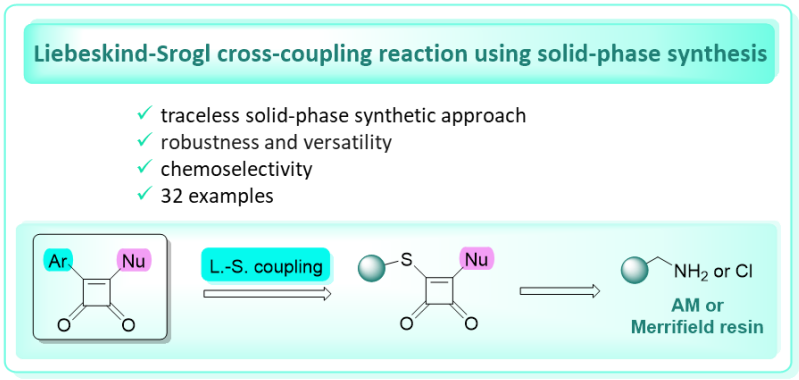

Keywords

Squaramides, Liebeskind-Srogl cross-coupling, solid-phase synthesis, chemoselectivity, tuberculosis.

Introduction

Squaramides represent an important category of new antituberculosis agents that gained the attention of medicinal chemists in 2017 following the release of the pioneering study on this subject.[1] These compounds inhibit mycobacterial ATP synthase and demonstrate superior efficacy against drug-resistant tuberculosis (Figure 1).[2–7] Moreover, they operate via a distinct mechanism compared to the clinically used bedaquiline, enhancing their potential as promising alternatives.

The carbon-carbon bond between the squaric cycle and the aryl substituent is crucial for antituberculosis activity, as shown in Figure 1. However, synthesizing this bond poses significant challenges. Previous methods have faced various obstacles that hindered the preparation of all required derivatives.[1–3] The Friedel–Crafts reaction, for instance, suffered from very low yields and was not applicable to various ranges of substrates.[1,2] Alternatively, the Liebeskind–Srogl Pd^0/Cu^I-mediated cross-coupling reaction offered several synthetic advantages, including mild, nonbasic conditions and high specificity for inorganic compounds. Nonetheless, these reactions have proven ineffective with certain boronic acids.[3] The solution-phase synthesis of these compounds proved highly dependent on the electronic properties of the boronic acids used in the cross-coupling step. As a result, some derivatives were obtained in very low yields (below 1%), or not at all. For this reason, other methods were sought to allow the use of a wider range of substrates.

Figure 1. Synthetic squaramides and their potential as antituberculosis agents. The structure of mycobacterial ATP synthase was created using Mol* Viewer and PDB: 7NJP.

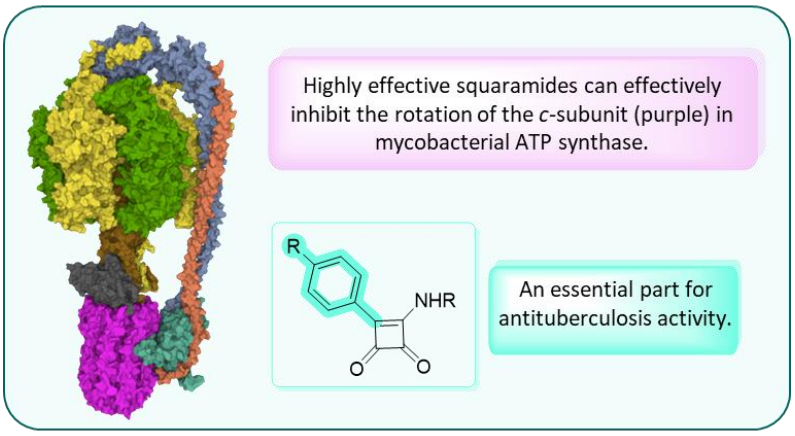

In our current research, we have utilized the Liebeskind–Srogl cross-coupling reaction on a solid support. This solid-phase synthetic approach offers many advantages over traditional solution synthesis, particularly in the field of medicinal chemistry. Solid-phase synthesis allows for the rapid and efficient generation of compounds without the necessity of isolating individual intermediates. This makes it a valuable method for developing new drug candidates and conducting extensive structure-activity relationship (SAR) studies. One of the key advantages of solid-phase synthesis is its compatibility with automated or high-throughput screenings. However, many resins used in this type of synthesis, including those studied here, can only work with a limited range of organic solvents. Polar protic solvents, such as alcohol and water, do not swell the resins adequately, which can lead to lower reactivity. Consequently, optimizing solid-phase synthetic sequences can be challenging, as only certain reaction parameters are adjustable. Additionally, the integration of solid-phase synthesis with

cross-coupling reactions is relatively rare, making the Liebeskind-Srogl cross-coupling reaction particularly unique.

The Liebeskind-Srogl reaction involves the formation of a new carbon-carbon bond between a thioester and a boronic acid facilitated by a metal catalyst. This cross-coupling reaction follows a distinct mechanism. Initially, Cu(I) coordinates with the thioester, making it more electron-deficient and promoting the efficient oxidative addition of the palladium catalyst. This step is followed by transmetallation and reductive elimination, which are typical phases of cross-coupling reactions, ultimately yielding the final product. Performing the synthesis on a solid phase, where the molecule is attached to a resin, does not negatively affect any of these reaction phases, allowing the reaction to proceed smoothly. On the contrary, the inherent properties of this reaction allow for traceless cleavage from the resin when appropriate solid support is selected, which is particularly beneficial for substituents that may be unstable under the acidic or basic conditions typically used for resin cleavage.

From a medicinal chemistry perspective, it is highly desirable to develop a rapid and efficient method for synthesizing a diverse range of squaramides that can be used for biological testing. This study presents an effective and robust approach to achieving that goal.

Results and Discussion

In the pilot studies, we selected two commercially available resins (Scheme 1) that featured suitable functional groups for conversion into the appropriate thioether: aminomethyl resin (AM resin) and Merrifield resin. The subsequent synthetic approach involves substituting the "right" part of the squaramide with various nucleophiles, followed by a Liebeskind-Srogl cross-coupling reaction, which simultaneously facilitates traceless cleavage from the resin. This process is clearly illustrated in Scheme 1.

Scheme 1. Design of synthetic pathways using various resins.

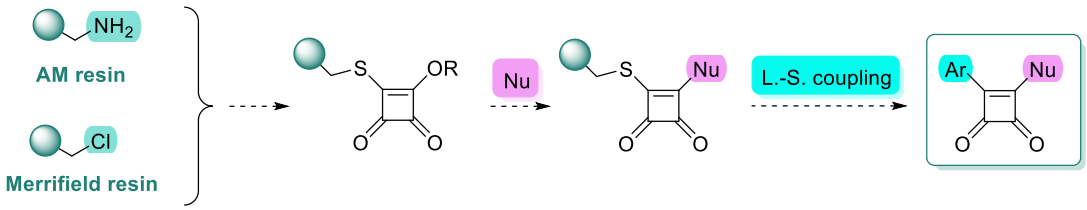

Initially, we concentrated on utilizing aminomethyl resin **1** as a solid support, which contains an amino functional group that can be readily substituted with an appropriate linker (Scheme 2). The first step in this reaction sequence involved the introduction of a suitable thio linker, specifically achieved through the acylation of 3-(tritylthio)propionic acid resin. We monitored the progress of this initial step

using the bromophenol blue test, which yielded a negative result, confirming that all amino groups on the aminomethyl resin had reacted completely. It should be noted that all yields were calculated based on the loading of the starting aminomethyl resin.

In the subsequent stage, the trityl-protecting group was removed, enabling a reaction of intermediate **3** with 3-(*tert*-butoxy)-4-methoxycyclobut-3-ene-1,2-dione (Scheme 2, synthesis of this precursor was carried out according to the publication by Shinada *et al*. and is described in Supporting information).[8] This was followed by reactions involving various nucleophiles, resulting in resin-bound precursors **5**. The final step of the reaction sequence involved a cross-coupling reaction carried out in the presence of copper(I) thiophene-2-carboxylate (CuTC), tri(2-furyl)phosphine (TFP), and a Pd catalyst, which led to the cleavage of the product **6** from the resin. The individual steps are discussed in detail below.

Scheme 2. Synthesis of squaramides **6** using aminomethyl resin.[a]

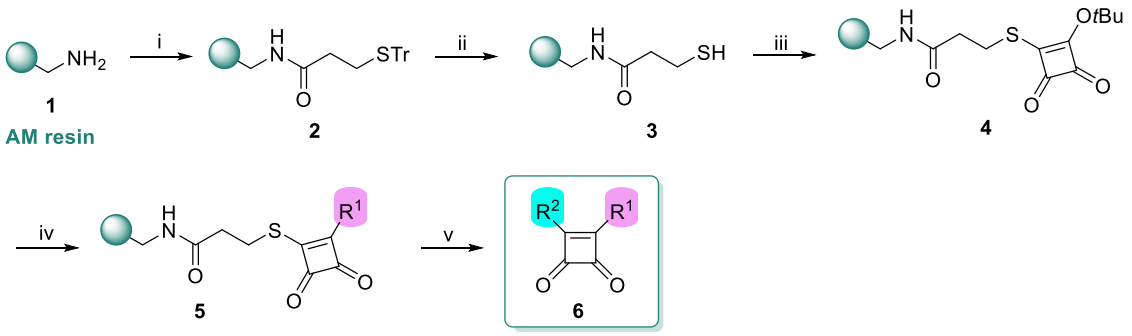

[a]Reagents and conditions: (i) 3-(tritylthio)propionic acid, DIC, DCM/DMF (1:1), rt, 18 h; (ii) TFA/TES (95:5), rt, 1 h; (iii) 3-(*tert*-butoxy)-4-methoxycyclobut-3-ene-1,2-dione, TEA, DCM, rt, 18 h; (iv) amines (or other nucleophiles), DCM, (TEA – for Nu-H·HCl), rt, 18 h; (v) R^2-$B(OH)_2$, CuTC, TFP, $Pd_2(dba)_3$, dioxan anhydrous, 50 °C, 18 h.

To assess the relevance of the key cross-coupling step for the chosen resin, we initiated preliminary studies using the readily available intermediate **5a** (see Table 1). At room temperature, the reaction showed only minimal conversion (Table 1, entry 1). Therefore, we raised the reaction temperature; however, even under these conditions, the conversion remained unsatisfactory (see Table 1, entry 2). The use of dioxane as a solvent in the reaction proved to be highly effective, resulting in a satisfactory yield of the desired product **6a**, as indicated in Table 1, entry 3. Additionally, attempts to modify the catalyst (see entries 4–5) or prolong the reaction time (entry 6) did not yield significant improvements in the overall outcome.

Table 1. Optimization of reaction conditions for Liebeskind-Srogl coupling on AM resin.

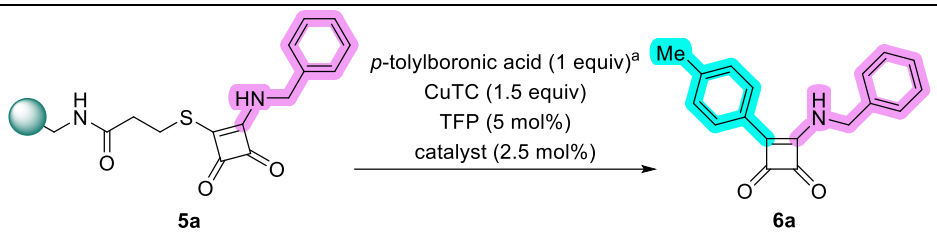

entry	catalyst	temperature	Solvent (anhydrous)	time	result
1	$Pd_2(dba)_3$	RT	THF	20 h	NI[b]
2	$Pd_2(dba)_3$	50 °C	THF	20 h	NI[b]
3	$Pd_2(dba)_3$	50 °C	Dioxan	20 h	25.3 mg (33%)[d]
4	$Pd(OAc)_2$	50 °C	Dioxan	20 h	NI[c]
5	$Pd(PPh_3)_4$	50 °C	Dioxan	20 h	21.6 mg (29%)[d]
6	$Pd_2(dba)_3$	50 °C	Dioxan	44 h	23.1 mg (30%)[d]

[a]The amount of all reagents is related to boronic acid. All components are in excess compared to AM resin (theoretical loading of AM resin (250 mg) is 0.28 mmol).
[b]NI: Not isolated, product detected only in trace amount.
[c]NI: Not isolated, complex mixture with many side products was formed.
[d]Product isolated from ~250 mg of resin.

The developed methodology enabled us to effectively introduce a range of boronic acids (see Table 2). We achieved successful reactions with electron-rich, electron-poor, and heterocyclic boronic acids. Notably, vinylboronic acid (**6m**) was coupled successfully. However, the final coupling was less effective with five-membered heterocycles where the -$B(OH)_2$ group was positioned at the 2-position of the heterocycle. Furthermore, the reaction was unsuccessful with the sterically hindered 2,6-(dimethylphenyl)boronic acid (**6n**).

Notable limitations of the developed methodology became evident when we attempted to introduce various nucleophiles onto the immobilized four-membered squarate skeleton. Only primary aliphatic amines yielded successful results. In contrast, heterocyclic amines **6p** produced only trace amounts of product, while aromatic amines resulted in no detectable final products **6**. Even elevating the temperature to 50 °C or changing the solvent to DMF during the substitution reaction did not enhance the outcome. Due to the absence of analysis following the substitution step, whether the challenge originated from the substitution itself or the subsequent coupling reaction remains uncertain. However, the findings suggest that the substitution step is more likely to be problematic, given that previous experiments have demonstrated the versatility and effectiveness of the coupling process.

Notably, the Libeskind-Srogl cross-coupling during the synthesis of derivative **6c** surprisingly proceeded as anticipated, resulting in the formation of the final compound. This was achieved despite the presence of an additional sulfur atom in the structure, which could potentially participate in this type of reaction. While we noted higher impurities than reactions involving other substituents, the final compound **6c** was still obtained in a slightly lower, yet acceptable, yield. The yields of the final compounds varied between 16% and 38%, primarily influenced by the electronic activation of the boronic acid in the final reaction step (Table 2).

Due to certain limitations, we faced with aminomethyl resin, we were unable to prepare some derivatives **6** (see Table 2). Consequently, we have decided to explore Merrifield resin with a chloromethyl functional group. We aim to thoroughly evaluate the scope and limitations of Merrifield resin, which may deepen our understanding of its capabilities and potentially lead to the development of new synthetic methodologies that could address the challenges we faced previously.

Scheme 3 offers a succinct overview of the synthetic pathway leading to the proposed squaramides **6** performed on Merrifield resin. The initial step of the synthesis involves the straightforward reaction between Merrifield resin and 3-ethoxy-4-mercaptocyclobut-3-ene-1,2-dione (the synthesis of this precursor was carried out according to the publication by Srivastava *et al*. and is detailed in the Supporting Information).[9] Similar to the previous case, the reaction sequence does not include a cleavable group that would aid in verifying successful reactions/sufficient conversions throughout the synthesis. As a result, the yields of the final products **6** are calculated based on the theoretical loading of the starting Merrifield resin, as outlined in the experimental section. The reaction sequence proceeded with various nucleophiles and concluded with a Liebeskind-Srogl cross-coupling reaction.

Scheme 3. Synthesis of squaramides **6** using Merrifield resin.[a]

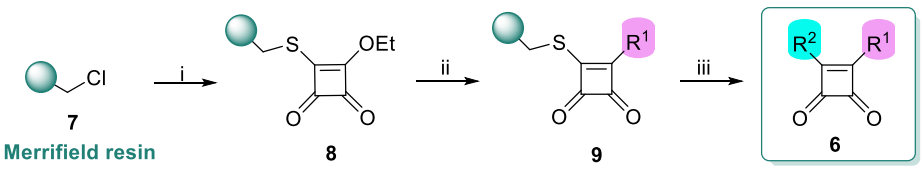

[a]Reagents and conditions: (i) 3-ethoxy-4-mercaptocyclobut-3-ene-1,2-dione, TEA, DMF, rt, 18 h; (ii) amines (or other nucleophiles), DCM, (TEA – for Nu-H·HCl), rt-50 °C, 18 h; (iii) R^2-$B(OH)_2$, CuTC, TFP, $Pd_2(dba)_3$, anhydrous dioxan, 50 °C, 18 h.

Squaramides **6** with various aromatic substituents were successfully synthesized utilizing Merrifield resin through the Liebeskind-Srogl cross-coupling reaction (Table 2). Both electron-rich and

electron-poor, as well as heteroaromatic boronic acids, were effectively incorporated. As previously observed, the reaction also proceeded successfully with a vinyl analog. Notably, the use of Merrifield resin facilitated the incorporation of 2-thienylboronic acid (**6l**), which had not been successfully achieved in the earlier synthesis using AM resin. Furthermore, unlike the AM resin approach, we were able to obtain derivative **6n**, which contains the sterically hindered 2,6-dimethylphenyl substituent. However, the yields for these two derivatives, **6l** and **6n**, are relatively low, at 14% and 31% (Table 2).

In our investigations concerning nucleophilic reactions, Merrifield resin demonstrated superior effectiveness compared to the AM resin method. We successfully introduced a range of aliphatic primary and secondary amines onto the central squaric acid scaffold, including specific amino acids (**6y** and **6ad**). The approach also yielded positive results with aromatic amines, even those that featured electron-withdrawing groups on the aromatic ring (**6ab**). Furthermore, we were able to incorporate various types of hydroxylamines, including *N*-substituted and *N*,*O*-disubstituted derivatives. It is noteworthy that the reaction conditions varied based on the nucleophiles employed. Aliphatic amines reacted efficiently at room temperature, as well as the two hydroxylamine derivatives, while aromatic amines necessitated an increase in temperature to 50 °C. Despite the method's apparent robustness and versatility, all our attempts to synthesize hydrazine derivatives (**6z**, **6ak**,**6al**) were unsuccessful. Even with the addition of $Zn(OTf)_2$ as an activator and elevated temperatures, we were unable to obtain any of the proposed hydrazine derivatives **6z**, **6ak**,**6al**. This limitation is likely due to the necessity of a polar solvent to facilitate the introduction of hydrazine onto the squaric acid framework, as suggested by solution-phase reaction conditions. Unfortunately, this solvent requirement conflicts with solid-phase synthesis and the resins chosen for our synthetic efforts. In the case of hydrazine derivatives **6z**, **6ak**,**6al**, difficulties arise during the substitution step rather than the coupling step, preventing us from obtaining the desired products.

It is important to note that we did not observe the formation of significant by-products or impurities during the synthesis of any derivatives after the cleavage step. The experiments conducted indicate that the final coupling step is not problematic. Instead, the issues arise during the reaction with nucleophiles. In the cases of unsuccessful synthesis of final derivatives, we observed the formation of a new C-C bond while the ethoxy group remained intact. This suggests that, although the final cleavage was successful, the preceding nucleophilic substitution did not occur. Furthermore, in the case of some hydrazine derivatives, we successfully isolated the “unsubstituted” derivative **6aa** after completing the entire reaction sequence, which supports our hypothesis regarding the reactivity. As seen in the previous reaction sequence, when the substitution reaction step was successfully completed, we obtained the final products **6**. The yield primarily depended on the electronic activation of the boronic acid, ranging from 14% to 51% (Table 2). Please note that we do not include derivative **6aa** in this yield calculation, as the substitution reaction step was not performed in that case.

Table 2: List of synthesized squaramides **6** using AM resin and Merrifield resin.

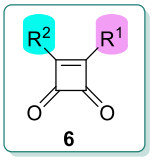

compd	R^2	R^1	Yield[a] (%) AM resin	Yield[b] (%) Merrifield resin
6a	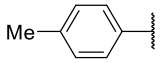	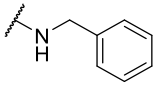	33	40
6b	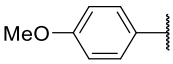	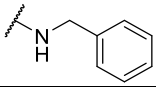	29	ND[f]
6c	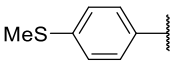	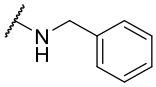	17	ND[f]
6d[10]	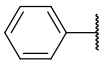	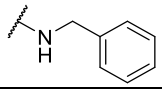	32	ND[f]
6e	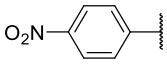	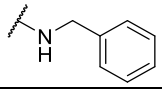	16	21
6f	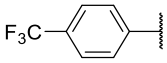	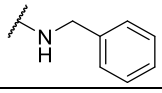	26	ND[f]
6g	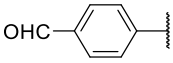	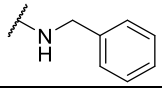	18	ND[f]
6h	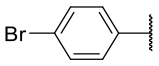	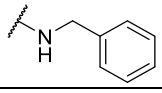	23	27
6i		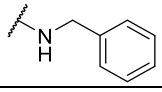	38	ND[f]
6j		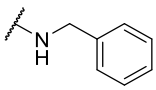	NI[c]	ND[f]
6k		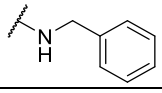	28	35
6l		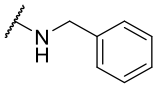	NI[c]	14
6m	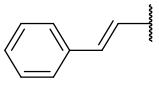	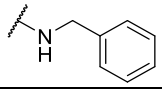	29	41
6n	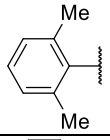	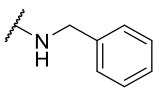	NI[c]	31
6o	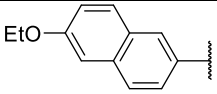	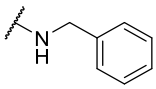	20	ND[f]
6p[3,g]	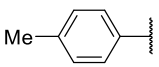	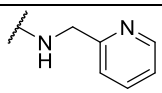	NI[c]	50

6q	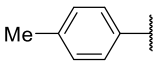	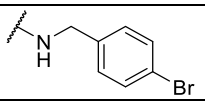	20	37
6r	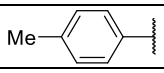	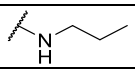	34	53
6s[11]	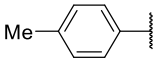	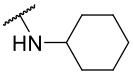	34	49
6t[11]	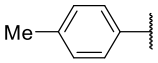	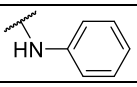	NI[d]	50
6u	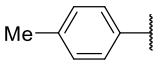	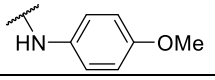	NI[c]	46
6v	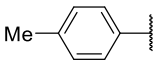	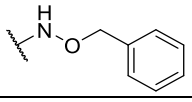	NI[d]	ND[f]
6w	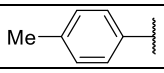	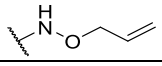	NI[d]	ND[f]
6x	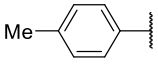		NI[d]	ND[f]
6y	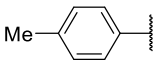	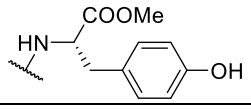	33	45
6z	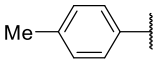	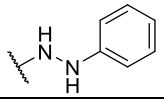	NI[d]	NI[c]
6aa[12]	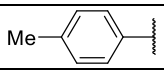		ND[f]	58
6ab	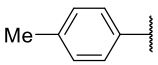	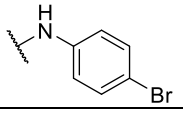	ND[f]	35
6ac	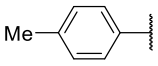	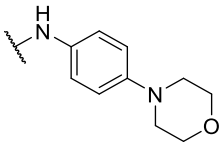	ND[f]	34
6ad	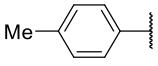	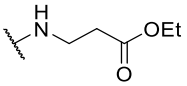	ND[f]	46
6ae	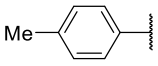	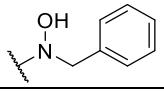	ND[f]	34
6af	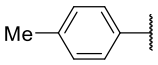	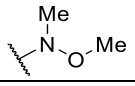	ND[f]	41
6ag[13]	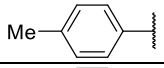	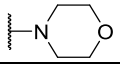	ND[f]	50
6ah	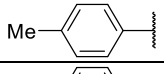	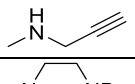	ND[f]	NI[d]
6ai	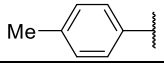	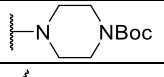	ND[f]	42
6aj	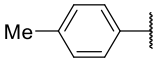	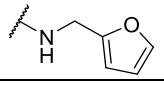	ND[f]	51
6ak	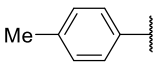	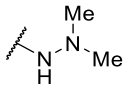	ND[f]	NI[d]

6al	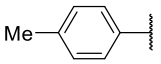	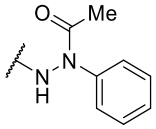	ND[f]	NI[e]

[a]Yields for AM resin calculated from a theoretical loading of the resin (over five reaction steps).
[b]Yields for Merrifield resin calculated from a theoretical loading of the resin (over three reaction steps).
[c]NI: Not isolated, product detected only in trace amount.
[d]NI: Not isolated, product was not detected after the coupling cleavage.
[e]NI: Not isolated, derivative **6aa** was obtained instead.
[f]ND: Not determined.
[g]Derivative **6p** was previously prepared also via a solution-phase synthesis using Liebeskind-Srogl cross-coupling, achieving an overall yield of 40%.[3]
Note: Derivatives with the citation noted in the left column have been already prepared in the past by solution-phase synthesis.

As confirmed by NMR analysis, three synthesized derivatives (**6m**, **6n**, **6i**) were isolated as mixtures of rotamers. The presence of bulky aromatic or vinyl substituents contributes to the formation of these rotameric mixtures, as their steric hindrance limits bond rotation. This occurrence has been documented in our previous studies involving structurally similar compounds.[3] Our investigations indicated that the energy barrier between the two rotameric forms is significantly high, rendering thermal interconversion unfeasible under standard experimental conditions. Additionally, variations in the deuterated solvent did not impact the observed ratio of rotameric forms. This phenomenon should be considered when synthesizing biologically active compounds of this type, as restricted bond rotation can significantly affect biological activity.

As highlighted in the text above, the utilization of Merrifield resin enabled the successful synthesis of certain derivatives that could not be produced using AM resin. The findings suggest that the Merrifield resin approach facilitates a more efficient Liebeskind-Srogl cross-coupling reaction in the final step while also enabling the substitution of the central core with a broader spectrum of nucleophiles. Table 2 presents an apparent comparison between the products **6** obtained from AM and Merrifield resins, clearly demonstrating the advantages of the latter. For instance, when employing Merrifield resin, boronic acids that did not react in the AM resin synthesis (specifically compounds **6l** and **6n**) were effectively coupled. Moreover, the Merrifield resin method proved to be more effective in the substitution step, successfully introducing aromatic amines (**6t** and **6u**) into the structure when the reaction was conducted at 50 °C. In contrast, these same derivatives were either undetectable or only present in trace amounts in the synthesis using AM resin.

Additionally, the Merrifield resin method consistently produced higher yields of the final products **6** than the AM resin approach. This difference may be attributed to the overall greater efficiency of the reaction sequence or the fact that the Merrifield resin synthesis involves one fewer reaction step.

To emphasize the distinct chemoselectivity of the Liebeskind-Srogl cross-coupling reaction, we carried out a solid-phase experiment involving the sequential modification of an intermediate using the Suzuki-Miyaura cross-coupling reaction (Scheme 4). Initially, 4-bromoaniline was introduced onto the central squaramide scaffold. This intermediate was then reacted with 4-methoxyphenylboronic acid under Suzuki coupling conditions, utilizing KOAc and a palladium catalyst in anhydrous DMF, following the procedures outlined by Piettre *et al*.[14] After thoroughly washing the reaction slurry with DMF and DCM, the intermediate **10** was subsequently reacted with *p*-tolylboronic acid *via* the Liebeskind-Srogl cross-coupling reaction, which simultaneously cleaved the final product **6am** from the resin. The successful isolation of the desired product **6am**, achieved with a yield of 23% (25.3 mg from a starting resin of 250 mg), demonstrated that both couplings can proceed independently. This finding paves the way for broader modification possibilities of target molecules.

Scheme 4. Synthesis of squaramides *via* chemoselective approach.[a]

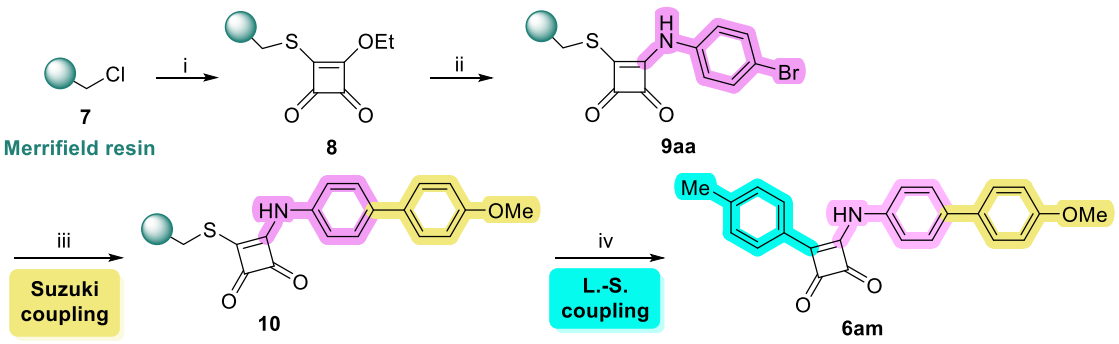

[a]Reagents and conditions: (i) 3-ethoxy-4-mercaptocyclobut-3-ene-1,2-dione, TEA, DMF, rt, 18 h; (ii) 4-bromoaniline, DCM, 50 °C, 18 h; (iii) 4-(methoxyphenyl)boronic acid, KOAc, $PdCl_2$(dppf), anhydrous DMF, 60 °C, 18 h; (iv) 4-tolylboronic acid, CuTC, TFP, $Pd_2(dba)_3$, anhydrous dioxan, 50 °C, 18 h.

Solid-phase synthesis and a combinatorial approach are commonly used to generate compound libraries due to their efficiency in producing structural diversity with minimal synthetic steps, thereby eliminating the need for intermediate isolation or purification. To enhance the potential applications of our developed methodology, we aimed to evaluate its scalability using Merrifield resin. To achieve this, we conducted a model reaction sequence using benzylamine as the nucleophile and 4-tolyl boronic acid for the final Liebeskind-Srogl cross-coupling step, leading to the final compound **6a** depicted in Scheme 5. In the coupling reaction, we reduced the ratios of the individual components compared to previous experiments. Assuming full utilization of the resin's theoretical loading capacity of 1.21 mmol/g, the reaction employed 2.5 equivalents of 4-tolyl boronic acid, 3 equivalents of CuTC,

5 mol% TFP, and 2.5 mol% $Pd_2(dba)_3$. A scale-up reaction was conducted using either 1 g or 5 g of Merrifield resin. As demonstrated in Scheme 5, the employed reaction methodology is applicable for all tested quantities.

Scheme 5. An overview of the scale-up process and the utilized instrumentation.

Table 3 outlines the advantages and disadvantages of utilizing the Liebeskind–Srogl cross-coupling reaction for the synthesis of squaramides through a solid-phase synthetic approach, in comparison to traditional solution synthesis methods. Based on extensive data collected during our projects, solid-phase synthesis has demonstrated greater overall efficiency. This increased efficiency can be primarily attributed to higher product yields and improved compatibility with a wider range of boronic acids.

While the reaction time for the cross-coupling step is similar in both methods, solid-phase synthesis significantly shortens the overall time required to produce the final products. In this approach, intermediates are attached to the resin, allowing for simple washing between steps. This eliminates the lengthy isolation and purification processes typically needed in other methods. Notably, the lack of intermediate purification does not complicate the isolation of the final product. In fact, our experience shows that purifying the final compound is often easier when it is synthesized on a solid support. This contributes to the higher yields of the final compounds obtained.

One common limitation of solid-phase synthesis is its scalability. However, in this case, it seems feasible to scale up. As we have demonstrated, the synthetic approach remains effective for at least up to a 5 g resin scale. Nevertheless, one drawback of the solid-phase synthesis method is its higher cost. This approach typically requires reagents in excess and involves relatively expensive resins. Although we were able to reduce the excess of reagents in our scale-up experiments, the higher material costs continue to contribute to the overall expense of this method.

Ultimately, the choice of method depends on the specific goals of the synthesis. However, for the rapid and efficient generation of large compound series, such as in SAR studies, we consider solid-phase synthesis to be the more beneficial approach.

Table 3: A comparison of synthetic methods utilizing the Liebeskind–Srogl cross-coupling reaction for the synthesis of squaramides.

	conventional synthesis (solution-phase)	**solid-phase synthesis**
yields of target compounds	lower	higher
boronic acid scope	limited	broader
reaction time	equal	equal
overall synthesis time requirement	higher	lower
purification	complicated	easier & faster
economic demands	lower	higher

Conclusion

In summary, we have developed a traceless solid-phase synthetic approach that enables the preparation of a diverse array of new squaramides, which show significant promise for the treatment of drug-resistant tuberculosis. Our approach emphasizes simplicity, allowing for manual execution without the necessity of isolating and purifying individual intermediates, and it is applicable across a broad spectrum of starting materials. Moreover, the specific type of cleavage from the resin through the Liebeskind-Srogl coupling reaction allows the presence of acid-labile groups. Additionally, we have confirmed remarkable chemoselectivity and the feasibility of scaling up the synthesis. The presented synthesis brings a unique application of the Liebeskind-Srogl cross-coupling in solid-phase synthesis. We anticipate that our findings will serve as a foundation for further exploration of the biological implications of the discovered reaction and the development of innovative squaramides with exceptional antituberculosis activity.

Experimental section

Materials and Methods

Solvents and chemicals were purchased from Sigma-Aldrich (St. Louis, Missouri, USA) or Fluorochem (UK). Analytical thin-layer chromatography (TLC) was performed using aluminum plates precoated with silica gel 60 F254. Synthesis was carried out on Domino Blocks in disposable polypropylene reaction vessels (Torviq, Tucson, AZ). All reactions were carried out at room temperature (21 °C) unless stated otherwise.

The LC-MS analyses were carried out on the UHPLC-MS system (Waters). This system consists of UHPLC chromatograph Acquity with a photodiode array detector and single quadrupole mass spectrometer and uses an XSelect C18 column (2.1 x 50 mm) at 30 °C and a flow rate of 600 µl/min. The mobile phase was (A) 10 mM ammonium acetate in HPLC grade water and (B) HPLC grade acetonitrile. A gradient was formed from 10% A to 80% B in 2.5 minutes and kept for 1.5 minutes. The

column was re-equilibrated with a 10% solution of B for 1 minute. The ESI source operated at a discharge current of 5 µA, vaporizer temperature of 350 °C, and capillary temperature of 200 °C.

NMR $^{1}H/^{13}C$ spectra were recorded on a JEOL ECA400II (400 MHz) spectrometer at magnetic field strengths of 9.39 T (with operating frequencies 399.78 MHz for ^{1}H and 100.53 MHz for ^{13}C) at ambient temperature (~21 °C). Chemical shifts (δ) are reported in parts per million (ppm), and coupling constants (J) are reported in Hertz (Hz). NMR spectra are recorded at rt (21 °C) and referenced to the residual signals of DMSO-d_6.

HRMS analysis was performed on an LC chromatograph (Dionex UltiMate 3000, Thermo Fischer Scientific, MA, USA) with mass spectrometer Exactive Plus Orbitrap high-resolution (Thermo Fischer Scientific, MA, USA) operating in positive scan mode in the range of 1000–1500 m/z. Electrospray was used as a source of ionization. Samples were diluted to a final concentration of 0.1 mg/mL in a solution of water and acetonitrile (50:50, v/v). The samples were injected into the mass spectrometer following HPLC separation on a Phenomenex Gemini column (C18, 50 x 2 mm, 3 µm particle) using an isocratic mobile phase of 0.01 M MeCN/ammonium acetate (80/20) at a flow rate of 0.3 mL/min.

Chemistry

AM resin synthetic approach

Amidation of 3-(tritylthio)propanoic acid with AM resin resulting in **2**

AM resin **1** (~1 g) was washed three times with DCM, three times with DMF, and reacted with 10 mL of solution of DIPEA in DMF (1:9; v:v) at rt for 20 min. The resin was washed five times with DMF, followed by an addition of solution of 3-(tritylthio)propanoic acid (3 mmol) and DIC (3 mmol) in 10 mL of DCM/DMF (1:1; v:v). The resin was reacted with the prepared mixture at rt for 18 h. Finally, the resin was washed three times with DMF and three times with DCM. A convenient conversion of the reaction was verified using the bromophenol blue test.

Deprotection of thiol resulting in **3**

Resin **2** (~1 g) was washed three times with DCM and reacted with 10 mL of TFA/TES solution (95:5; v:v) at rt for 1 h. The resin was washed five times with DCM.

Immobilization of central four-membered skeleton resulting in **4**

Resin **3** (~1 g) was washed three times with DCM and reacted with a solution of 3-(tert-butoxy)-4-methoxycyclobut-3-ene-1,2-dione and TEA in DCM at rt for 18 h. The resin was washed five times with DCM.

Nucleophile introduction resulting in **5**

Resin **4** (~250 mg) was washed three times with DCM and reacted with a solution of appropriate nucleophile (1 mmol) in DCM at rt for 18 h. The resin was washed three times with DCM. If the

nucleophile was added to the reaction as a hydrochloride, an equimolar amount of TEA (1 mmol) was added.

Liebeskind-Srogl cross-coupling cleavage resulting in **6** (procedure for both AM resin and Merrifield resin)

Resin **5** (~250 mg) was washed three times with DCM, three times with THF anhydrous, and once with anhydrous dioxan. Then, appropriate boronic acid (1.6 mmol), CuTC (2.4 mmol), TFP (0.08 mmol), and $Pd_2(dba)_3$ (0.04 mmol) were added. Finally, anhydrous dioxane (3 mL) was drawn into the syringe, and the reaction mixture was shaken for 18 h at 50 °C. The reaction mixture was poured into a saturated solution of NH_4Cl (30 mL), and the syringe was washed three times with EtOAc (5 mL). After the separation of both layers, the EtOAc was collected, and the residual NH_4Cl solution was extracted with another two portions of EtOAc (2 x 30 mL). Combined organic layers were washed with a saturated solution of NH_4Cl (30 mL) and brine (30 mL) and dried over anhydrous $MgSO_4$. The solvent was evaporated under reduced pressure. Product **6** was purified by LC using DCM/MeOH (grad.). Product **6** was precipitated from DCM by the addition of hexane if repurification was needed.

Merrifield resin synthetic approach

Immobilization of squaric scaffold (nucleophilic substitution of Merrifield resin by thio derivative of squaric acid) resulting in **8**

Merrifield resin **7** (~1 g) was washed three times with DCM, three times with DMF and reacted with a solution of 3-ethoxy-4-mercaptocyclobut-3-ene-1,2-dione (3 mmol) and TEA (3 mmol) in DMF (10 mL) at rt for 18 h. The resin was washed three times with DMF and three times with DCM.

Nucleophile introduction resulting in **9**

Resins **8** (~250 mg) were washed three times with DCM and reacted with a solution of appropriate nucleophile (1 mmol) in DCM at rt for 18 h. The resins were washed three times with DCM. In the case of aromatic amines, the resins were shaken with reaction mixtures at 50 °C for 18 h. If the nucleophile was added to the reaction as a hydrochloride, an equimolar amount of TEA (1 mmol) was added.

Suzuki-Miyaura cross-coupling reaction resulting in ***10aa***

Resin **9aa** (~250 mg) was washed three times with DCM, three times with DMF anhyd. Then, 4-methoxyphenyl boronic acid (1.8 mmol), KOAc (2.7 mmol), and $PdCl_2$(dppf) (0.09 mmol) were added. Finally, DMF anhyd (3 mL) was drawn into the syringe, and the reaction mixture was shaken for 18 h at 60 °C. The resin was washed five times with DMF and five times with DCM.

Scale-up of the reaction sequence

The scale-up procedures were consistent with the method used for smaller amounts of starting resin, differing only in the ratio of the reactants.

For a 1 g resin scale, immobilization was performed using a solution of 3-ethoxy-4-mercaptocyclobut-3-ene-1,2-dione (3 mmol) and TEA (3 mmol) in DMF (10 mL). The subsequent substitution step employed a solution of benzylamine (3 mmol) in DCM (10 mL). The Liebeskind-Srogl cross-coupling reaction was carried out with *p*-tolylboronic acid (3.02 mmol), CuTC (3.63 mmol), TFP (0.121 mmol), and $Pd_2(dba)_3$ (0.06 mmol) in anhydrous 1,4-dioxane (10 mL).

For the 5 g resin scale, a solution of 3-ethoxy-4-mercaptocyclobut-3-ene-1,2-dione (15 mmol) and TEA (15 mmol) in DMF (50 mL) was used for immobilization. The substitution step utilized a solution of benzylamine (15 mmol) in DCM (50 mL). The Liebeskind-Srogl cross-coupling reaction was performed with *p*-tolylboronic acid (15.13 mmol), CuTC (18.15 mmol), TFP (0.3 mmol), and $Pd_2(dba)_3$ (0.15 mmol) in anhydrous 1,4-dioxane (50 mL).

Analytical data for individual compounds

3-(benzylamino)-4-(p-tolyl)cyclobut-3-ene-1,2-dione **6a**

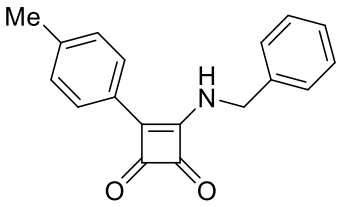

Product **6a** was obtained as a white solid. Yield: 25.3 mg (33%) using AM resin, 33.2 mg (40%) using Merrifield resin. ^{1}H NMR (400 MHz, DMSO-d_6) δ 9.53 (br s, 1H), 7.93 (d, *J* = 7.9 Hz, 2H), 7.44 – 7.26 (m, 7H), 4.92 (s, 2H), 2.37 (s, 3H). ^{13}C NMR (101 MHz, DMSO-d_6) δ 193.2, 188.7, 178.2, 162.1, 140.8, 138.2, 129.6, 128.6, 127.6, 127.5, 126.5, 126.2, 47.5, 21.2. HRMS: m/z: calcd. for $C_{18}H_{16}NO_2^+$: 278.1176 $[M+H]^+$; found: 278.1177.

3-(benzylamino)-4-(4-methoxyphenyl)cyclobut-3-ene-1,2-dione **6b**

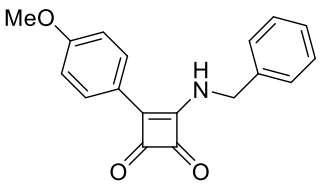

Product **6b** was obtained as a white solid. Yield: 19.2 mg (29%) using AM resin. ^{1}H NMR (400 MHz, DMSO-$_d$6) δ 9.47 (t, *J* = 6.3 Hz, 1H), 8.09 – 7.90 (m, 2H), 7.39 (d, *J* = 4.4 Hz, 4H), 7.34 – 7.25 (m, 1H), 7.16 – 7.03 (m, 2H), 4.91 (d, *J* = 6.1 Hz, 2H), 3.31 (s, 3H).^{13}C NMR (101 MHz, DMSO-d_6) δ 192.5, 188.6, 177.8, 162.2, 161.1, 138.3, 128.6, 128.2, 127.6, 127.5, 122.1, 114.5, 55.4, 47.4. HRMS: m/z: calcd. for $C_{18}H_{16}NO_3^+$: 294.1125 $[M+H]^+$; found: 294.1127.

3-(benzylamino)-4-(4-(methylthio)phenyl)cyclobut-3-ene-1,2-dione **6c**

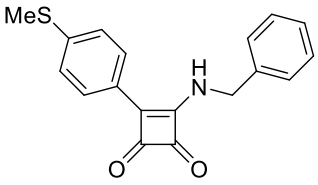

Product **6c** was obtained as a yellow solid. Yield: 15.1 mg (17%) using AM resin. ^{1}H NMR (400 MHz, DMSO-d_6) δ 9.56 (t, *J* = 6.2 Hz, 1H), 8.03 – 7.93 (m, 2H), 7.43 – 7.35 (m, 6H), 7.35 – 7.28 (m, 1H), 4.92 (d, *J* = 6.1 Hz, 2H), 2.54 (s, 3H). ^{13}C NMR (101 MHz, DMSO-d_6) δ 192.8, 188.6, 178.0, 161.5, 142.2, 138.1, 128.6, 127.6, 127.6, 126.5, 125.5, 125.4, 47.5, 14.1. HRMS: m/z: calcd. for $C_{18}H_{16}NO_2S^+$: 310.0896 $[M+H]^+$; found: 310.0896.

3-(benzylamino)-4-phenylcyclobut-3-ene-1,2-dione **6d**

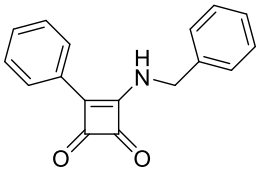

Product **6d** was obtained as a white solid. Yield: 23.8 mg (32%) using AM resin. ^{1}H NMR (400 MHz, DMSO-d_6) δ 9.61 (br s, 1H), 8.02 (d, *J* = 7.4 Hz, 2H), 7.64 – 7.28 (m, 8H), 4.93 (s, 2H). ^{13}C NMR (101 MHz, DMSO-d_6) δ 193.5, 188.6, 178.5, 161.7, 138.1, 130.6, 129.2, 129.0, 128.6, 127.6, 127.6, 126.1, 47.5. HRMS: m/z: calcd. for $C_{17}H_{14}NO_2^+$: 264.1019 $[M+H]^+$; found: 264.1020.

3-(benzylamino)-4-(4-nitrophenyl)cyclobut-3-ene-1,2-dione **6e**

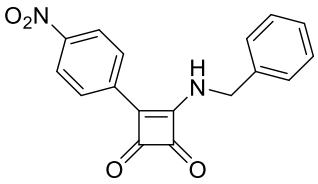

Product **6e** was obtained as a yellow solid. Yield: 13.7 mg (16%) using AM resin, 19.6 mg (21%) using Merrifield resin. ^{1}H NMR (400 MHz, DMSO-d_6) δ 9.99 (br s, 1H), 8.39 – 8.33 (m, 2H), 8.26 – 8.19 (m, 2H), 7.47 – 7.36 (m, 4H), 7.35 – 7.30 (m, 1H), 4.96 (s, 2H). ^{13}C NMR (101 MHz, DMSO-d_6) δ 193.9, 188.3, 178.6, 157.7, 147.3, 137.6, 134.8, 128.6, 127.7, 126.8, 124.2, 47.8. HRMS: m/z: calcd. for $C_{17}H_{13}N_2O_4^+$: 309.0870 $[M+H]^+$; found:309.0868 .

3-(benzylamino)-4-(4-(trifluoromethyl)phenyl)cyclobut-3-ene-1,2-dione **6f**

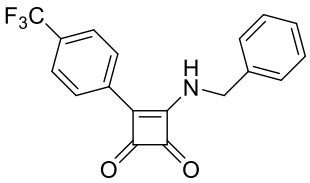

Product **6f** was obtained as a white solid. Yield: 24.2 mg (26%) using AM resin. ^{1}H NMR (400 MHz, DMSO-d_6) δ 9.85 (s, 1H), 8.19 (d, *J* = 8.2 Hz, 2H), 7.89 (d, *J* = 8.2 Hz, 2H), 7.44 – 7.36 (m, 4H), 7.35 – 7.28 (m, 1H), 4.95 (s, 2H). ^{13}C NMR (101 MHz, DMSO-d_6) δ 194.4, 189.0, 179.2, 159.6, 138.3, 133.2, 130.1 (q, *J* = 31.9 Hz), 129.2, 128.2, 127.1, 126.4 (q, *J* = 3.6 Hz), 124.5 (q, *J* = 272.4 Hz), 48.2. HRMS: m/z: calcd. for $C_{18}H_{13}F_3NO_2^+$: 332.0893 $[M+H]^+$; found: 332.0895.

4-(2-(benzylamino)-3,4-dioxocyclobut-1-en-1-yl)benzaldehyde **6g**

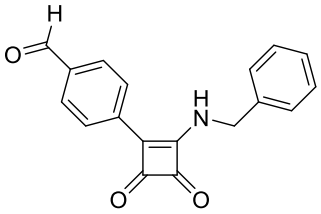

Product **6g** was obtained as a yellow solid. Yield: 14.4 mg (18%) using AM resin. ^{1}H NMR (400 MHz, DMSO-d_6) δ 10.04 (s, 1H), 9.86 (br s, 1H), 8.19 (d, *J* = 8.3 Hz, 2H), 8.03 (d, *J* = 8.3 Hz, 2H), 7.44 – 7.37 (m, 4H), 7.36 – 7.29 (m, 1H), 4.95 (s, 2H). ^{13}C NMR (101 MHz, DMSO-d_6) δ 193.8, 192.5, 188.5, 178.6, 159.3, 137.7, 136.4, 134.1, 129.9, 128.6, 127.7, 127.6, 126.4, 47.7. HRMS: m/z: calcd. for $C_{18}H_{14}NO_3^+$: 292.0968 $[M+H]^+$; found: 292.0972.

3-(benzylamino)-4-(4-bromophenyl)cyclobut-3-ene-1,2-dione **6h**

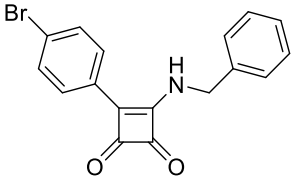

Product **6h** was obtained as a white solid. Yield: 21.6 mg (23%) using AM resin, 27.7 mg (27%) using Merrifield resin. ^{1}H NMR (400 MHz, DMSO-d_6) δ 9.69 (br s, 1H), 7.98 – 7.93 (m, 2H), 7.79 – 7.72 (m, 2H), 7.42 – 7.35 (m, 4H), 7.35 – 7.29 (m, 1H), 4.92 (s, 2H). ^{13}C NMR (101 MHz, DMSO-d_6) δ 193.4, 188.4, 178.3, 160.1, 137.9, 132.1, 128.6, 128.2, 127.9, 127.6, 127.6, 123.8, 47.6. HRMS: m/z: calcd. for $C_{17}H_{13}BrNO_2^+$: 342.0124 $[M+H]^+$; found: 342.0123.

3-(benzylamino)-4-(furan-3-yl)cyclobut-3-ene-1,2-dione **6i**

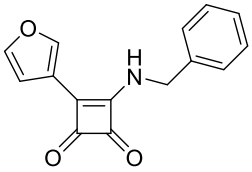

Product **6i** was obtained as a white solid. Yield: 21.3 mg (38%) using AM resin. ^{1}H NMR (400 MHz, DMSO-d_6), 95:5 mixture of two rotamers. Major rotamer δ 9.34 (t, *J* = 6.3 Hz, 1H), 8.48 (t, *J* = 1.2 Hz, 1H), 7.91 (t, *J* = 1.7 Hz, 1H), 7.41 – 7.28 (m, 5H), 7.12 (dd, *J* = 2.0, 0.5 Hz, 1H), 4.90 (d, *J* = 6.2 Hz, 2H). Minor rotamer, characteristic signals: δ 9.73 (t, *J* = 6.0 Hz, 1H), 8.25 (s, 1H), 7.81 (t, *J* = 1.7 Hz, 1H), 4.72 (d, *J* = 6.3 Hz, 2H). ^{13}C NMR (101 MHz, DMSO-d_6), 95:5 mixture of two rotamers. Major rotamer δ 192.3, 187.7, 177.7, 156.7, 145.0, 142.8, 138.0, 128.7, 127.6, 127.5, 114.7, 107.4, 47.3. Minor rotamer was not detected. HRMS: m/z: calcd. for $C_{15}H_{12}NO_3^+$: 254.0812 $[M+H]^+$; found: 254.0812.

3-(benzylamino)-4-(thiophen-3-yl)cyclobut-3-ene-1,2-dione **6k**

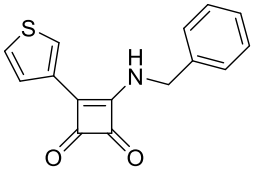

Product **6k** was obtained as a pale-yellow solid. Yield: 21.1 mg (28%) using AM resin, 28.4 mg (35%) using Merrifield resin. ^{1}H NMR (400 MHz, DMSO-d_6) δ 9.47 (t, *J* = 5.5 Hz, 1H), 8.37 (t, *J* = 2.4 Hz, 1H), 7.79 (d, *J* = 2.0 Hz, 2H), 7.39 (d, *J* = 4.4 Hz, 4H), 7.35 – 7.29 (m, 1H), 4.92 (d, *J* = 4.7 Hz, 2H). ^{13}C NMR (101 MHz, DMSO-d_6) δ 191.2, 186.6, 176.2, 156.8, 138.0, 131.5, 129.1, 128.6, 128.6, 128.3, 127.6, 47.5.HRMS: m/z: calcd. for $C_{15}H_{12}NO_2S^+$: 270.0583 $[M+H]^+$; found: 270.0585.

3-(benzylamino)-4-(thiophen-2-yl)cyclobut-3-ene-1,2-dione **6l**

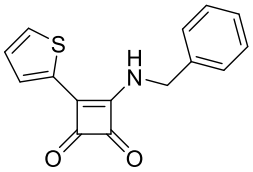

Product **6l** was obtained as a yellow solid. Yield: 11.2 mg (14%) using Merrifield resin. ^{1}H NMR (400 MHz, DMSO-d_6) δ 9.56 (t, *J* = 6.2 Hz, 1H), 7.97 (d, *J* = 5.0 Hz, 1H), 7.88 (d, *J* = 3.8 Hz, 1H), 7.44 – 7.27 (m, 6H), 4.92 (d, *J* = 6.0 Hz, 2H). ^{13}C NMR (101 MHz, DMSO-d_6) δ 191.8, 187.1, 176.7, 157.4, 138.6, 132.0, 129.6, 129.2, 129.1, 128.9, 128.2, 48.1. HRMS: m/z: calcd. for $C_{15}H_{12}NO_2S^+$: 270.0583 $[M+H]^+$; found: 270.0580.

(E)-3-(benzylamino)-4-styrylcyclobut-3-ene-1,2-dione **6m**

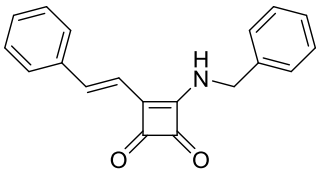

Product **6m** was obtained as a yellow solid. Yield: 23.8 mg (29%) using AM resin, 35.6 mg (41%) using Merrifield resin. ^{1}H NMR (400 MHz, DMSO-d_6), 76:24 mixture of two rotamers. Major rotamer δ 9.5 (t, *J* = 6.0 Hz, 1H), 7.6 (d, *J* = 16.3 Hz, 1H), 7.6 – 7.5 (m, 3H), 7.4 – 7.3 (m, 7H), 7.3 (d, *J* = 16.2 Hz, 1H), 4.9 (d, *J* = 5.3 Hz, 2H). Minor rotamer, characteristic signals: δ 9.8 (d, J = 6.3 Hz, 1H), 7.8 (d, J = 15.8 Hz, 1H), 7.1 (d, J = 15.8 Hz, 1H), 4.8 (d, J = 5.4 Hz, 2H). ^{13}C NMR (101 MHz, DMSO-d_6), 76:24 mixture of two rotamers. Signals are not specified for major and minor rotamer. δ 192.9, 192.2, 189.3, 188.6, 178.8, 162.3, 161.2, 137.8, 137.4, 136.1, 136.0, 135.9, 129.4, 129.2, 129.0, 128.9, 128.7, 128.7, 127.7, 127.7, 127.5, 127.4, 127.2, 116.7, 115.4, 47.4, 47.2. HRMS: m/z: calcd. for $C_{19}H_{16}NO_2^+$: 290.1176 $[M+H]^+$; found: 290.1177.

3-(benzylamino)-4-(2,6-dimethylphenyl)cyclobut-3-ene-1,2-dione **6n**

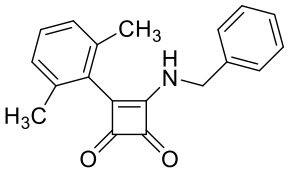

Product **6n** was obtained as a brown solid. Yield: 27.3 mg (31%) using Merrifield resin. ^{1}H NMR (400 MHz, DMSO-d_6), 63:37 mixture of two rotamers. Major rotamer δ 9.37 (t, *J* = 6.3 Hz, 1H), 7.66 – 7.03 (m, 7H), 6.83 (dd, *J* = 6.1, 2.5 Hz, 1H), 4.82 (d, *J* = 6.3 Hz, 2H), 2.20 (s, 6H). Minor rotamer, characteristic signals: δ 9.92 (t, *J* = 6.4 Hz, 1H), 4.13 (d, *J* = 6.3 Hz, 2H), 2.02 (s, 6H). ^{13}C NMR (101 MHz, DMSO-d_6), 63:37 mixture of two rotamers. Signals are not specified for major and minor rotamer. δ 194.3, 193.4, 189.0, 188.3, 181.8, 180.8, 167.6, 166.3, 138.1, 137.2, 135.8, 135.3, 129.2, 129.1, 129.0, 128.6, 128.4, 128.0, 127.5, 127.5, 127.3, 127.1, 127.0, 47.4, 47.1, 19.9, 19.7. HRMS: m/z: calcd. for $C_{19}H_{18}NO_2^+$: 292.1332 $[M+H]^+$; found: 292.1332.

3-(benzylamino)-4-(6-ethoxynaphthalen-2-yl)cyclobut-3-ene-1,2-dione **6o**

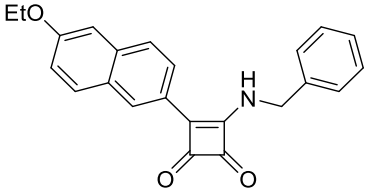

Product **6o** was obtained as a pale-yellow solid. Yield: 19.6 mg (20%) using AM resin. ^{1}H NMR (400 MHz, DMSO-d_6) δ 9.63 (br s, 1H), 8.51 (d, *J* = 1.9 Hz, 1H), 8.08 (dd, *J* = 8.6, 1.7 Hz, 1H), 7.91 (t, *J* = 8.9 Hz, 2H), 7.45 – 7.36 (m, 5H), 7.35 – 7.29 (m, 1H), 7.23 (dd, *J* = 8.9, 2.5 Hz, 1H), 4.98 (d, *J* = 4.1 Hz, 2H),

4.18 (q, *J* = 7.0 Hz, 2H), 1.41 (t, *J* = 7.0 Hz, 3H). ^{13}C NMR (101 MHz, DMSO-d_6) δ 193.1, 188.8, 178.3, 162.3, 158.0, 138.2, 135.2, 130.3, 128.7, 128.0, 127.6, 127.4, 125.9, 124.5, 123.7, 119.8, 106.9, 63.4, 47.6, 14.6. HRMS: m/z: calcd. for $C_{23}H_{20}NO_3^+$: 358.1438 $[M+H]^+$; found: 358.1437.

3-((pyridin-2-ylmethyl)amino)-4-(p-tolyl)cyclobut-3-ene-1,2-dione **6p**

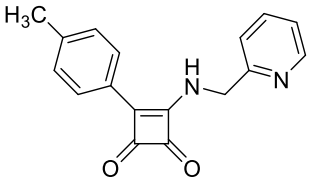

Product **6p** was obtained as a brown solid. Yield: 42.1 mg (50%) using Merrifield resin. ^{1}H NMR (400 MHz, DMSO-d_6) δ 9.55 (t, *J* = 6.0 Hz, 1H), 8.55 (ddd, *J* = 4.8, 1.7, 0.9 Hz, 1H), 7.99 – 7.89 (m, 2H), 7.81 (td, *J* = 7.7, 1.8 Hz, 1H), 7.45 (dt, *J* = 7.9, 1.1 Hz, 1H), 7.37 (d, *J* = 7.9 Hz, 2H), 7.32 (ddd, *J* = 7.6, 4.8, 1.1 Hz, 1H), 5.01 (d, *J* = 6.0 Hz, 2H), 2.38 (s, 3H). ^{13}C NMR (101 MHz, DMSO-d_6) δ 193.0, 188.9, 179.0, 162.0, 157.1, 149.2, 140.8, 137.0, 129.6, 126.6, 126.2, 122.7, 121.6, 48.9, 21.2. HRMS: m/z: calcd. for $C_{17}H_{15}N_2O_2^+$: 279.1128 $[M+H]^+$; found: 279.1125.

3-((4-bromobenzyl)amino)-4-(p-tolyl)cyclobut-3-ene-1,2-dione **6q**

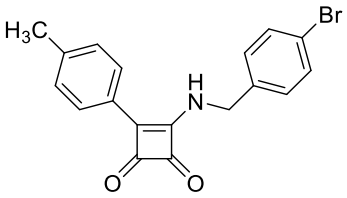

Product **6q** was obtained as a white solid. Yield: 20.1 mg (20%) using AM resin, 40.1 mg (37%) using Merrifield resin^{1}H NMR (400 MHz, DMSO-d_6) δ 9.51 (t, *J* = 6.2 Hz, 1H), 8.00 – 7.85 (m, 2H), 7.61 – 7.54 (m, 2H), 7.41 – 7.32 (m, 4H), 4.88 (d, *J* = 6.0 Hz, 2H), 2.37 (s, 3H) ^{13}C NMR (101 MHz, DMSO-d_6) δ 193.1, 188.7, 178.3, 162.2, 140.9, 137.6, 131.5, 129.9, 129.6, 126.5, 126.2, 120.7, 46.8, 21.2.

3-(propylamino)-4-(p-tolyl)cyclobut-3-ene-1,2-dione **6r**

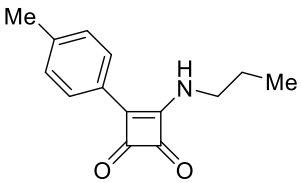

Product **6r** was obtained as a white solid. Yield: 22.1 mg (34%) using AM resin, 36.8 mg (53%) using Merrifield resin. ^{1}H NMR (400 MHz, DMSO-d_6) δ 9.04 (t, *J* = 6.2 Hz, 1H), 7.94 – 7.86 (m, 2H), 7.36 (d, *J* = 8.1 Hz, 2H), 3.66 (q, *J* = 6.7 Hz, 2H), 2.37 (s, 3H), 1.64 (h, *J* = 7.3 Hz, 2H), 0.91 (t, *J* = 7.4 Hz, 3H). ^{13}C NMR

(101 MHz, DMSO-d_6) δ 193.1, 188.6, 178.4, 161.6, 140.6, 129.5, 126.7, 126.0, 45.9, 23.7, 21.2, 10.7. HRMS: m/z: calcd. for $C_{14}H_{16}NO_2^+$: 230.1176 $[M+H]^+$; found: 230.1180.

3-(cyclohexylamino)-4-(p-tolyl)cyclobut-3-ene-1,2-dione **6s**

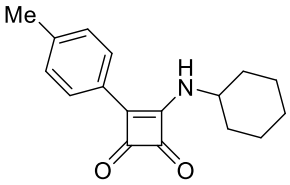

Product **6s** was obtained as a pale-yellow solid. Yield: 25.7 mg (34%) using AM resin, 39.6 mg (49%) using Merrifield resin. ^{1}H NMR (400 MHz, DMSO-d_6) δ 8.83 (br s, 1H), 7.94 (d, *J* = 8.2 Hz, 2H), 7.35 (d, *J* = 7.9 Hz, 2H), 4.14 (t, *J* = 10.7 Hz, 1H), 2.37 (s, 3H), 1.92 (dd, *J* = 12.1, 3.9 Hz, 2H), 1.78 (dt, *J* = 13.2, 3.4 Hz, 2H), 1.63 (dt, *J* = 12.7, 3.5 Hz, 1H), 1.46 (qd, *J* = 12.3, 3.4 Hz, 2H), 1.37 – 1.20 (m, 2H), 1.18 – 1.04 (m, 1H). ^{13}C NMR (101 MHz, DMSO-d_6) δ 192.9, 188.5, 177.4, 161.5, 140.5, 129.4, 126.6, 126.2, 54.1, 33.3, 24.7, 21.2. HRMS: m/z: calcd. for $C_{17}H_{20}NO_2^+$: 270.1489 $[M+H]^+$; found: 270.1490.

3-(phenylamino)-4-(p-tolyl)cyclobut-3-ene-1,2-dione **6t**

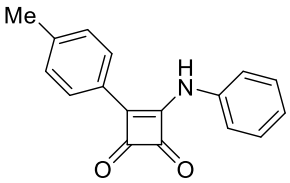

Product **6t** was obtained as a yellow solid. Yield: 39.8 mg (50%) using Merrifield resin. ^{1}H NMR (400 MHz, DMSO-d_6) δ 10.79 (br s, 1H), 9.14 – 6.65 (m, 9H), 2.39 (s, 3H). ^{13}C NMR (101 MHz, DMSO-d_6) δ 190.8, 190.1, 177.7, 163.8, 141.1, 137.2, 129.4, 128.6, 127.1, 126.0, 125.6, 122.7, 21.3. HRMS: m/z: calcd. for $C_{17}H_{14}NO_2^+$: 264.1019 $[M+H]^+$; found: 264.1019.

3-((4-methoxyphenyl)amino)-4-(p-tolyl)cyclobut-3-ene-1,2-dione **6u**

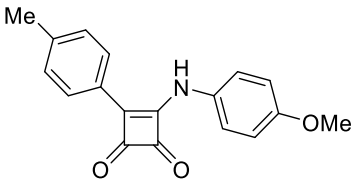

Product **6u** was obtained as a yellow solid. Yield: 41.1 mg (46%) using Merrifield resin. ^{1}H NMR (400 MHz, DMSO-d_6) δ 11.44 – 10.17 (m, 1H), 8.27 – 6.06 (m, 8H), 3.78 (s, 3H), 2.39 (s, 3H). ^{13}C NMR (101 MHz, DMSO-d_6) δ 190.6, 189.8, 177.5, 163.0, 157.3, 141.0, 130.2, 129.5, 126.6, 126.2, 124.3, 113.8, 55.3, 21.3. HRMS: m/z: calcd. for $C_{18}H_{16}NO_3^+$: 294.1125 $[M+H]^+$; found: 294.1126.

Methyl (3,4-dioxo-2-(p-tolyl)cyclobut-1-en-1-yl)-L-tyrosinate **6y**

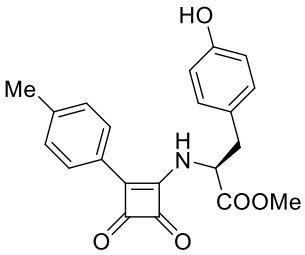

Product **6x** was obtained as an orange solid. Yield: 33.6 mg (33%) using AM resin, 49.2 mg (45%) using Merrifield resin. ^{1}H NMR (400 MHz, DMSO-d_6) δ 9.29 (d, *J* = 9.0 Hz, 1H), 9.20 (br s, 1H), 7.90 (d, *J* = 8.2 Hz, 2H), 7.38 (d, *J* = 8.0 Hz, 2H), 7.21 – 6.96 (m, 2H), 6.75 – 6.55 (m, 2H), 5.16 (ddd, *J* = 10.6, 9.2, 4.5 Hz, 1H), 3.73 (s, 3H), 3.23 (dd, *J* = 14.0, 4.6 Hz, 1H), 3.00 (dd, *J* = 13.9, 10.7 Hz, 1H), 2.38 (s, 3H). ^{13}C NMR (101 MHz, DMSO-d_6) δ 192.2, 188.6, 178.4, 170.7, 162.3, 156.0, 141.2, 130.2, 129.6, 126.6, 126.4, 126.1, 115.1, 58.3, 52.5, 36.5, 21.3. HRMS: m/z: calcd. for $C_{21}H_{20}NO_5^+$: 366.1336 $[M+H]^+$; found: 366.1336.

3-ethoxy-4-(p-tolyl)cyclobut-3-ene-1,2-dione **6aa**

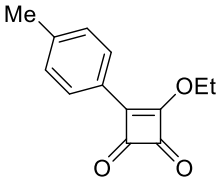

Product **6z** was obtained as a yellow solid. Yield: 38.2 mg (58%) using Merrifield resin. ^{1}H NMR (400 MHz, DMSO-d_6) δ 7.83 (d, *J* = 8.3 Hz, 2H), 7.41 (d, *J* = 7.9 Hz, 2H), 4.90 (q, *J* = 7.1 Hz, 2H), 2.39 (s, 3H), 1.48 (t, *J* = 7.1 Hz, 3H). ^{13}C NMR (101 MHz, DMSO-d_6) δ 194.4, 192.8, 191.9, 170.7, 143.0, 130.0, 126.8, 124.9, 71.3, 21.4, 15.4. HRMS: m/z: calcd. for $C_{13}H_{13}O_3^+$: 217.0859 $[M+H]^+$; found: 217.0857.

3-((4-bromophenyl)amino)-4-(p-tolyl)cyclobut-3-ene-1,2-dione **6ab**

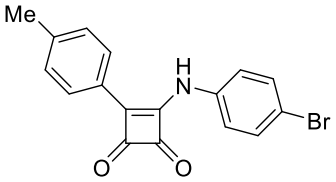

Product **6aa** was obtained as a yellow solid. Yield: 36.6 mg (35%) using Merrifield resin. ^{1}H NMR (400 MHz, DMSO-d_6) δ 10.83 (br s, 1H), 7.95 (br s, 1H), 7.70 – 7.15 (m, 7H), 2.39 (s, 3H). ^{13}C NMR (101 MHz, DMSO-d_6) δ 190.5, 190.1, 177.6, 164.1, 141.3, 136.7, 131.5, 129.5, 127.1, 125.9, 124.6, 117.9, 21.3. HRMS: m/z: calcd. for $C_{17}H_{13}BrNO_2^+$: 342.0124 $[M+H]^+$; found: 342.0124.

3-((4-morpholinophenyl)amino)-4-(p-tolyl)cyclobut-3-ene-1,2-dione **6ac**

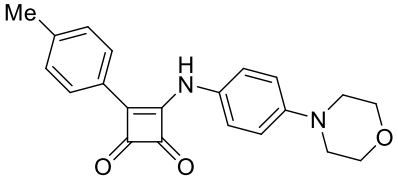

Product **6ab** was obtained as a brown solid. Yield: 35.5 mg (34%) using Merrifield resin. ^{1}H NMR (400 MHz, DMSO-d_6) δ 11.35 – 10.39 (m, 1H), 8.19 – 6.55 (m, 8H), 3.75 (t, *J* = 4.7 Hz, 4H), 3.12 (t, *J* = 4.7 Hz, 4H), 2.40 (s, 3H). ^{13}C NMR (101 MHz, DMSO-d_6) δ 190.6, 189.7, 177.3, 162.9, 149.0, 141.0, 129.5, 129.0, 126.6, 126.3, 123.7, 114.8, 66.0, 48.4, 21.3. HRMS: m/z: calcd. for $C_{21}H_{21}N_2O_3^+$: 349.1547 $[M+H]^+$; found: 349.1545.

ethyl 3-((3,4-dioxo-2-(p-tolyl)cyclobut-1-en-1-yl)amino)propanoate **6ad**

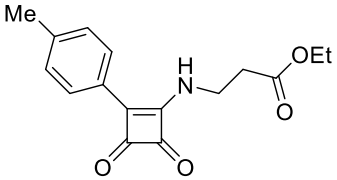

Product **6ac** was obtained as a white solid. Yield: 39.9 mg (46%) using Merrifield resin. ^{1}H NMR (400 MHz, DMSO-d_6) δ 9.00 (br s, 1H), 7.88 (d, *J* = 8.2 Hz, 2H), 7.35 (d, *J* = 8.0 Hz, 2H), 4.05 (q, *J* = 7.1 Hz, 2H), 3.96 (t, *J* = 7.0 Hz, 2H), 2.72 (t, *J* = 6.7 Hz, 2H), 2.37 (s, 3H), 1.15 (t, *J* = 7.1 Hz, 3H). ^{13}C NMR (101 MHz, DMSO-d_6) δ 192.8, 188.7, 178.6, 170.6, 161.5, 140.7, 129.6, 126.5, 126.0, 60.1, 38.9, 34.6, 21.2, 14.0. HRMS: m/z: calcd. for $C_{16}H_{18}NO_4^+$: 288.1230 $[M+H]^+$; found: 288.1233.

3-(benzyl(hydroxy)amino)-4-(p-tolyl)cyclobut-3-ene-1,2-dione **6ae**

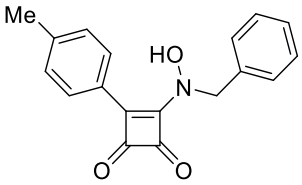

Product **6ad** was obtained as a white solid. Yield: 29.8 mg (34%) using Merrifield resin. ^{1}H NMR (400 MHz, DMSO-d_6) δ 11.70 (s, 1H), 8.01 (d, *J* = 8.3 Hz, 2H), 7.45 – 7.33 (m, 5H), 7.29 (d, *J* = 8.1 Hz, 2H), 5.10 (s, 2H), 2.34 (s, 3H). ^{13}C NMR (101 MHz, DMSO-d_6) δ 188.6, 185.8, 172.7, 160.3, 140.2, 134.7, 129.2, 128.7, 128.5, 128.3, 128.2, 126.2, 57.1, 21.1. HRMS: m/z: calcd. $C_{18}H_{16}NO_3^+$: 294.1125 $[M+H]^+$; found: 294.1124.

3-(methoxy(methyl)amino)-4-(p-tolyl)cyclobut-3-ene-1,2-dione **6af**

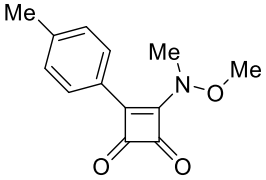

Product **6ae** was obtained as a pale-yellow solid. Yield: 28.8 mg (41%) using Merrifield resin. ^{1}H NMR (400 MHz, DMSO-d_6) δ 7.89 (d, J = 8.3 Hz, 2H), 7.34 (d, J = 8.0 Hz, 2H), 3.72 (s, 3H), 3.65 (s, 3H), 2.36 (s, 3H). ^{13}C NMR (101 MHz, DMSO-d_6) δ 188.1, 186.1, 172.9, 160.3, 140.4, 129.5, 127.8, 125.8, 61.6, 37.2, 21.1. HRMS: m/z: calcd. $C_{13}H_{14}NO_3^+$: 232.0968 $[M+H]^+$; found: 232.0968.

3-morpholino-4-(p-tolyl)cyclobut-3-ene-1,2-dione **6ag**

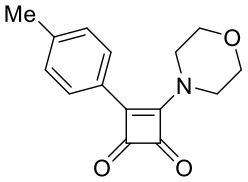

Product **6af** was obtained as a white solid. Yield: 38.8 mg (50%) using Merrifield resin. ^{1}H NMR (400 MHz, DMSO-d_6) δ 7.48 (d, J = 8.2 Hz, 2H), 7.33 (d, J = 7.9 Hz, 2H), 3.98 (br s, 2H), 3.75 (br s, 4H), 3.55 (br s, 2H), 2.36 (s, 3H). ^{13}C NMR (101 MHz, DMSO-d_6) δ 192.8, 187.9, 177.4, 162.6, 139.7, 129.3, 127.5, 125.8, 65.8, 65.4, 49.0, 47.0, 21.0. HRMS: m/z: calcd. $C_{15}H_{16}NO_3^+$: 258.1125 $[M+H]^+$; found: 258.1123.

tert-butyl 4-(3,4-dioxo-2-(p-tolyl)cyclobut-1-en-1-yl)piperazine-1-carboxylate **6ai**

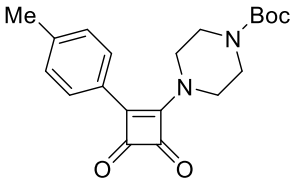

Product **6ah** was obtained as a white solid. Yield: 45.5 mg (42%) using Merrifield resin. ^{1}H NMR (400 MHz, DMSO-d_6) δ 7.49 (d, J = 8.1 Hz , 2H), 7.34 (d, J = 7.9 Hz, 2H), 3.95 (br s, 2H), 3.52 (br s, 6H), 2.36 (s, 3H), 1.42 (s, 9H). ^{13}C NMR (101 MHz, DMSO-d_6) δ 192.7, 187.9, 177.7, 162.8, 153.6, 139.7, 129.4, 127.5, 125.8, 79.4, 48.5, 46.5, 42.7, 27.9, 21.0.HRMS: m/z: calcd. $C_{20}H_{25}N_2O_4^+$: 357.1809 $[M+H]^+$; found: 357.1810.

3-((furan-2-ylmethyl)amino)-4-(p-tolyl)cyclobut-3-ene-1,2-dione **6aj**

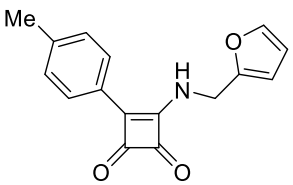

Product **6ai** was obtained as a white solid. Yield: 40.9 mg (51%) using Merrifield resin. ^{1}H NMR (400 MHz, DMSO-d_6) δ 9.53 (br s, 1H), 7.92 (d, *J* = 8.2 Hz, 2H), 7.65 (dd, *J* = 1.5, 0.7 Hz, 1H), 7.34 (d, *J* = 8.0 Hz, 2H), 6.46 – 6.38 (m, 2H), 4.91 (s, 2H), 2.36 (s, 3H). ^{13}C NMR (101 MHz, DMSO-d_6) δ 192.8, 188.8, 178.4, 162.3, 150.9, 143.0, 140.9, 129.6, 126.4, 126.2, 110.7, 108.2, 40.5, 21.2. HRMS: m/z: calcd. $C_{16}H_{14}NO_3^+$: 268.0968 $[M+H]^+$; found: 268.0968.

3-(((4'-methoxy-[1,1'-biphenyl]-4-yl)methyl)amino)-4-(*p*-tolyl)cyclobut-3-ene-1,2-dione **6am**

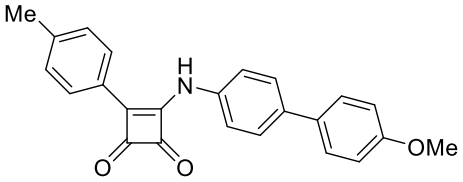

Product **6am** was obtained as a yellow solid. Yield: 25.3 mg (23%) using Merrifield resin. ^{1}H NMR (400 MHz, DMSO-d_6) δ 10.80 (br s, 1H), 8.28 – 7.23 (m, 10H), 7.11 – 6.94 (m, 2H), 3.80 (s, 3H), 2.40 (s, 3H). ^{13}C NMR (101 MHz, DMSO-d_6) δ 190.6, 190.1, 177.6, 163.8, 158.9, 141.2, 136.9, 136.0, 131.6, 129.4, 127.6, 127.1, 126.2, 126.1, 123.0, 114.4, 55.2, 21.3. HRMS: m/z: calcd. $C_{24}H_{20}NO_3^+$: 370.1438 $[M+H]^+$; found: 370.1439.

Declaration of Competing Interest

The authors declare that they have no known competing financial interests or personal relationships that could have appeared to influence the work reported in this paper.

Data availability

The data supporting the findings of this study are available in the published article as well as in its supplementary materials.

Acknowledgments

This work was financially supported by Palacky University Olomouc (project IGA_PrF_2024_028 and IGA_PrF_2025_014).

Author contributions

J.C. designed and performed the synthetic experiments, analyzed the experimental data, and wrote the experimental section. L.B. initiated the project, designed the synthetic experiments, analyzed the results, and was responsible for funding acquisition. L.B. and J.C. wrote the paper. Both authors have approved the final version of the manuscript.

References

(1) Tantry, S. J.; Markad, S. D.; Shinde, V.; Bhat, J.; Balakrishnan, G.; Gupta, A. K.; Ambady, A.; Raichurkar, A.; Kedari, C.; Sharma, S.; Mudugal, N. V; Narayan, A.; Naveen Kumar, C. N.; Nanduri, R.; Bharath, S.; Reddy, J.; Panduga, V.; Prabhakar, K. R.; Kandaswamy, K.; Saralaya, R.; Kaur, P.; Dinesh, N.; Guptha, S.; Rich, K.; Murray, D.; Plant, H.; Preston, M.; Ashton, H.; Plant, D.; Walsh, J.; Alcock, P.; Naylor, K.; Collier, M.; Whiteaker, J.; McLaughlin, R. E.; Mallya, M.; Panda, M.; Rudrapatna, S.; Ramachandran, V.; Shandil, R.; Sambandamurthy, V. K.; Mdluli, K.; Cooper, C. B.; Rubin, H.; Yano, T.; Iyer, P.; Narayanan, S.; Kavanagh, S.; Mukherjee, K.; Balasubramanian, V.; Hosagrahara, V. P.; Solapure, S.; Ravishankar, S.; Hameed P, S. Discovery of Imidazo[1,2-a]Pyridine Ethers and Squaramides as Selective and Potent Inhibitors of Mycobacterial Adenosine Triphosphate (ATP) Synthesis. *J. Med. Chem.* **2017**, *60* (4), 1379–1399.

(2) Chasák, J.; Oorts, L.; Dak, M.; Šlachtová, V.; Bazgier, V.; Berka, K.; De Vooght, L.; Smiejkowska, N.; Calster, K. Van; Van Moll, L.; Cappoen, D.; Cos, P.; Brulíková, L. Expanding the Squaramide Library as Mycobacterial ATP Synthase Inhibitors: Innovative Synthetic Pathway and Biological Evaluation. *Bioorg. Med. Chem.* **2023**, *95*, 117504.

(3) Chasák, J.; Van Moll, L.; Matheeussen, A.; De Vooght, L.; Cos, P.; Brulíková, L. The Liebeskind–Srogl Cross-Coupling Reaction as a Crucial Step in the Synthesis of New Squaramide-Based Antituberculosis Agents. *ACS Omega* **2024**, *9* (32), 34808–34828.

(4) Chasák, J.; Šlachtová, V.; Urban, M.; Brulíková, L. Squaric Acid Analogues in Medicinal Chemistry. *Eur. J. Med. Chem.* **2021**, *209*, 112872.

(5) Chen, J.; Ekiert, D. C. A Tale of Two Inhibitors: Diarylquinolines and Squaramides. *EMBO J.* **2023**, *42* (15), e114912.

(6) Courbon, G. M.; Palme, P. R.; Mann, L.; Richter, A.; Imming, P.; Rubinstein, J. L. Mechanism of Mycobacterial ATP Synthase Inhibition by Squaramides and Second Generation Diarylquinolines. *EMBO J.* **2023**, *42* (15), e113687.

(7) Ahmed, S.; A.E., P.; and Saxena, A. K. Molecular Docking-Based Interaction Studies on Imidazo[1,2-a] Pyridine Ethers and Squaramides as Anti-Tubercular Agents. *SAR QSAR Environ. Res.* **2023**, *34* (6), 435–457.

(8) Shinada, T.; Yamasaki, A.; Kiniwa, Y.; Shimamoto, K.; Ohfune, Y. Thiol Addition to T-Butyl Methyl Squarate. Efficient Synthesis of Novel Sulfur-Linked Squaryl Group-Containing Glutamate Analogs. *Tetrahedron Lett.* **2009**, *50* (30), 4354–4357.

(9) Srivastava, D.; Kushwaha, A.; Kociok-Köhn, G.; Gosavi, S. W.; Chauhan, R.; Kumar, A.; Muddassir, M. The Supramolecular Frameworks and Electrocatalytic Properties of Two New Structurally Diverse Tertiary Phosphane-Appended Nickel(Ii) and Copper(i) Thiosquarates.

CrystEngComm **2023**, *25* (48), 6822–6836.

(10) Schmidt, W.; Ried, H. A. Die Präparative Chemie Der Cyclobutendione; I. Synthese von Cyclobutendion Und Dessen Alkyl-, Alkenyl-Und Aryl-Derivaten. *Synthesis (Stuttg).* **1978**, *1978* (01), 1–22.

(11) Ivanovsky, S. A.; Mikhail V., D.; Dmitry V., K.; and Ivachtchenko, A. V. Synthesis of the Substituted 3-Cyclobutene-1,2-diones. *Synth. Commun.* **2007**, *37* (15), 2527–2542.

(12) Asby, D. J.; Radigois, M. G.; Wilson, D. C.; Cuda, F.; Chai, C. L. L.; Chen, A.; Bienemann, A. S.; Light, M. E.; Harrowven, D. C.; Tavassoli, A. Triggering Apoptosis in Cancer Cells with an Analogue of Cribrostatin 6 That Elevates Intracellular ROS. *Org. Biomol. Chem.* **2016**, *14* (39), 9322–9330.

(13) Schmidt Günter; Diedrich, Heike, A. H. S. Oxokohlenstoffe Und Verwandte Verbindungen; 15. Mitteilung.1Meerwein-Arylierung von Semiquadratsäure Und Semiquadratsäureamiden. Eine Allgemeine Darstellungsmethode von 3-Aryl-4-Hydroxy- Und 3-Amino-4-Aryl-3-Cyclobuten-1,2-Dionen. *Synthesis (Stuttg).* **1990**, *1990* (07), 579–582.

(14) Piettre, S. R.; Baltzer, S. A New Approach to the Solid-Phase Suzuki Coupling Reaction. *Tetrahedron Lett.* **1997**, *38* (7), 1197–1200.

Supporting information

Solid-Phase Synthesis of Aryl Squaramides Using Liebeskind-Srogl Cross-Coupling

Jan Chasák,[a] Lucie Brulíková[a,*]

[a]*Department of Organic Chemistry, Faculty of Science, Palacký University, 17. listopadu 12, 77146, Olomouc, Czech Republic*

The corresponding author's email address: lucie.brulikova@upol.cz

Contents

Scheme S1. Synthesis of 3-(tert-butoxy)-4-methoxycyclobut-3-ene-1,2-dione 4

Scheme S2. Synthesis of 3-ethoxy-4-mercaptocyclobut-3-ene-1,2-dione..... 4

Fig S1. ^{1}H NMR spectra of 3-(tert-butoxy)-4-methoxycyclobut-3-ene-1,2-dione 5

Fig S2. ^{13}C NMR spectra of 3-(tert-butoxy)-4-methoxycyclobut-3-ene-1,2-dione 5

Fig S3. ^{1}H NMR spectra of 3-ethoxy-4-mercaptocyclobut-3-ene-1,2-dione..... 6

Fig S4. ^{13}C NMR spectra of 3-ethoxy-4-mercaptocyclobut-3-ene-1,2-dione..... 6

Fig S5. ^{1}H NMR spectra of 3-(benzylamino)-4-(p-tolyl)cyclobut-3-ene-1,2-dione **6a**..... 7

Fig S6. ^{13}C NMR spectra of 3-(benzylamino)-4-(p-tolyl)cyclobut-3-ene-1,2-dione **6a**..... 7

Fig S7. ^{1}H NMR spectra of 3-(benzylamino)-4-(4-methoxyphenyl)cyclobut-3-ene-1,2-dione **6b** 8

Fig S8. ^{13}C NMR spectra of 3-(benzylamino)-4-(4-methoxyphenyl)cyclobut-3-ene-1,2-dione **6b** 8

Fig S9. ^{1}H NMR spectra of 3-(benzylamino)-4-(4-(methylthio)phenyl)cyclobut-3-ene-1,2-dione **6c**..... 9

Fig S10. ^{13}C NMR spectra of 3-(benzylamino)-4-(4-(methylthio)phenyl)cyclobut-3-ene-1,2-dione **6c**... 9

Fig S11. ^{1}H NMR spectra of 3-(benzylamino)-4-phenylcyclobut-3-ene-1,2-dione **6d** 10

Fig S12. ^{13}C NMR spectra of 3-(benzylamino)-4-phenylcyclobut-3-ene-1,2-dione **6d** 10

Fig S13. ^{1}H NMR spectra of 3-(benzylamino)-4-(4-nitrophenyl)cyclobut-3-ene-1,2-dione **6e**..... 11

Fig S14. ^{13}C NMR spectra of 3-(benzylamino)-4-(4-nitrophenyl)cyclobut-3-ene-1,2-dione **6e**..... 11

Fig S15. ^{1}H NMR spectra of 3-(benzylamino)-4-(4-(trifluoromethyl)phenyl)cyclobut-3-ene-1,2-dione **6f** 12

Fig S16. ^{13}C NMR spectra of 3-(benzylamino)-4-(4-(trifluoromethyl)phenyl)cyclobut-3-ene-1,2-dione **6f**..... 12

Fig S17. ^{1}H NMR spectra of 4-(2-(benzylamino)-3,4-dioxocyclobut-1-en-1-yl)benzaldehyde **6g**..... 13

Fig S18. ^{13}C NMR spectra of 4-(2-(benzylamino)-3,4-dioxocyclobut-1-en-1-yl)benzaldehyde **6g**..... 13

Fig S19. ^{1}H NMR spectra of 3-(benzylamino)-4-(4-bromophenyl)cyclobut-3-ene-1,2-dione **6h**..... 14

Fig S20. ^{13}C NMR spectra of 3-(benzylamino)-4-(4-bromophenyl)cyclobut-3-ene-1,2-dione **6h**..... 14

Fig S21. ^{1}H NMR spectra of 3-(benzylamino)-4-(furan-3-yl)cyclobut-3-ene-1,2-dione **6i** 15
Fig S22. ^{13}C NMR spectra of 3-(benzylamino)-4-(furan-3-yl)cyclobut-3-ene-1,2-dione **6i** 15
Fig S23. ^{1}H NMR spectra of 3-(benzylamino)-4-(thiophen-3-yl)cyclobut-3-ene-1,2-dione **6k** 16
Fig S24. ^{13}C NMR spectra of 3-(benzylamino)-4-(thiophen-3-yl)cyclobut-3-ene-1,2-dione **6k** 16
Fig S25. ^{1}H NMR spectra of 3-(benzylamino)-4-(thiophen-2-yl)cyclobut-3-ene-1,2-dione **6l** 17
Fig S26. ^{13}C NMR spectra of 3-(benzylamino)-4-(thiophen-2-yl)cyclobut-3-ene-1,2-dione **6l** 17
Fig S27. ^{1}H NMR spectra of (E)-3-(benzylamino)-4-styrylcyclobut-3-ene-1,2-dione **6m**..... 18
Fig S28. ^{13}C NMR spectra of (E)-3-(benzylamino)-4-styrylcyclobut-3-ene-1,2-dione **6m**..... 18
Fig S29. ^{1}H NMR spectra of 3-(benzylamino)-4-(2,6-dimethylphenyl)cyclobut-3-ene-1,2-dione **6n** 19
Fig S30. ^{13}C NMR spectra of 3-(benzylamino)-4-(2,6-dimethylphenyl)cyclobut-3-ene-1,2-dione **6n** ... 19
Fig S31. ^{1}H NMR spectra of 3-(benzylamino)-4-(6-ethoxynaphthalen-2-yl)cyclobut-3-ene-1,2-dione **6o** 20
Fig S32. ^{13}C NMR spectra of 3-(benzylamino)-4-(6-ethoxynaphthalen-2-yl)cyclobut-3-ene-1,2-dione **6o** 20
Fig S33. ^{1}H NMR spectra of 3-((pyridin-2-ylmethyl)amino)-4-(p-tolyl)cyclobut-3-ene-1,2-dione **6p**.... 21
Fig S34. ^{13}C NMR spectra of 3-((pyridin-2-ylmethyl)amino)-4-(p-tolyl)cyclobut-3-ene-1,2-dione **6p**... 21
Fig S35. ^{1}H NMR spectra of 3-((4-bromobenzyl)amino)-4-(p-tolyl)cyclobut-3-ene-1,2-dione **6q**..... 22
Fig S36. ^{13}C NMR spectra of 3-((4-bromobenzyl)amino)-4-(p-tolyl)cyclobut-3-ene-1,2-dione **6q**..... 22
Fig S37. ^{1}H NMR spectra of 3-(propylamino)-4-(p-tolyl)cyclobut-3-ene-1,2-dione **6r** 23
Fig S38. ^{13}C NMR spectra of 3-(propylamino)-4-(p-tolyl)cyclobut-3-ene-1,2-dione **6r** 23
Fig S39. ^{1}H NMR spectra of 3-(cyclohexylamino)-4-(p-tolyl)cyclobut-3-ene-1,2-dione **6s**..... 24
Fig S40. ^{13}C NMR spectra of 3-(cyclohexylamino)-4-(p-tolyl)cyclobut-3-ene-1,2-dione **6s**..... 24
Fig S41. ^{1}H NMR spectra of 3-(phenylamino)-4-(p-tolyl)cyclobut-3-ene-1,2-dione **6t**..... 25
Fig S42. ^{13}C NMR spectra of 3-(phenylamino)-4-(p-tolyl)cyclobut-3-ene-1,2-dione **6t**..... 25
Fig S43. ^{1}H NMR spectra of 3-((4-methoxyphenyl)amino)-4-(p-tolyl)cyclobut-3-ene-1,2-dione **6u**..... 26
Fig S44. ^{13}C NMR spectra of 3-((4-methoxyphenyl)amino)-4-(p-tolyl)cyclobut-3-ene-1,2-dione **6u**.... 26
Fig S45. ^{1}H NMR spectra of methyl (3,4-dioxo-2-(p-tolyl)cyclobut-1-en-1-yl)-L-tyrosinate **6y** 27
Fig S46. ^{13}C NMR spectra of methyl (3,4-dioxo-2-(p-tolyl)cyclobut-1-en-1-yl)-L-tyrosinate **6y** 27
Fig S47. ^{1}H NMR spectra of 3-ethoxy-4-(p-tolyl)cyclobut-3-ene-1,2-dione **6aa**..... 28
Fig S48. ^{13}C NMR spectra of 3-ethoxy-4-(p-tolyl)cyclobut-3-ene-1,2-dione **6aa**..... 28
Fig S49. ^{1}H NMR spectra of 3-((4-bromophenyl)amino)-4-(p-tolyl)cyclobut-3-ene-1,2-dione **6ab** 29
Fig S50. ^{13}C NMR spectra of 3-((4-bromophenyl)amino)-4-(p-tolyl)cyclobut-3-ene-1,2-dione **6ab** 29
Fig S51. ^{1}H NMR spectra of 3-((4-morpholinophenyl)amino)-4-(p-tolyl)cyclobut-3-ene-1,2-dione **6ac**30
Fig S52. ^{13}C NMR spectra of 3-((4-morpholinophenyl)amino)-4-(p-tolyl)cyclobut-3-ene-1,2-dione **6ac** 30

Fig S53. ^{1}H NMR spectra of ethyl 3-((3,4-dioxo-2-(p-tolyl)cyclobut-1-en-1-yl)amino)propanoate **6ad** 31

Fig S54. ^{13}C NMR spectra of ethyl 3-((3,4-dioxo-2-(p-tolyl)cyclobut-1-en-1-yl)amino)propanoate **6ad**31

Fig S55. ^{1}H NMR spectra of 3-(benzyl(hydroxy)amino)-4-(p-tolyl)cyclobut-3-ene-1,2-dione **6ae** 32

Fig S56. ^{13}C NMR spectra of 3-(benzyl(hydroxy)amino)-4-(p-tolyl)cyclobut-3-ene-1,2-dione **6ae** 32

Fig S57. ^{1}H NMR spectra of 3-(methoxy(methyl)amino)-4-(p-tolyl)cyclobut-3-ene-1,2-dione **6af**..... 33

Fig S58. ^{13}C NMR spectra of 3-(methoxy(methyl)amino)-4-(p-tolyl)cyclobut-3-ene-1,2-dione **6af**..... 33

Fig S59. ^{1}H NMR spectra of 3-morpholino-4-(p-tolyl)cyclobut-3-ene-1,2-dione **6ag**..... 34

Fig S60. ^{13}C NMR spectra of 3-morpholino-4-(p-tolyl)cyclobut-3-ene-1,2-dione **6ag**..... 34

Fig S61. ^{1}H NMR spectra of tert-butyl 4-(3,4-dioxo-2-(p-tolyl)cyclobut-1-en-1-yl)piperazine-1-carboxylate **6ai** 35

Fig S62. ^{13}C NMR spectra of tert-butyl 4-(3,4-dioxo-2-(p-tolyl)cyclobut-1-en-1-yl)piperazine-1-carboxylate **6ai** 35

Fig S63. ^{1}H NMR spectra of 3-((furan-2-ylmethyl)amino)-4-(p-tolyl)cyclobut-3-ene-1,2-dione **6aj** 36

Fig S64. ^{13}C NMR spectra of 3-((furan-2-ylmethyl)amino)-4-(p-tolyl)cyclobut-3-ene-1,2-dione **6aj** 36

Fig S65. ^{1}H NMR spectra of 3-((4'-methoxy-[1,1'-biphenyl]-4-yl)amino)-4-(p-tolyl)cyclobut-3-ene-1,2-dione **6am**..... 37

Fig S66. ^{13}C NMR spectra of 3-((4'-methoxy-[1,1'-biphenyl]-4-yl)amino)-4-(p-tolyl)cyclobut-3-ene-1,2-dione **6am**..... 37

Scheme S1. *Synthesis of 3-(tert-butoxy)-4-methoxycyclobut-3-ene-1,2-dione*

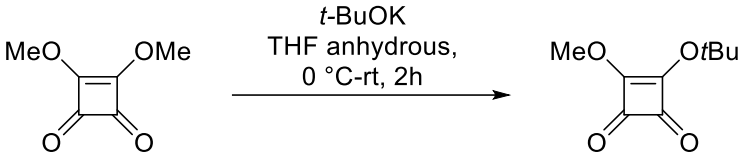

3,4-dimethoxy-3-cyclobutene-1,2-dione (2 g, 14.1 mmol) was placed in annealed Schlenk flasks and dissolved in THF dry (50 mL) under argon at 0 °C. Then, *t*BuOK (1.57 g, 14.1 mmol) was added portion wisely. The mixture was stirred for 2 h at 0 °C and another 2 h at rt. Then, the reaction mixture was quenched with saturated NH_4Cl (30 mL) and extracted with Et_2O (3x 30 mL). The combined organic phases were washed with brine (30 mL), dried over $MgSO_4$ and evaporated under reduced pressure. The product was purified by LC using DCM/MeOH 9:0.15 as mobile phase. The product was obtained as a white solid. Yield: 1.5g (56%). ^{1}H NMR (400 MHz, Chloroform-*d*) δ 4.38 (s, 3H), 1.57 (s, 9H). ^{13}C NMR (101 MHz, $CDCl_3$) δ 189.63, 188.64, 185.80, 184.79, 87.54, 60.94, 28.71. HRMS: m/z: calcd. for $C_9H_{13}O_4^+$: 185.0808 $[M+H]^+$; found: 185.0812.

Scheme S2. *Synthesis of 3-ethoxy-4-mercaptocyclobut-3-ene-1,2-dione*

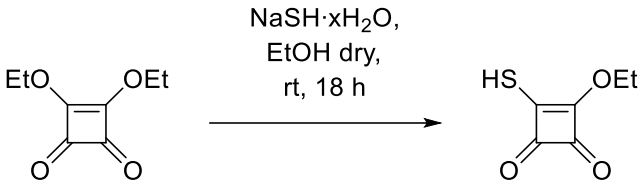

3,4-diethoxy-3-cyclobutene-1,2-dione (340 mg, 2 mmol) was placed in annealed Schlenk flasks and dissolved in EtOH dry (5 mL) under argon atmosphere. Then $NaSH{\cdot}xH_2O$ was added portion wisely. The mixture was stirred for 18 h at rt. Solids from the reaction mixture were filtered and the filtrate was precipitated by the addition of Et_2O (30 mL). Formed precipitation was filtered and washed by Et_2O (20 mL). The product was obtained as yellow solid. Yield: 302.4mg (96%). ^{1}H NMR (400 MHz, DMSO-d_6) δ 4.73 (q, *J* = 7.0 Hz, 2H), 1.32 (t, *J* = 7.1 Hz, 3H). ^{13}C NMR (101 MHz, DMSO-d_6) δ 207.30, 203.92, 197.30, 192.29, 66.88, 15.97. HRMS: m/z: calcd. for $C_6H_5O_3S^-$: 156.9953 $[M-H]^+$; found: 156.9954.

Fig S1. *^{1}H NMR spectra of 3-(tert-butoxy)-4-methoxycyclobut-3-ene-1,2-dione*

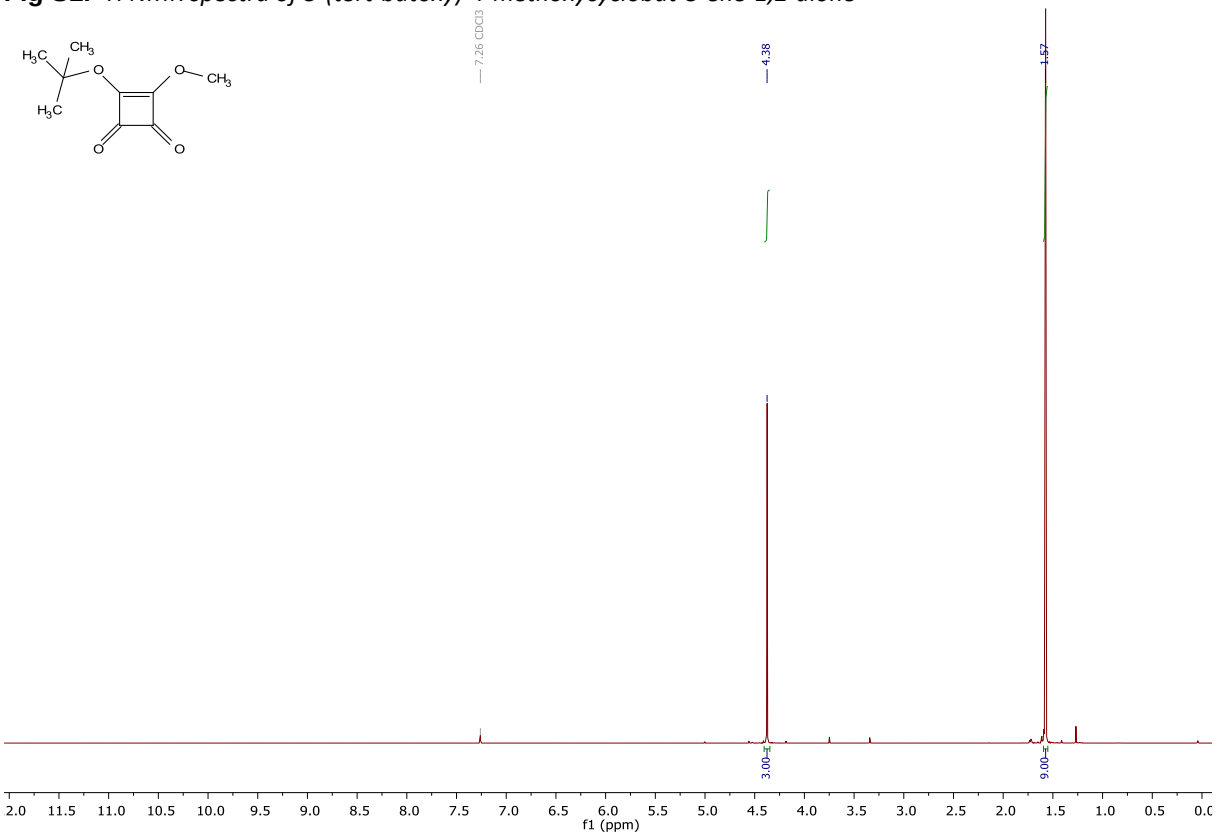

Fig S2. *^{13}C NMR spectra of 3-(tert-butoxy)-4-methoxycyclobut-3-ene-1,2-dione*

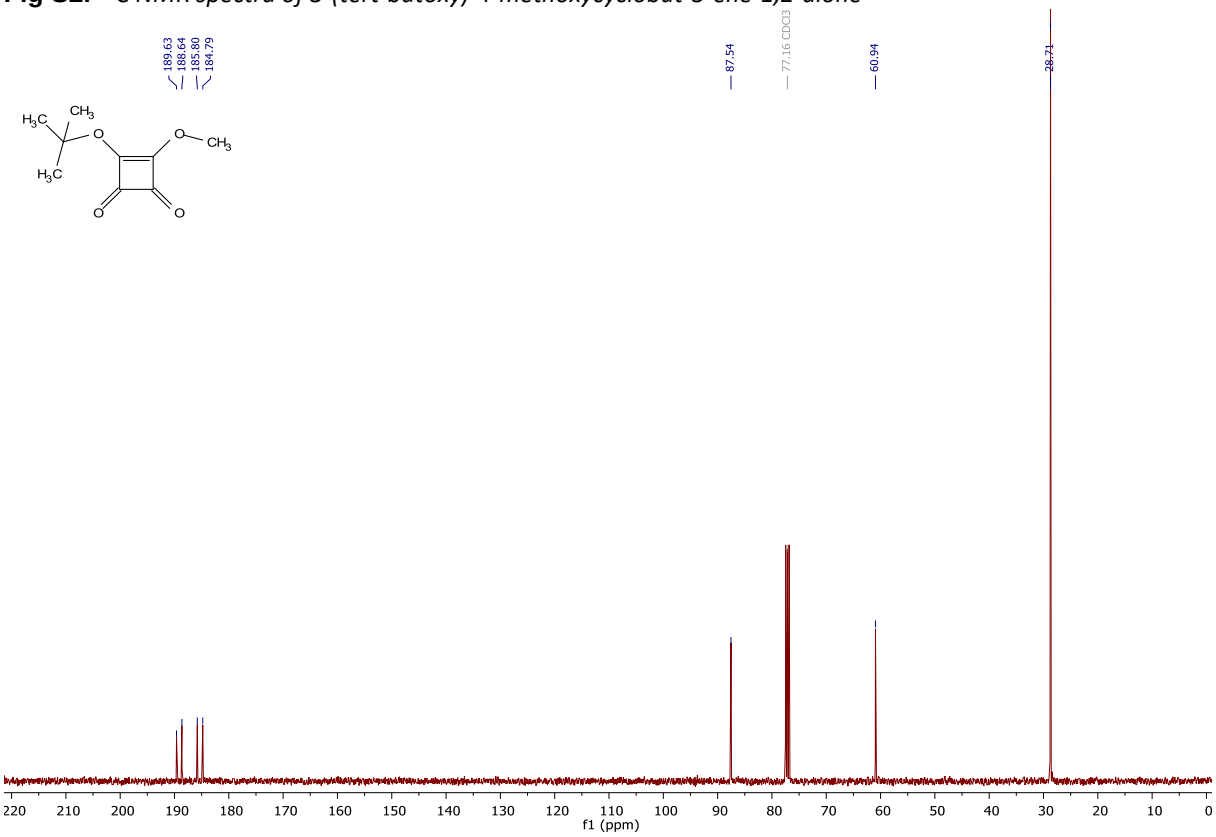

Fig S3. *^{1}H NMR spectra of 3-ethoxy-4-mercaptocyclobut-3-ene-1,2-dione*

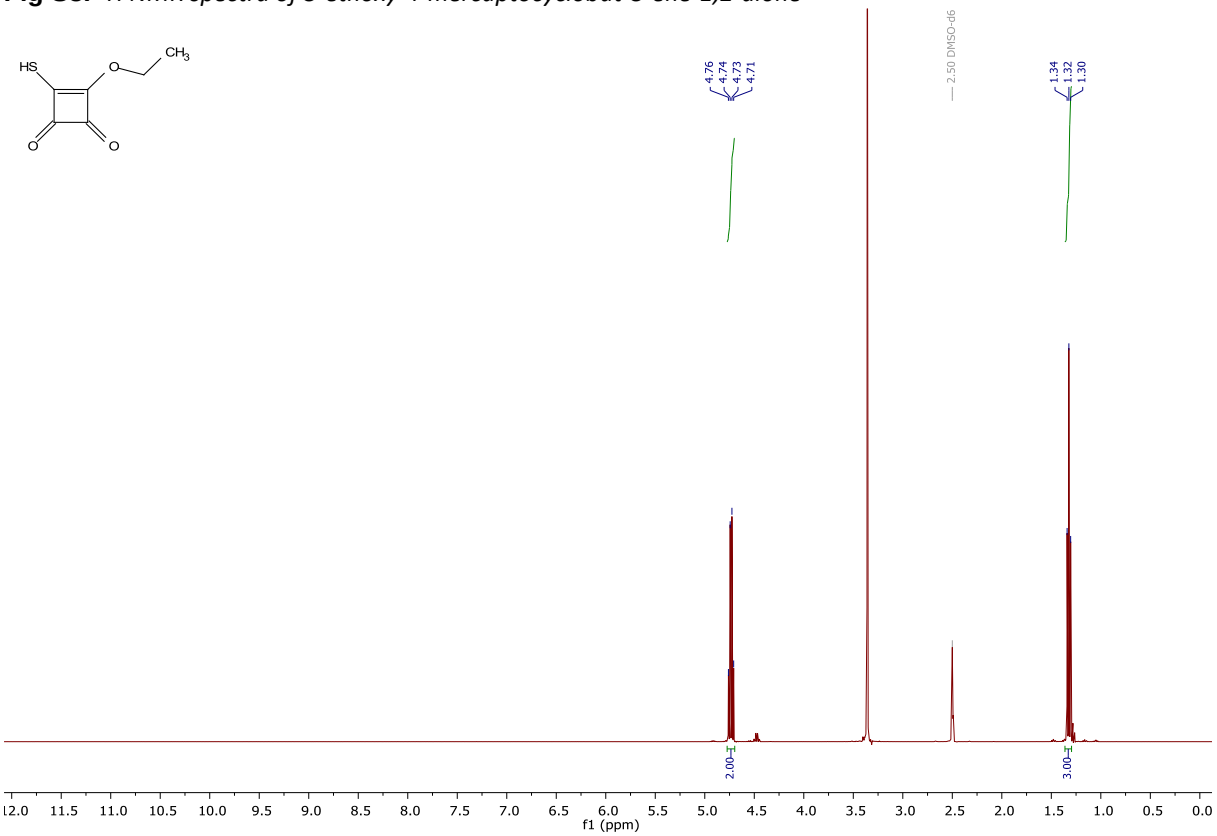

Fig S4. *^{13}C NMR spectra of 3-ethoxy-4-mercaptocyclobut-3-ene-1,2-dione*

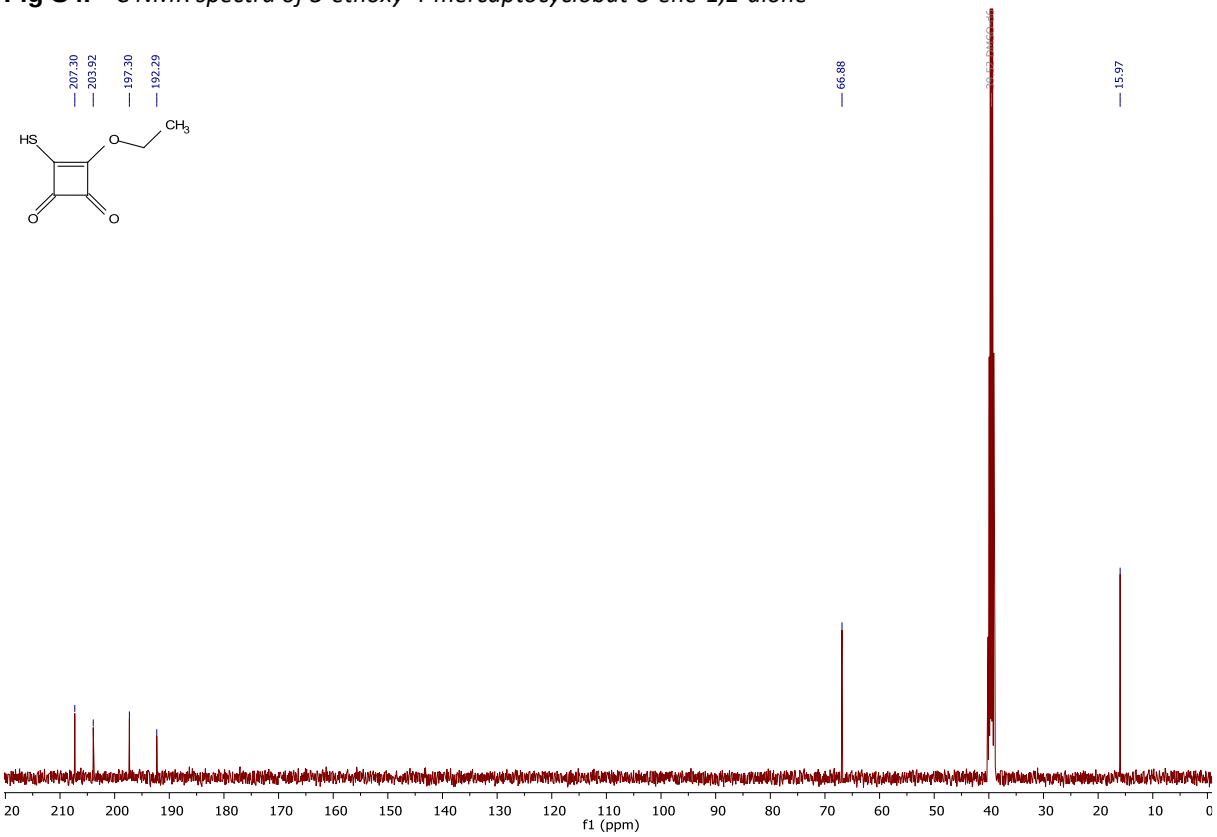

Fig S5. *^{1}H NMR spectra of 3-(benzylamino)-4-(p-tolyl)cyclobut-3-ene-1,2-dione* ***6a***

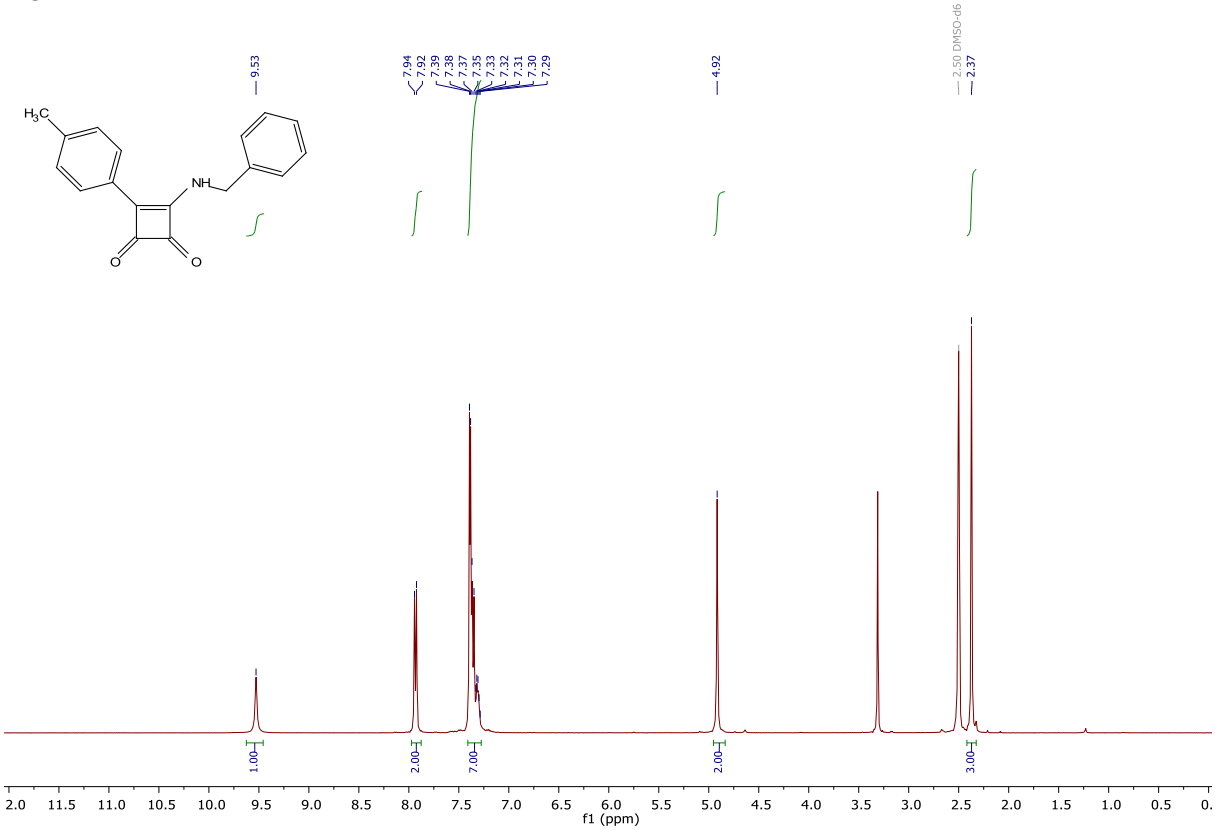

Fig S6. *^{13}C NMR spectra of 3-(benzylamino)-4-(p-tolyl)cyclobut-3-ene-1,2-dione* ***6a***

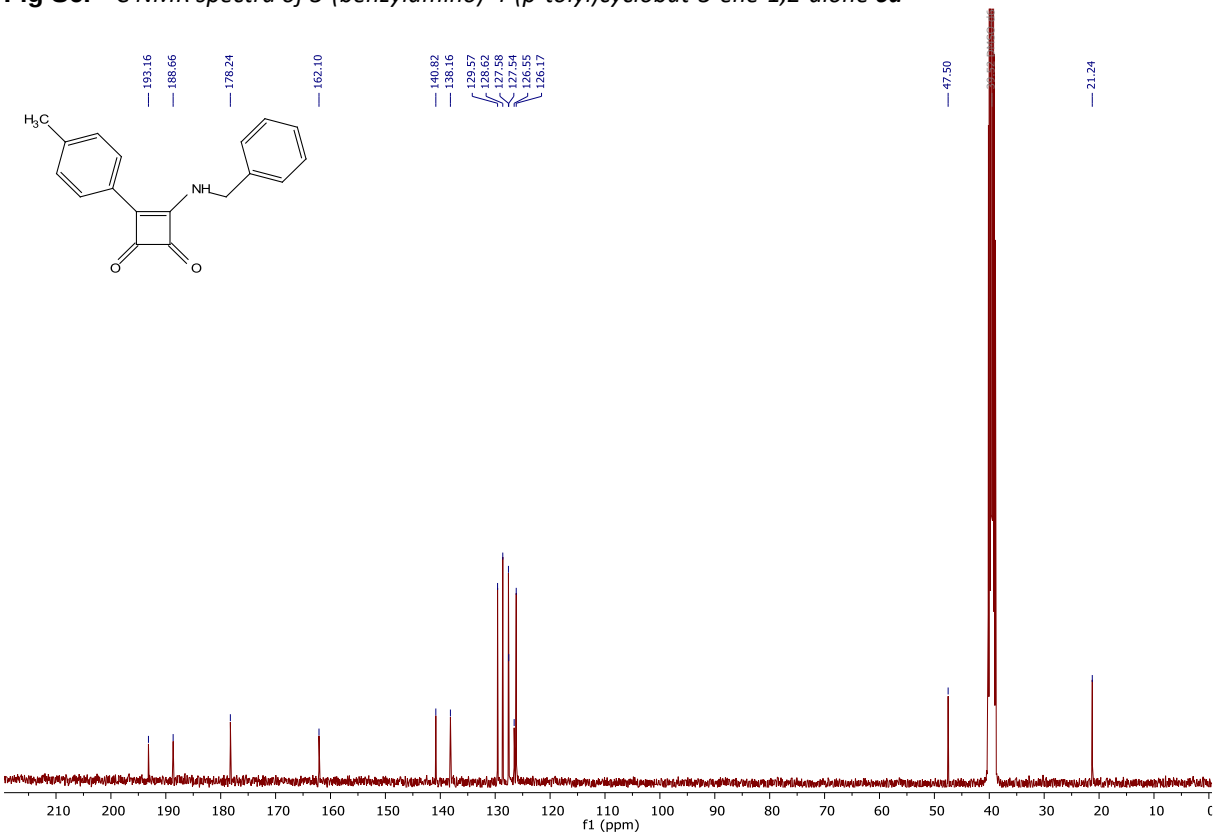

Fig S7. *^{1}H NMR spectra of 3-(benzylamino)-4-(4-methoxyphenyl)cyclobut-3-ene-1,2-dione* ***6b***

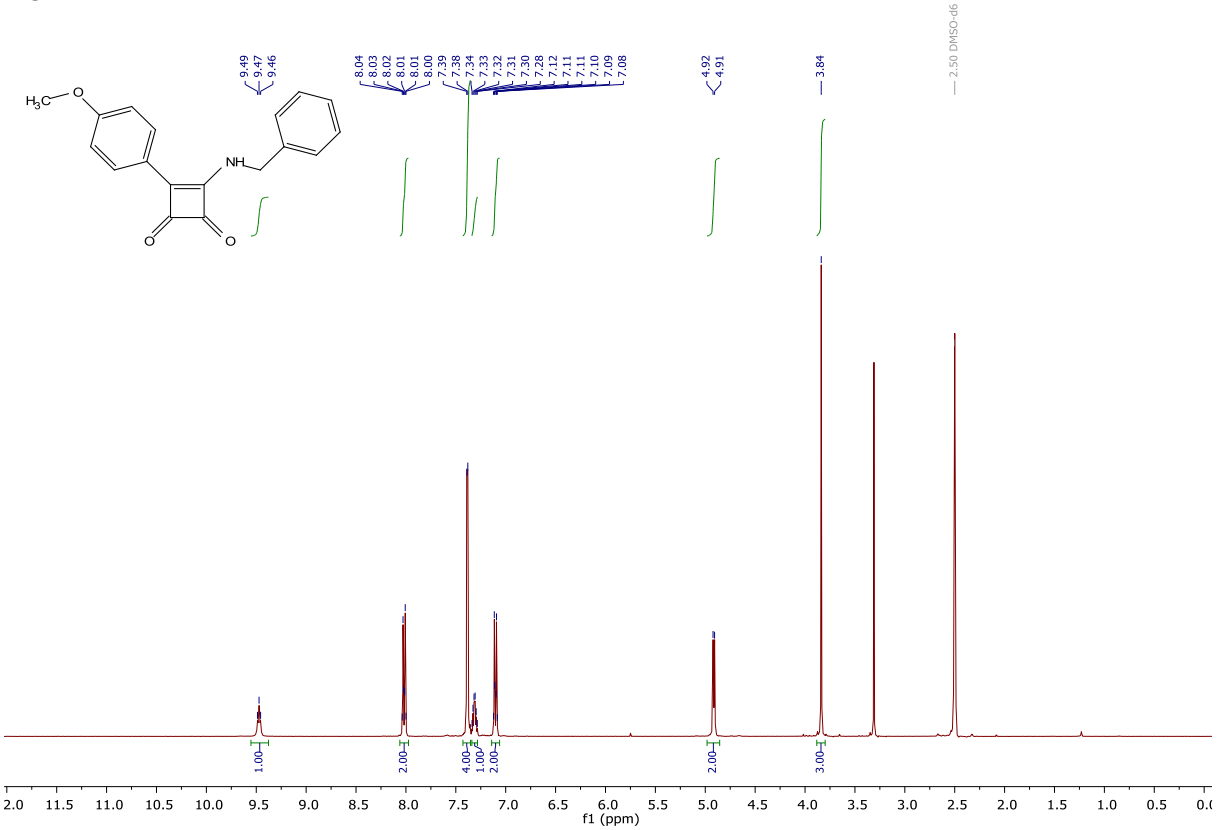

Fig S8. *^{13}C NMR spectra of 3-(benzylamino)-4-(4-methoxyphenyl)cyclobut-3-ene-1,2-dione* ***6b***

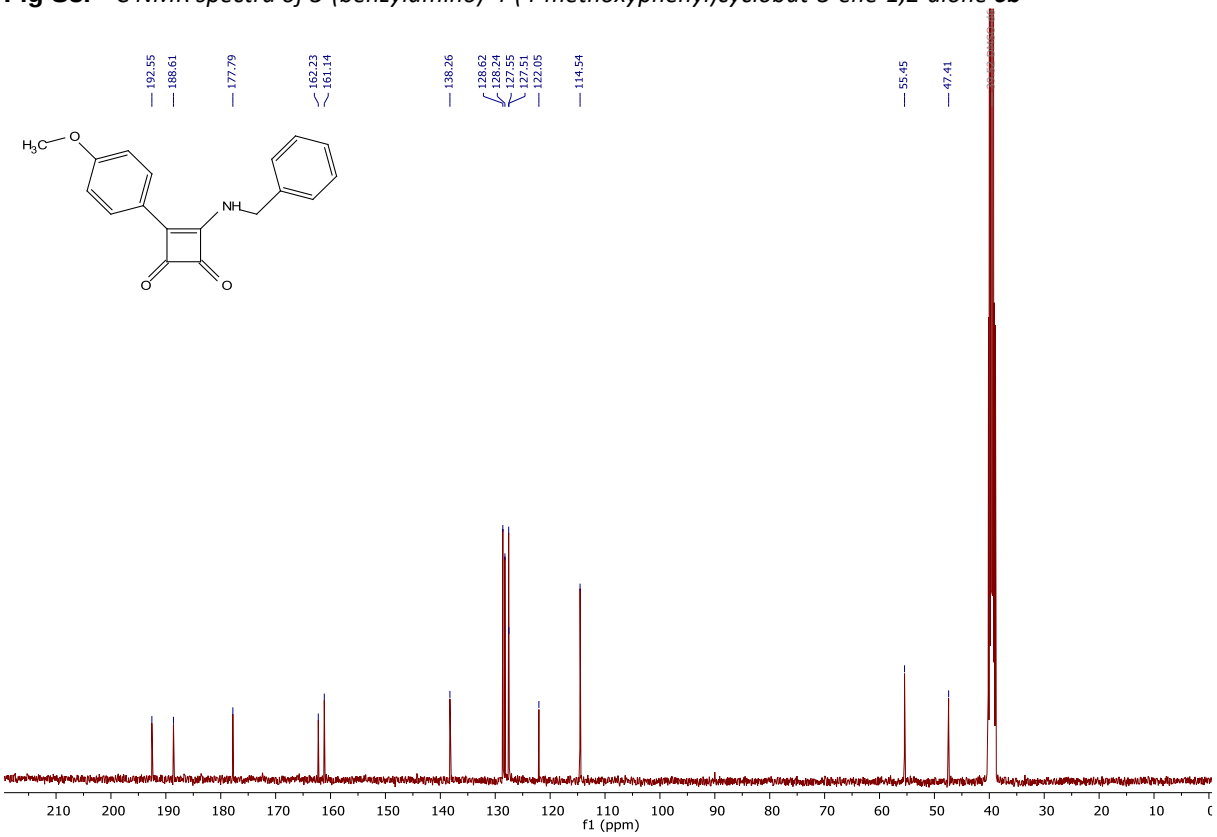

Fig S9. *^{1}H NMR spectra of 3-(benzylamino)-4-(4-(methylthio)phenyl)cyclobut-3-ene-1,2-dione* ***6c***

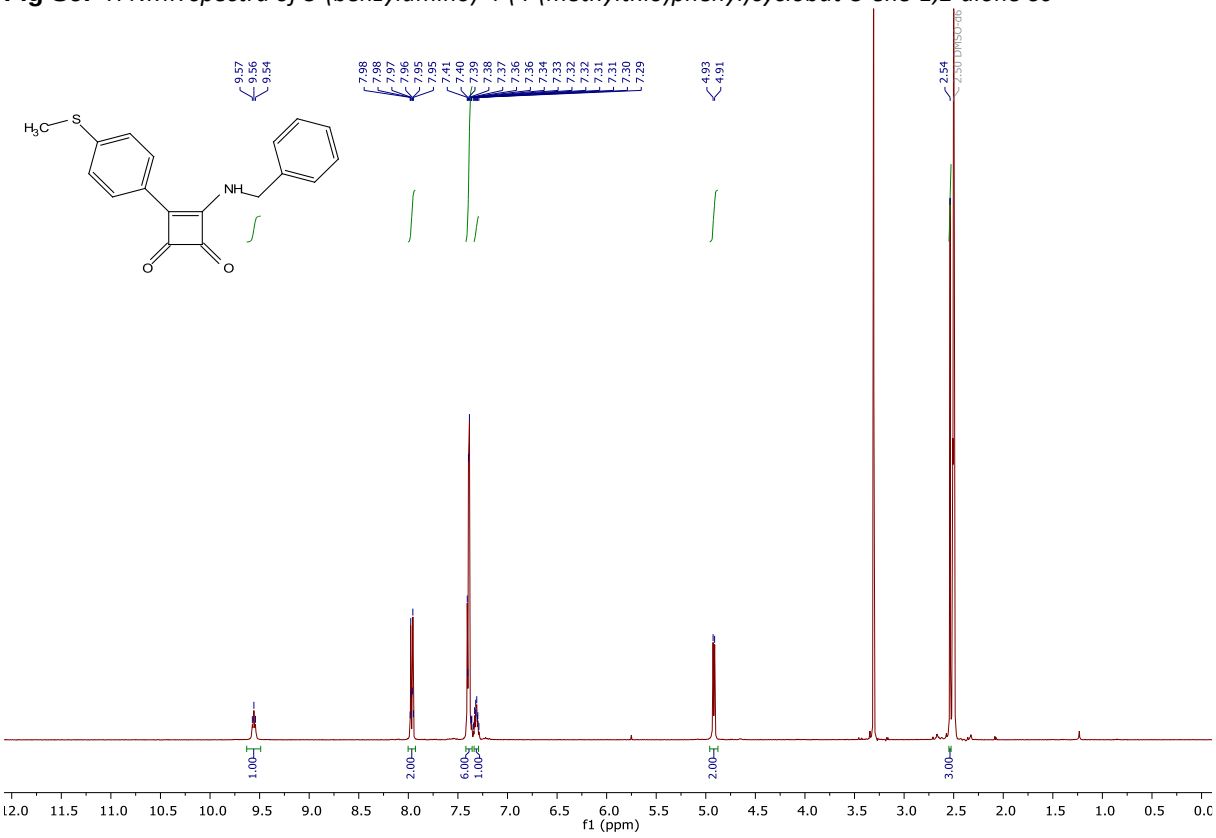

Fig S10. *^{13}C NMR spectra of 3-(benzylamino)-4-(4-(methylthio)phenyl)cyclobut-3-ene-1,2-dione* ***6c***

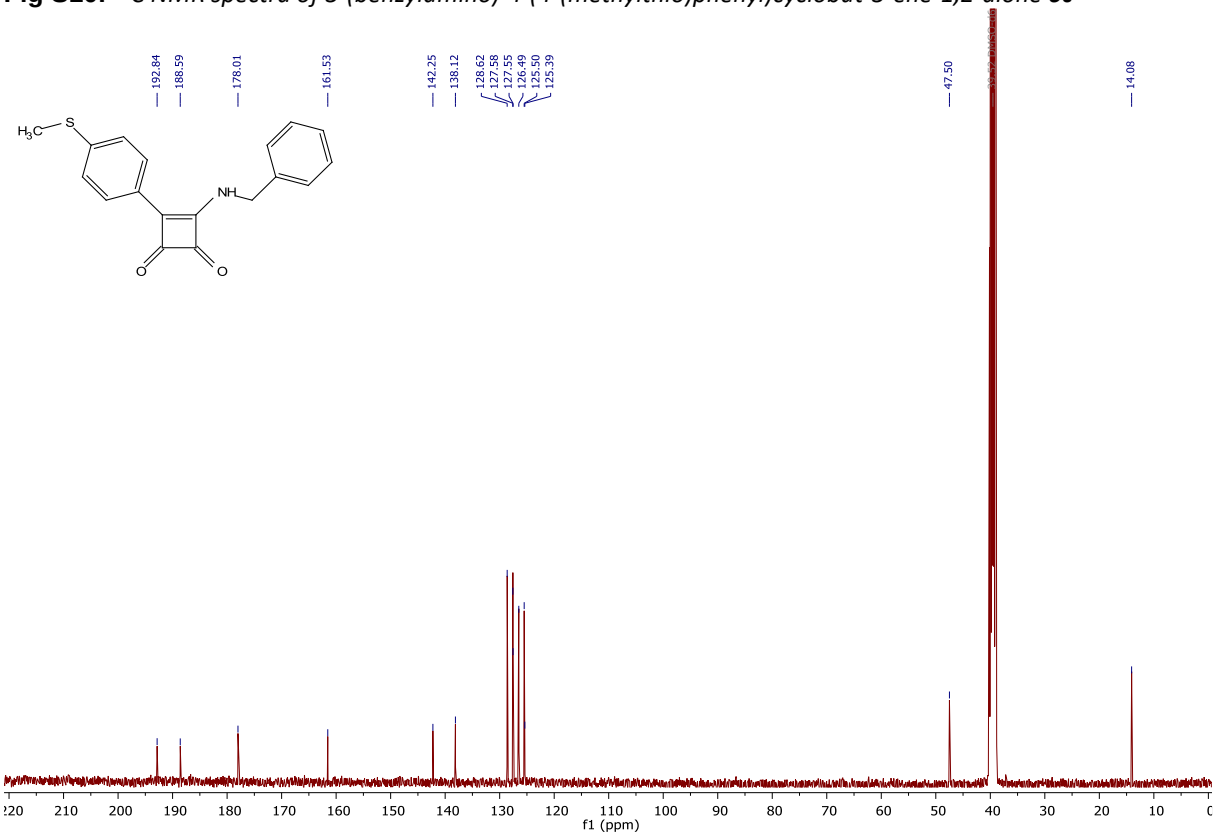

Fig S11. *^{1}H NMR spectra of 3-(benzylamino)-4-phenylcyclobut-3-ene-1,2-dione* ***6d***

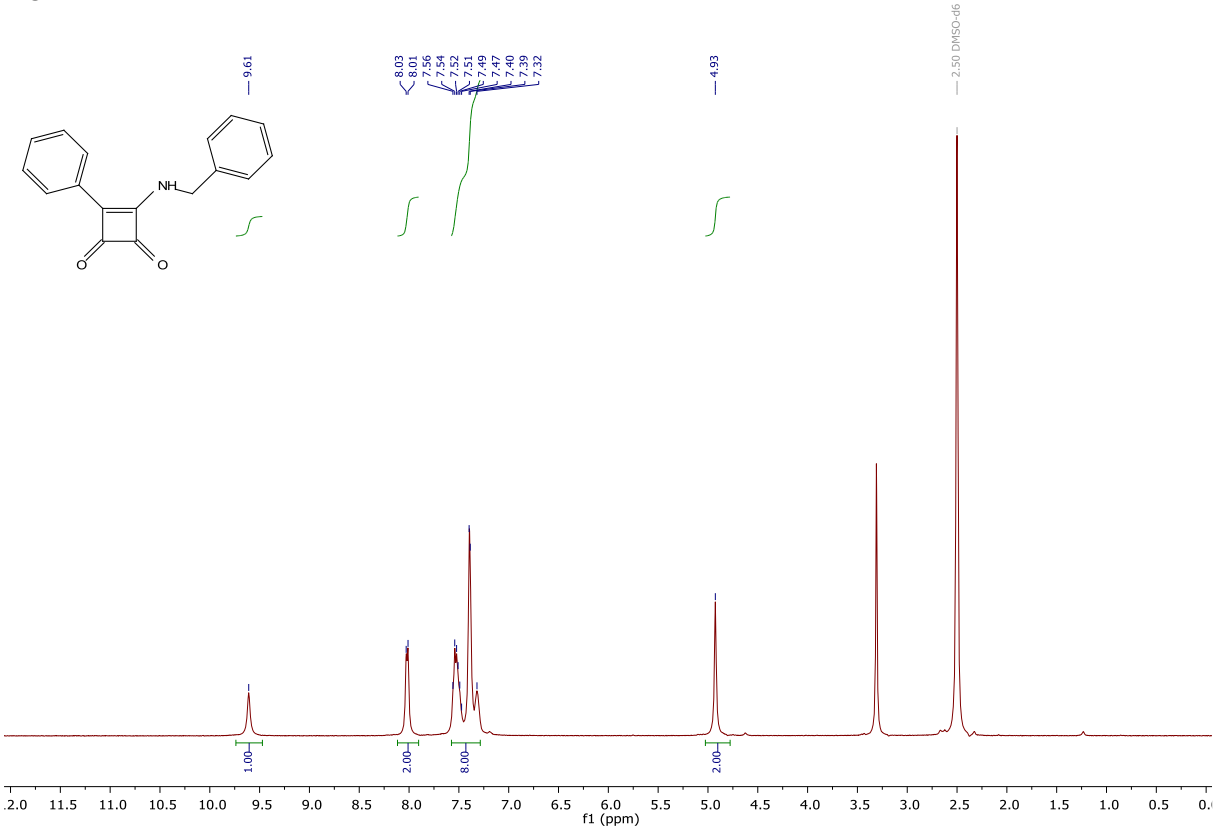

Fig S12. *^{13}C NMR spectra of 3-(benzylamino)-4-phenylcyclobut-3-ene-1,2-dione* ***6d***

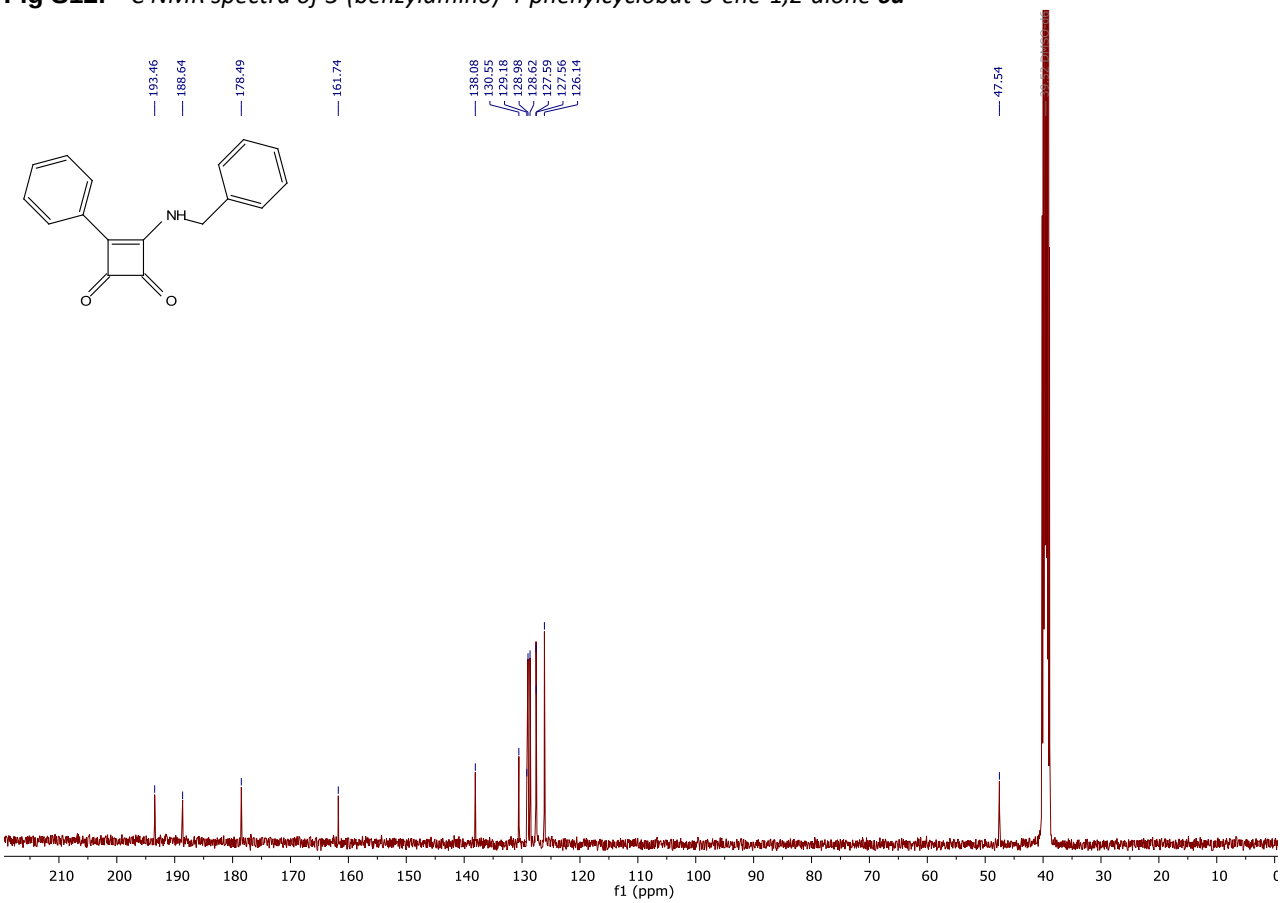

Fig S13. *^{1}H NMR spectra of 3-(benzylamino)-4-(4-nitrophenyl)cyclobut-3-ene-1,2-dione* ***6e***

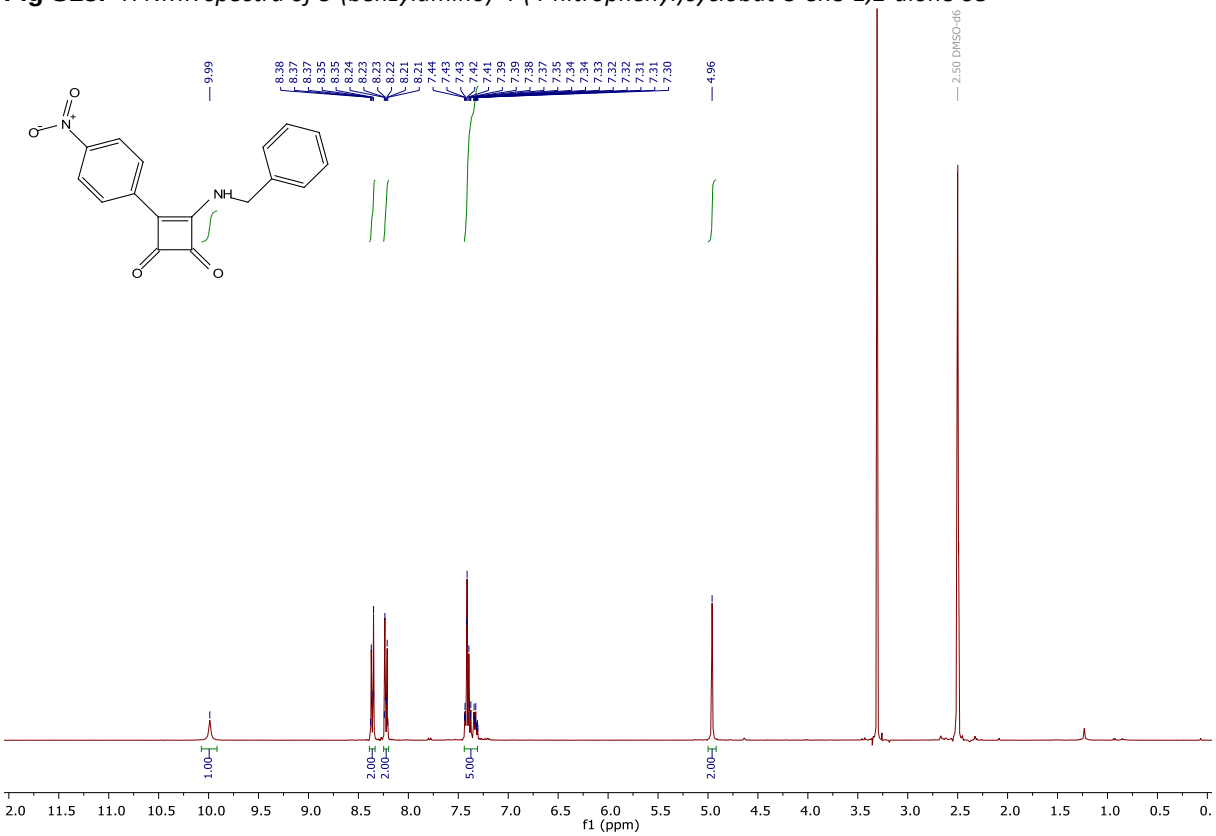

Fig S14. *^{13}C NMR spectra of 3-(benzylamino)-4-(4-nitrophenyl)cyclobut-3-ene-1,2-dione* ***6e***

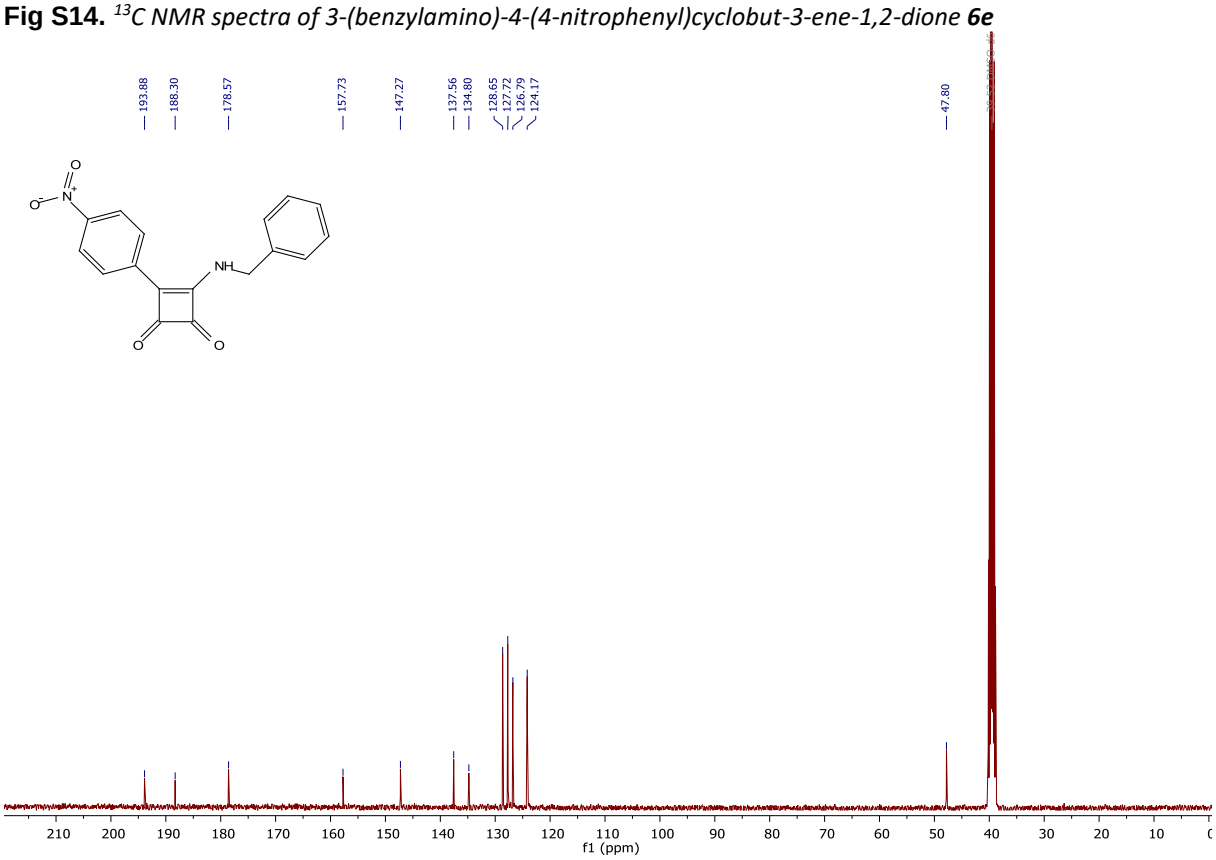

Fig S15. *^{1}H NMR spectra of 3-(benzylamino)-4-(4-(trifluoromethyl)phenyl)cyclobut-3-ene-1,2-dione* ***6f***

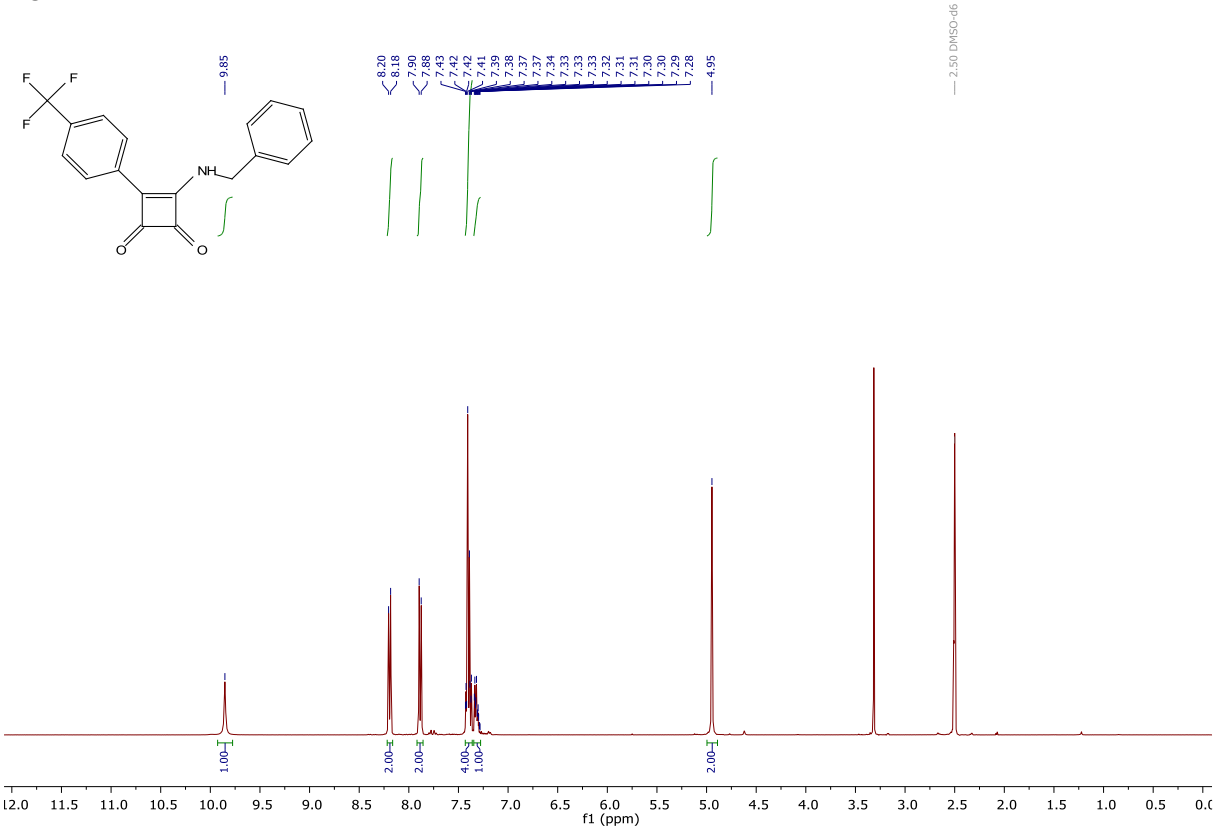

Fig S16. *^{13}C NMR spectra of 3-(benzylamino)-4-(4-(trifluoromethyl)phenyl)cyclobut-3-ene-1,2-dione* ***6f***

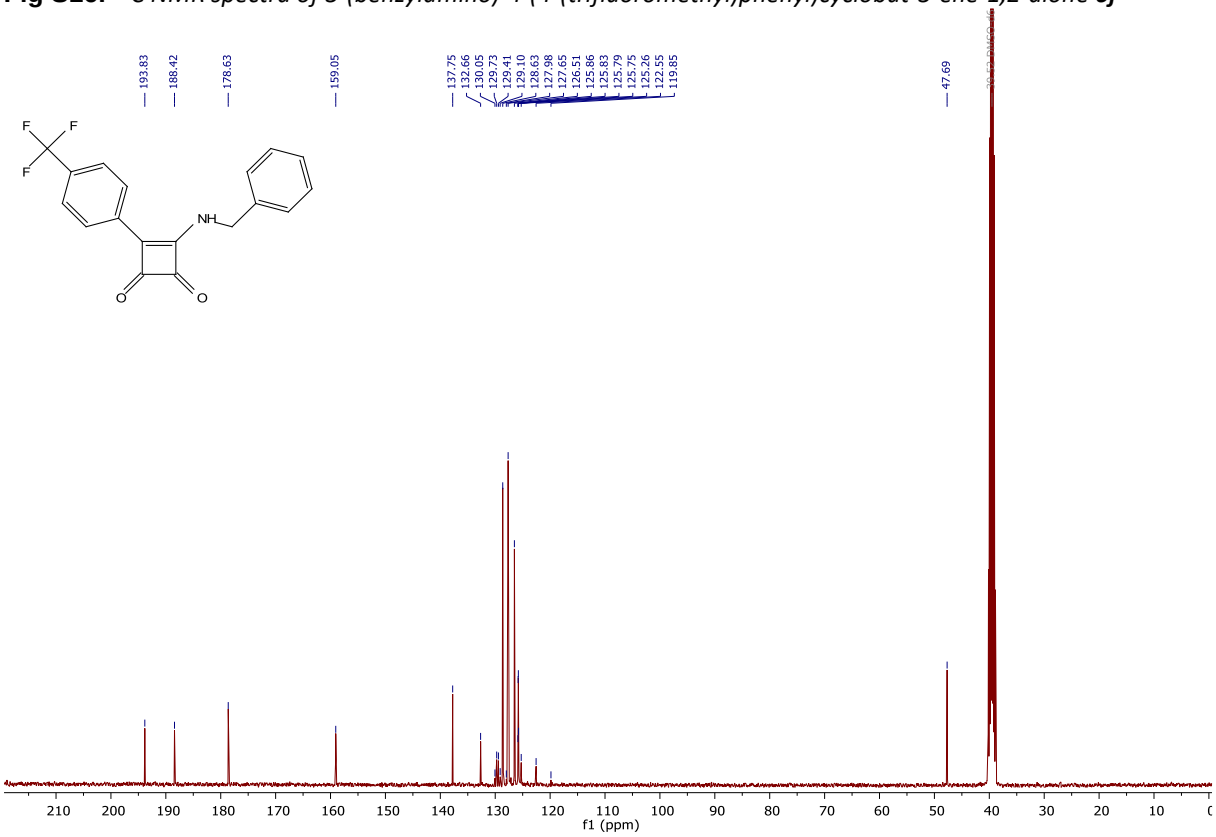

Fig S17. *^{1}H NMR spectra of 4-(2-(benzylamino)-3,4-dioxocyclobut-1-en-1-yl)benzaldehyde* ***6g***

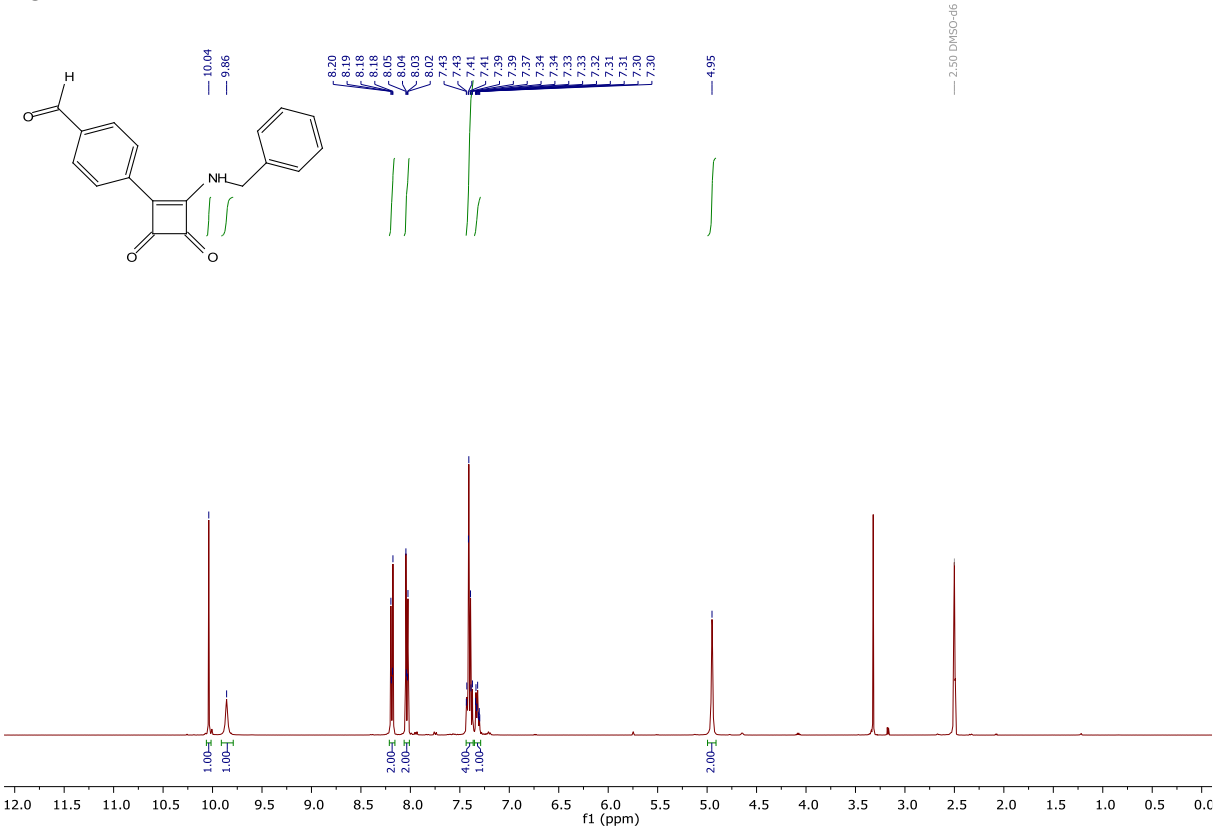

Fig S18. *^{13}C NMR spectra of 4-(2-(benzylamino)-3,4-dioxocyclobut-1-en-1-yl)benzaldehyde* ***6g***

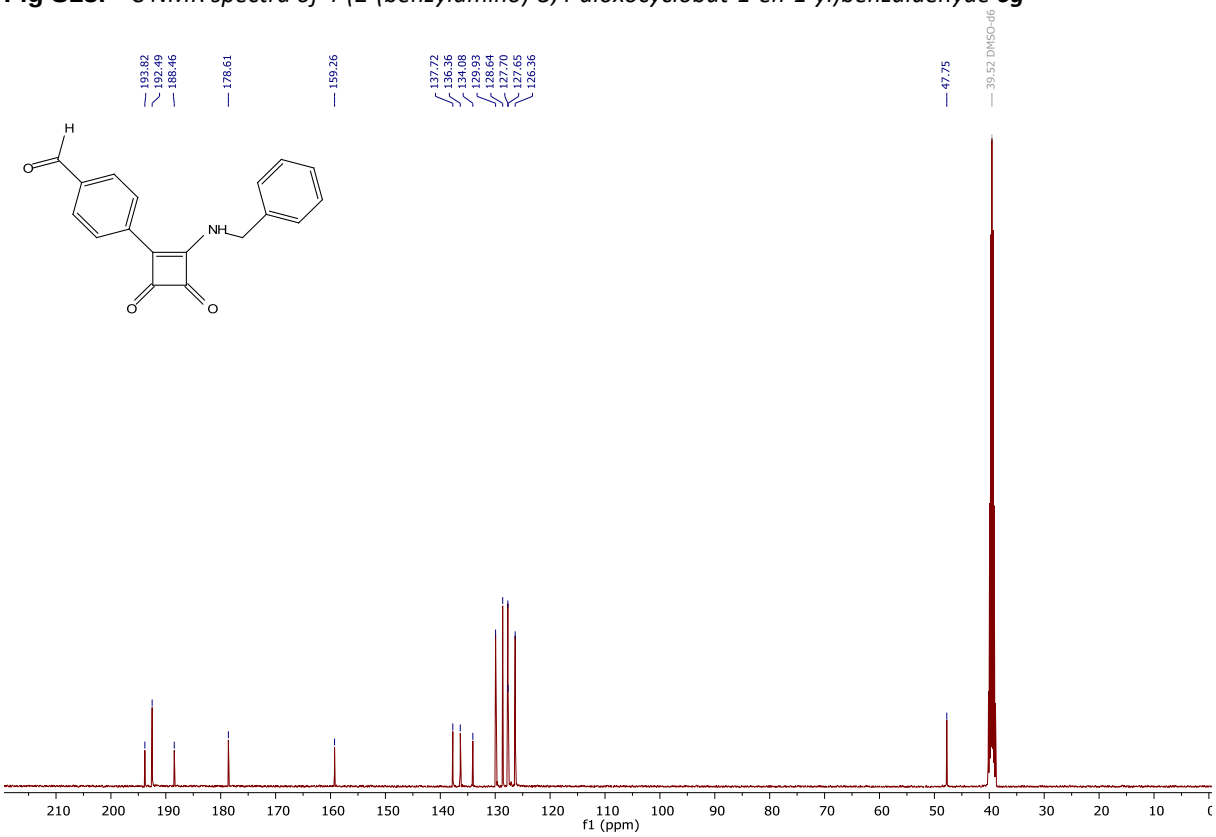

Fig S19. *^{1}H NMR spectra of 3-(benzylamino)-4-(4-bromophenyl)cyclobut-3-ene-1,2-dione* ***6h***

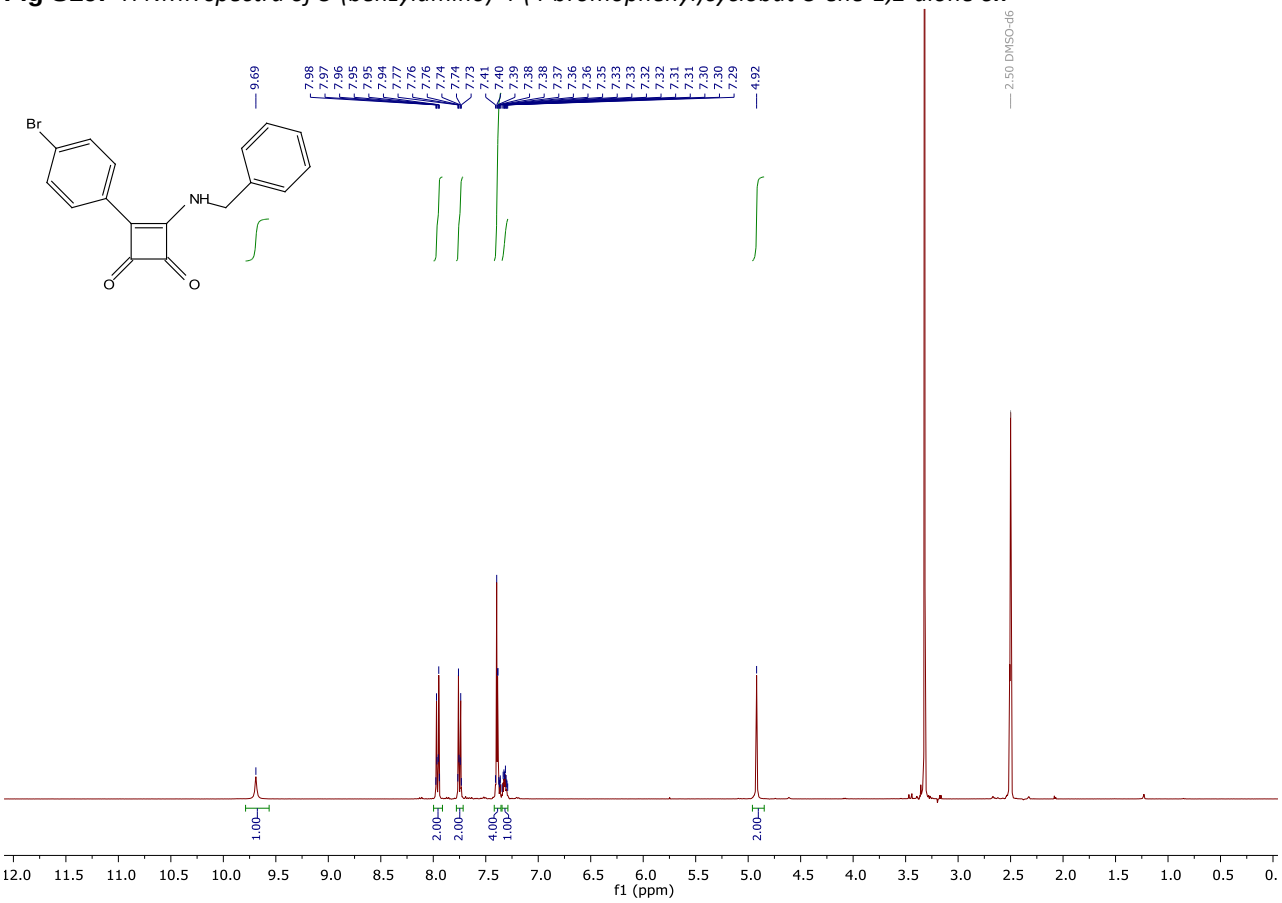

Fig S20. *^{13}C NMR spectra of 3-(benzylamino)-4-(4-bromophenyl)cyclobut-3-ene-1,2-dione* ***6h***

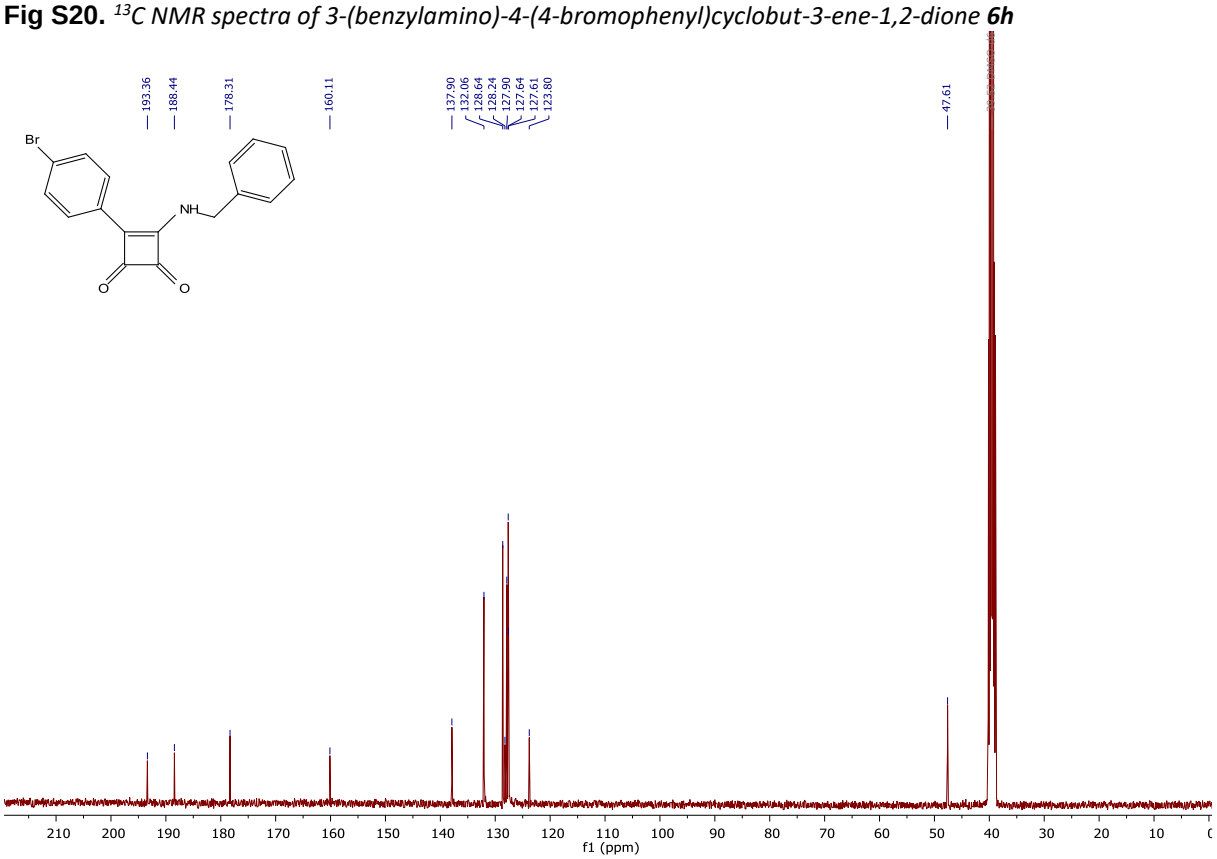

Fig S21. *^{1}H NMR spectra of 3-(benzylamino)-4-(furan-3-yl)cyclobut-3-ene-1,2-dione* ***6i***

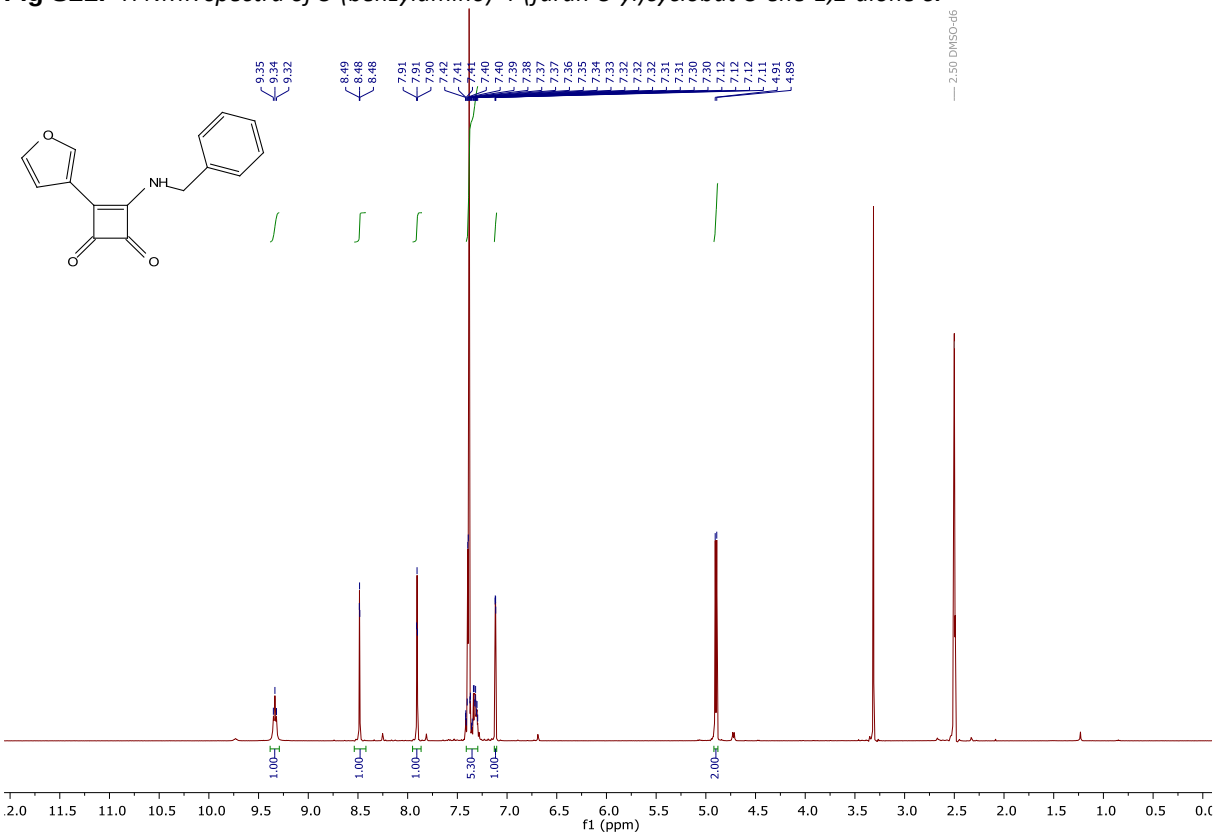

Fig S22. *^{13}C NMR spectra of 3-(benzylamino)-4-(furan-3-yl)cyclobut-3-ene-1,2-dione* ***6i***

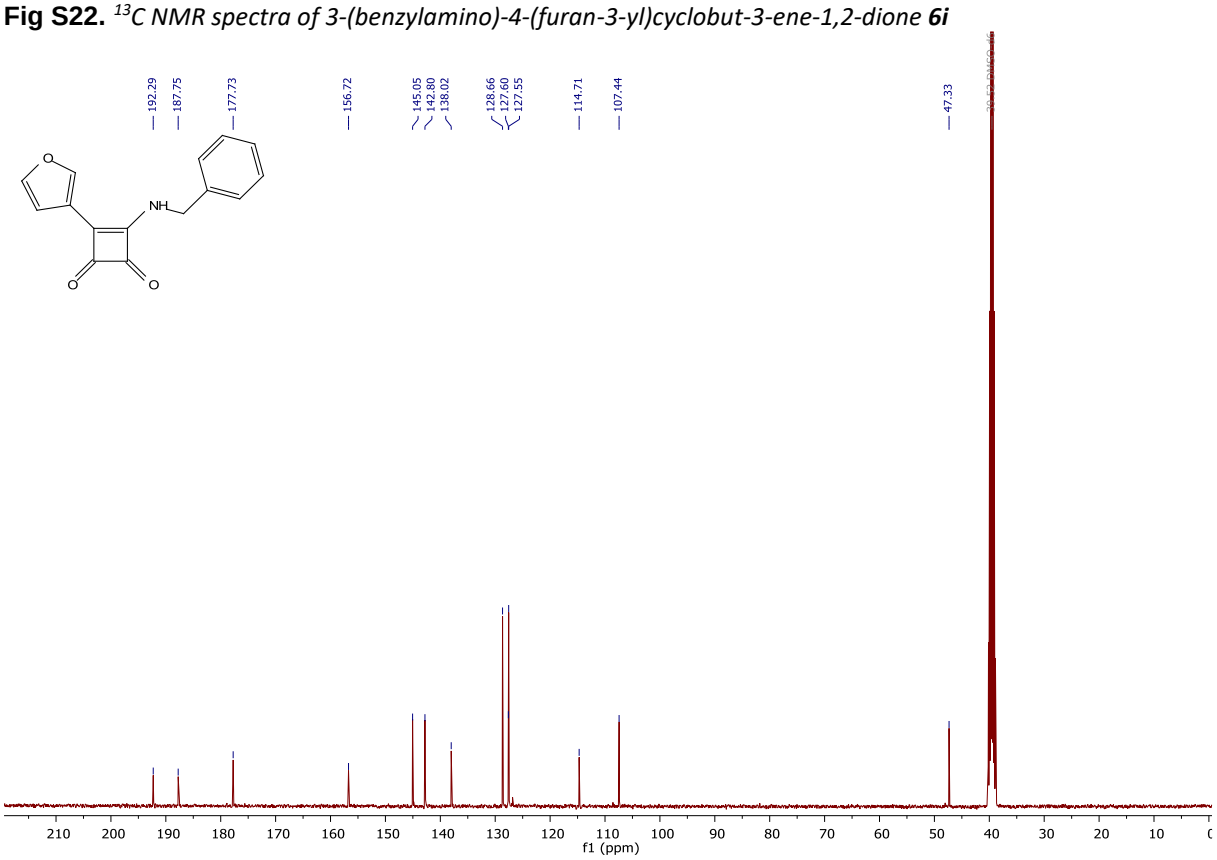

Fig S23. *^{1}H NMR spectra of 3-(benzylamino)-4-(thiophen-3-yl)cyclobut-3-ene-1,2-dione* ***6k***

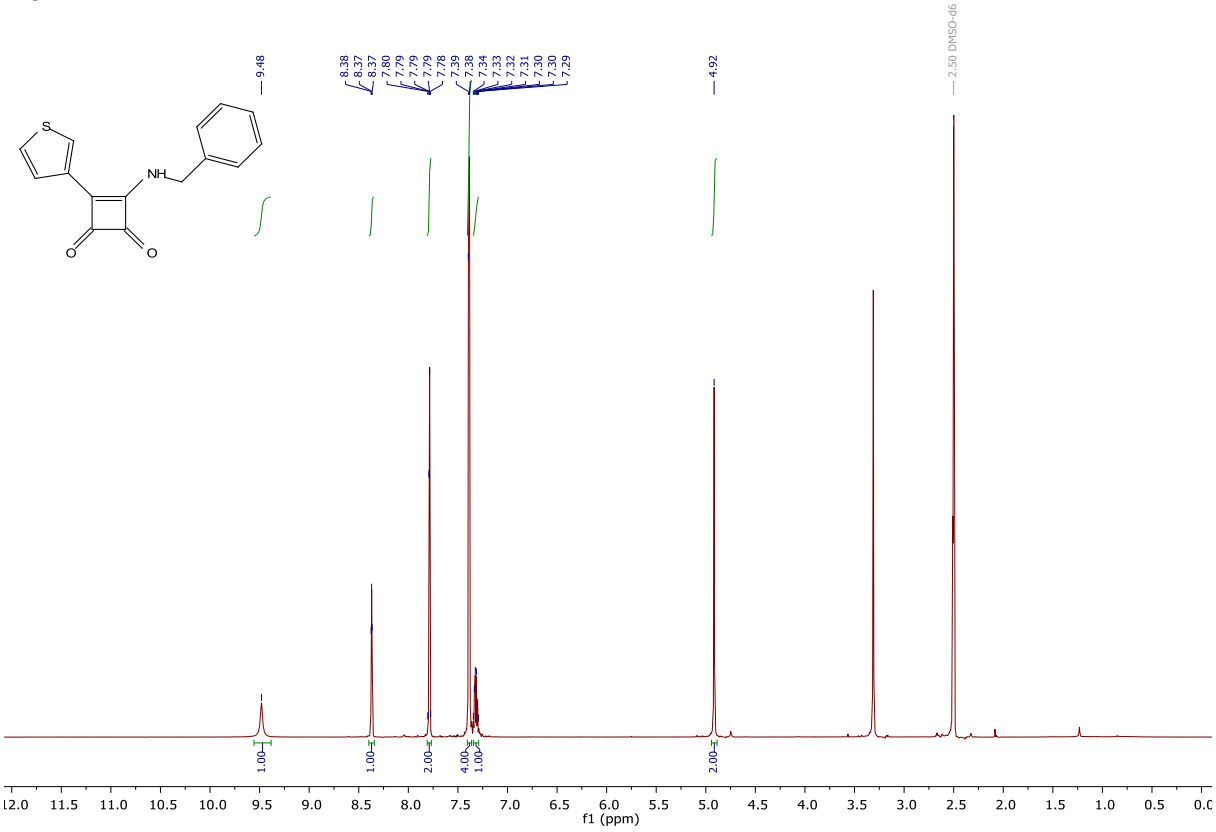

Fig S24. *^{13}C NMR spectra of 3-(benzylamino)-4-(thiophen-3-yl)cyclobut-3-ene-1,2-dione* ***6k***

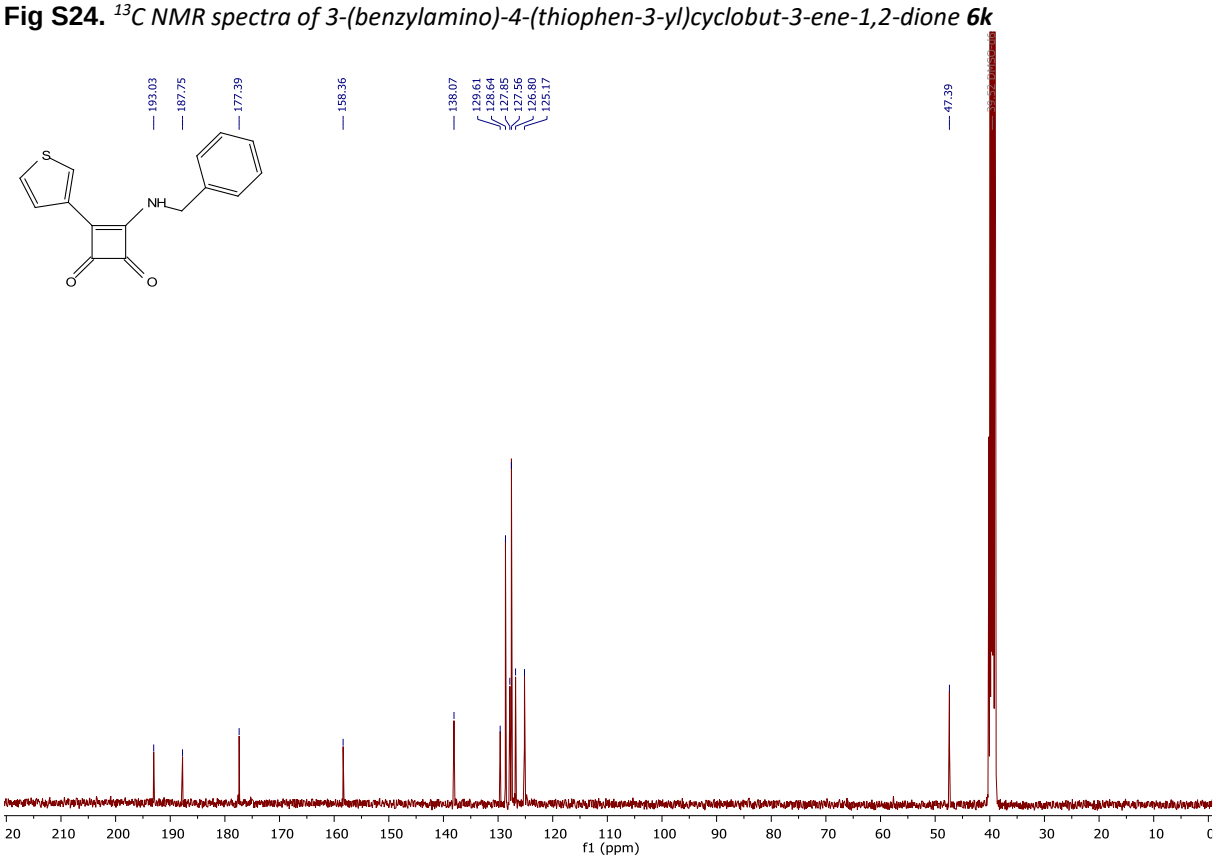

Fig S25. *^{1}H NMR spectra of 3-(benzylamino)-4-(thiophen-2-yl)cyclobut-3-ene-1,2-dione* ***6l***

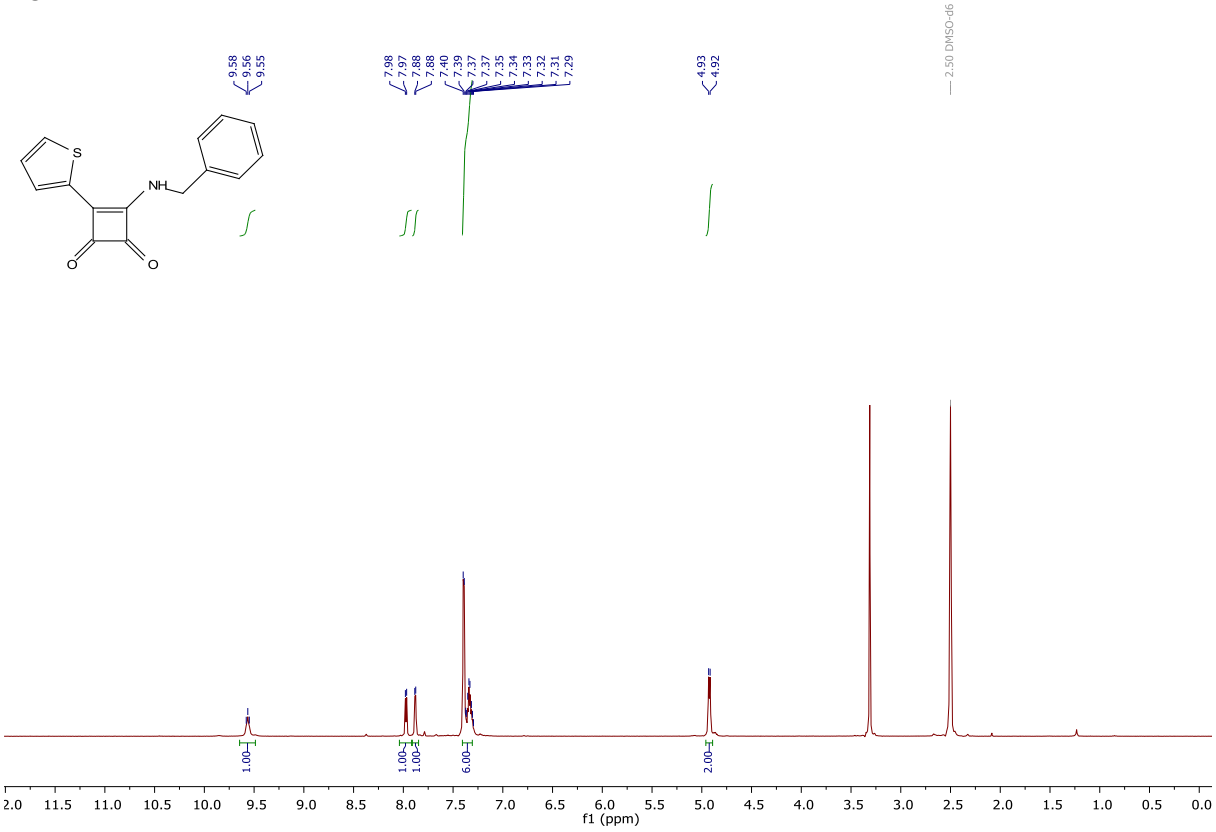

Fig S26. *^{13}C NMR spectra of 3-(benzylamino)-4-(thiophen-2-yl)cyclobut-3-ene-1,2-dione* ***6l***

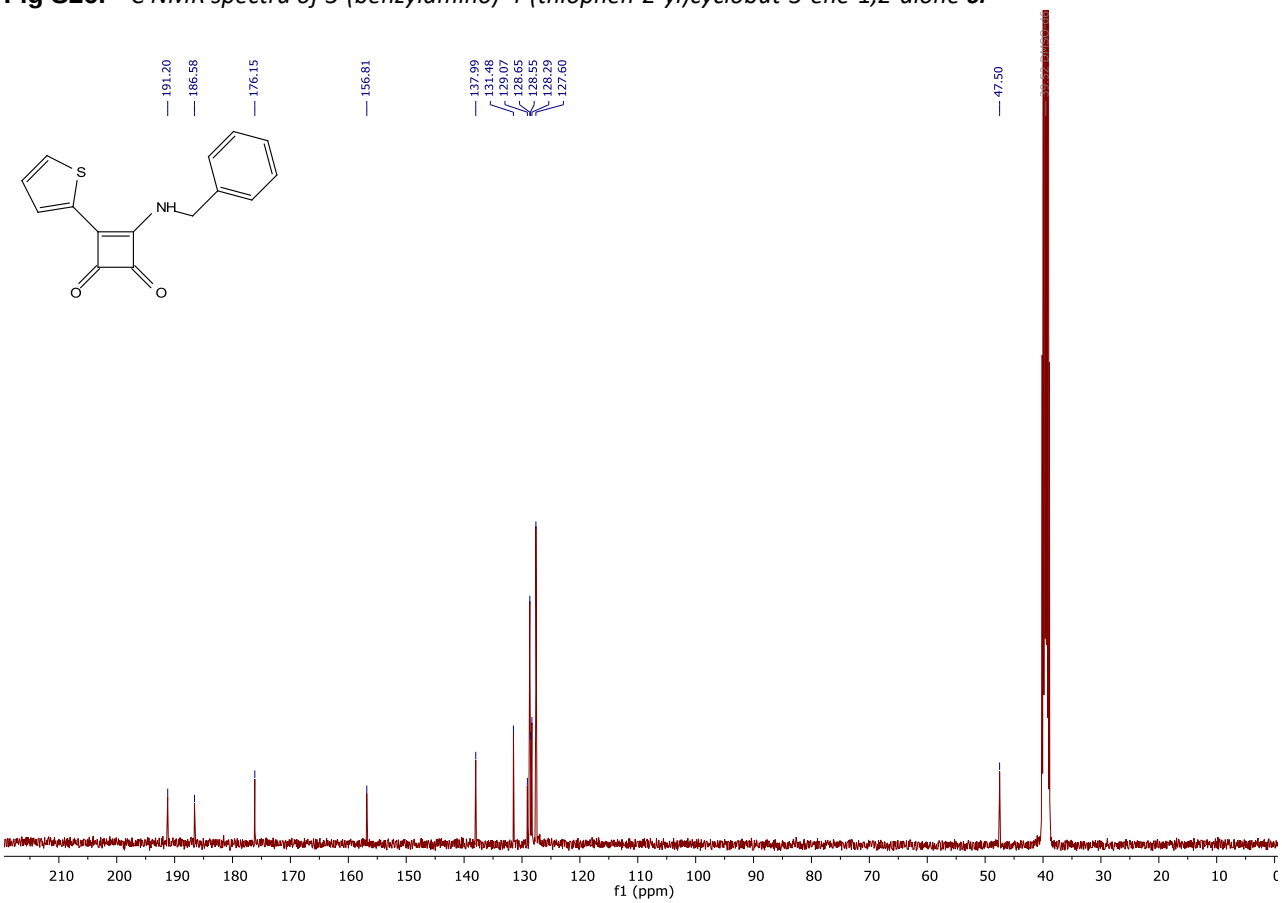

Fig S27. *^{1}H NMR spectra of (E)-3-(benzylamino)-4-styrylcyclobut-3-ene-1,2-dione* ***6m***

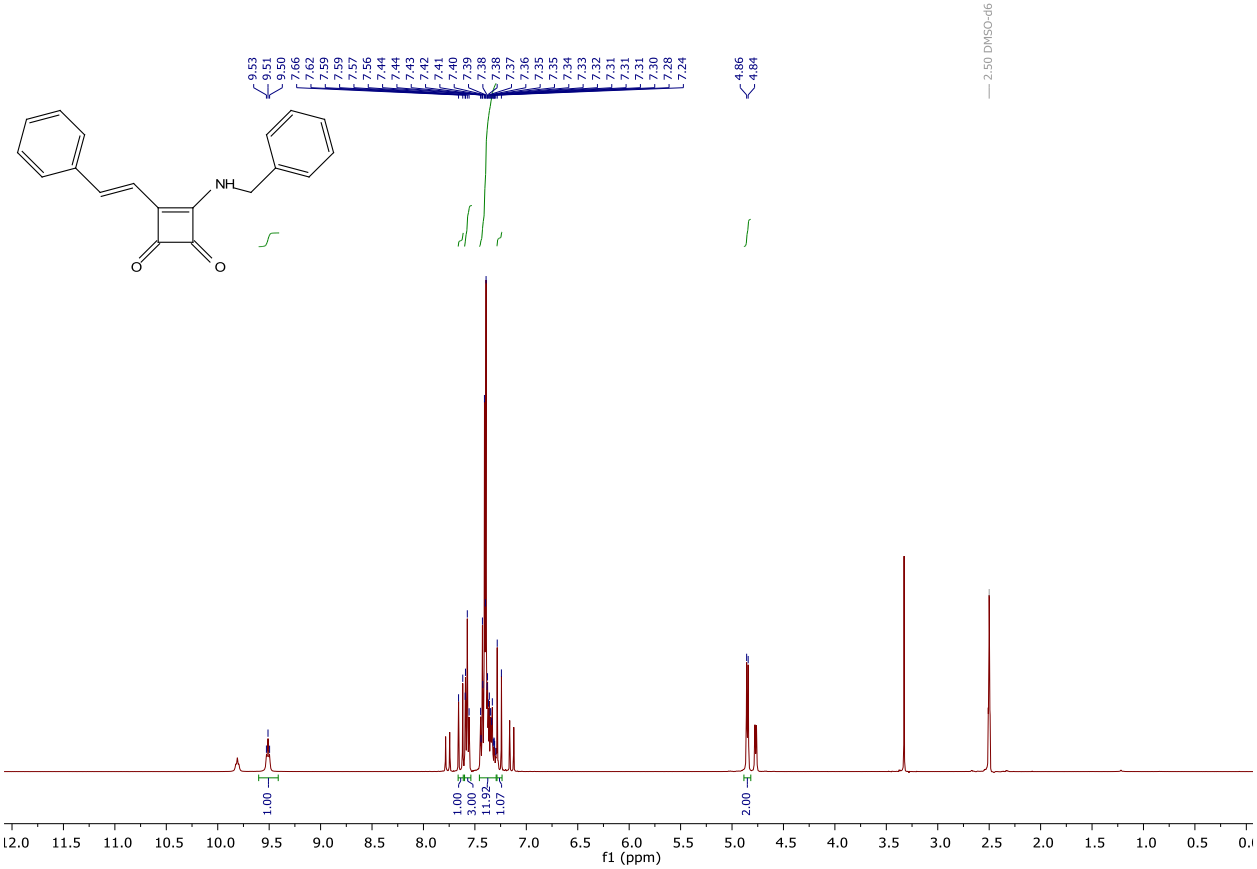

Fig S28. *^{13}C NMR spectra of (E)-3-(benzylamino)-4-styrylcyclobut-3-ene-1,2-dione* ***6m***

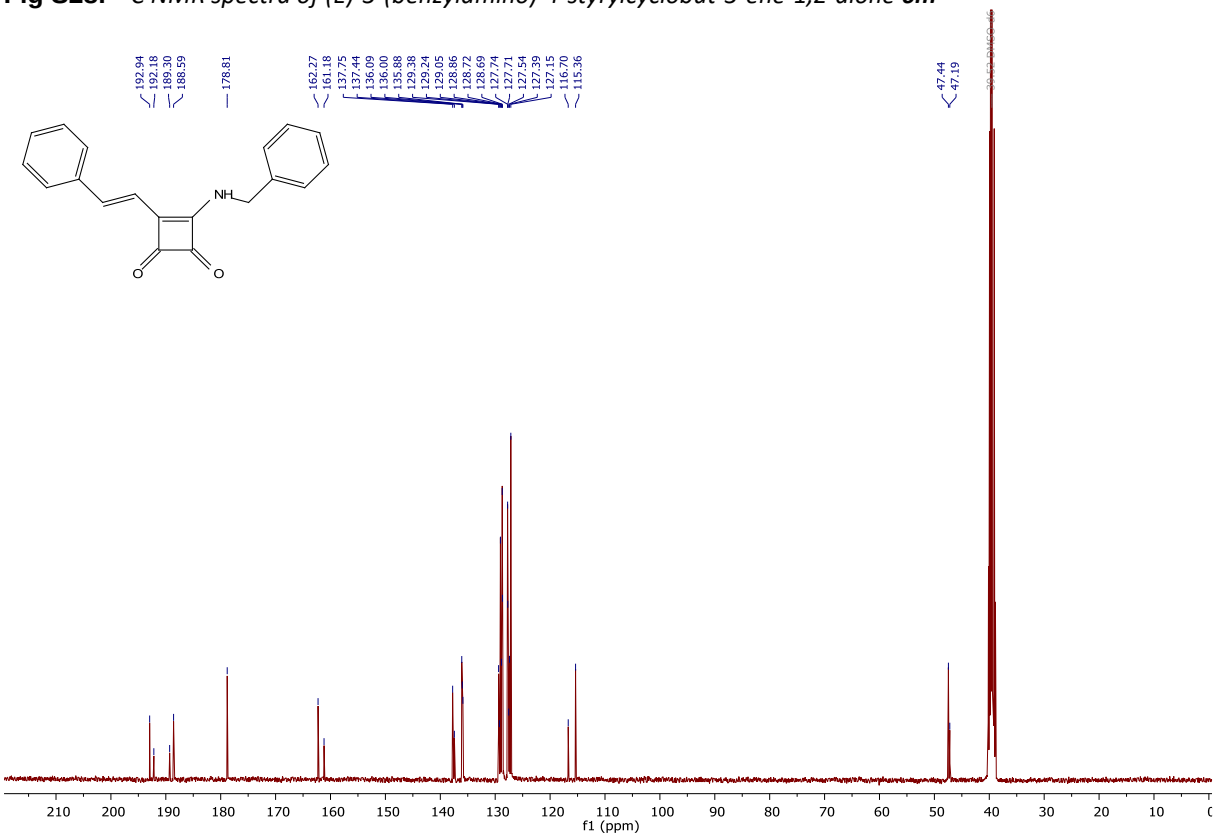

Fig S29. *^{1}H NMR spectra of 3-(benzylamino)-4-(2,6-dimethylphenyl)cyclobut-3-ene-1,2-dione* ***6n***

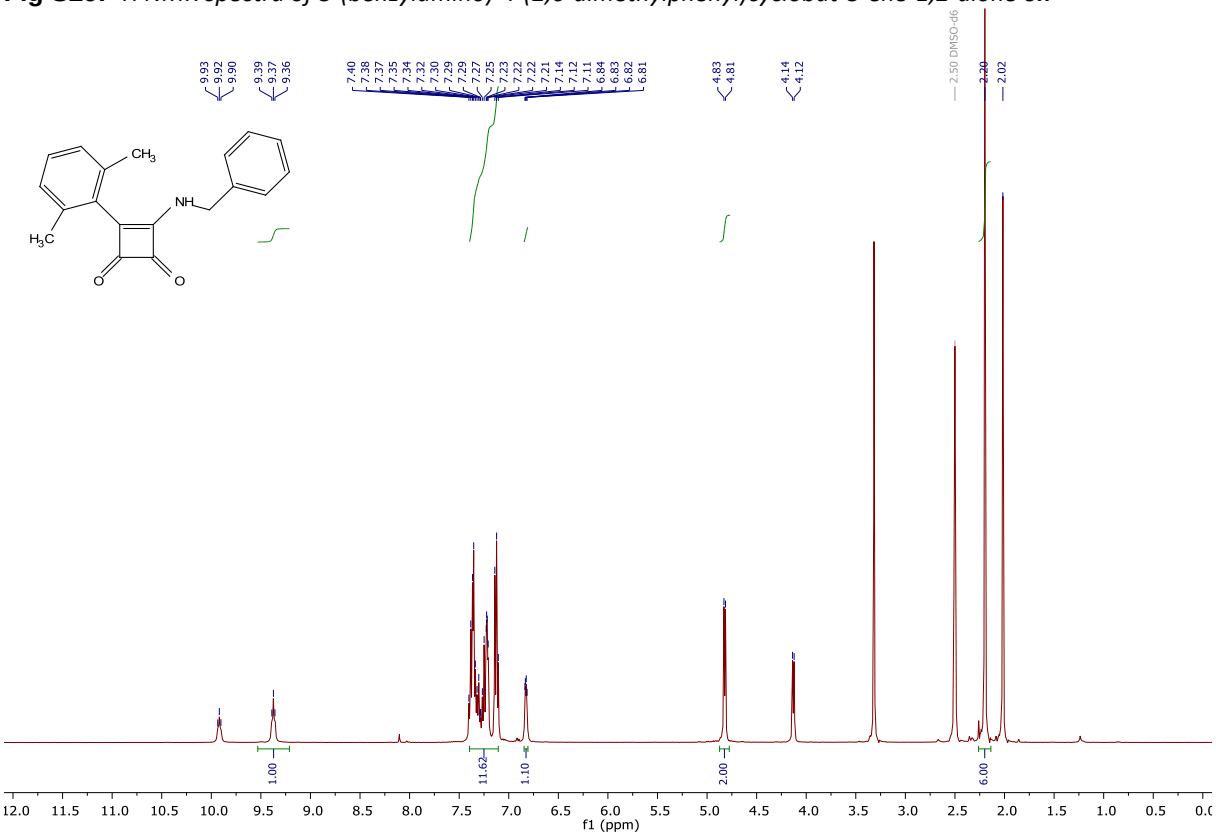

Fig S30. *^{13}C NMR spectra of 3-(benzylamino)-4-(2,6-dimethylphenyl)cyclobut-3-ene-1,2-dione* ***6n***

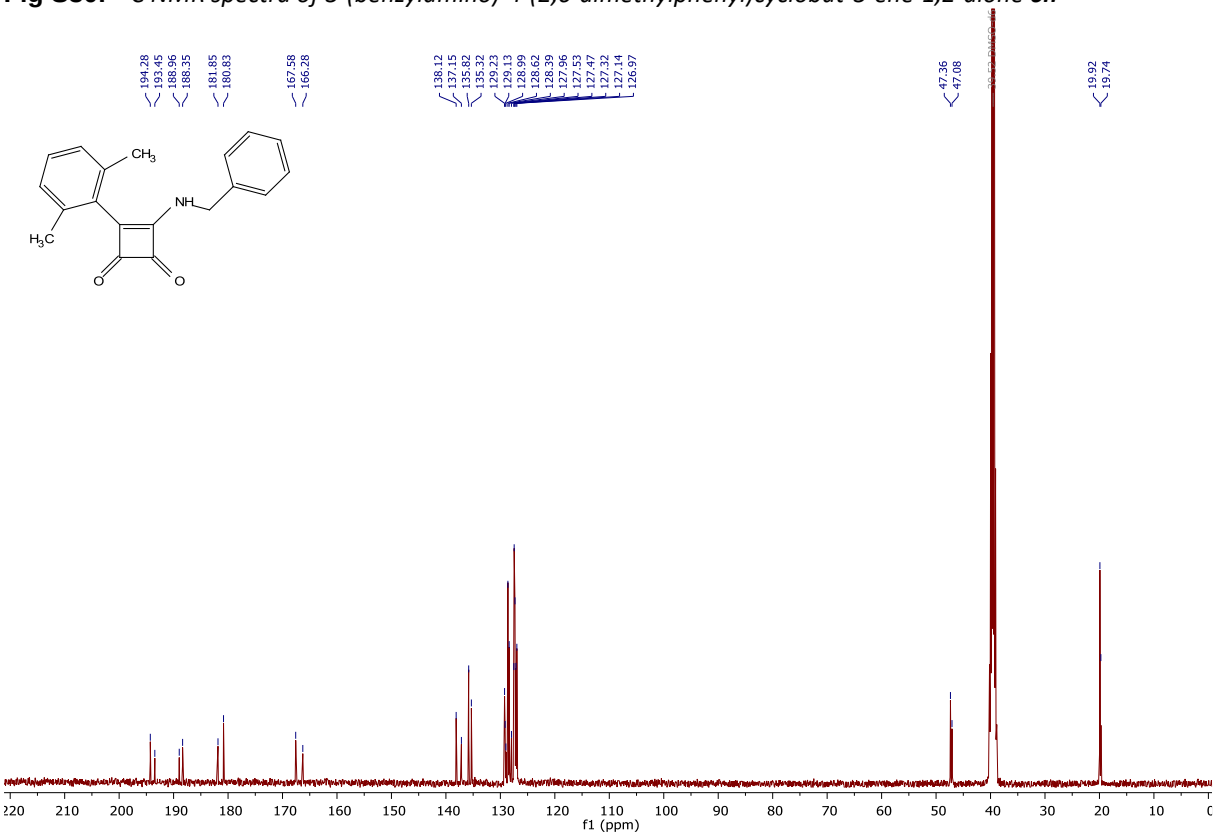

Fig S31. *^{1}H NMR spectra of 3-(benzylamino)-4-(6-ethoxynaphthalen-2-yl)cyclobut-3-ene-1,2-dione* ***6o***

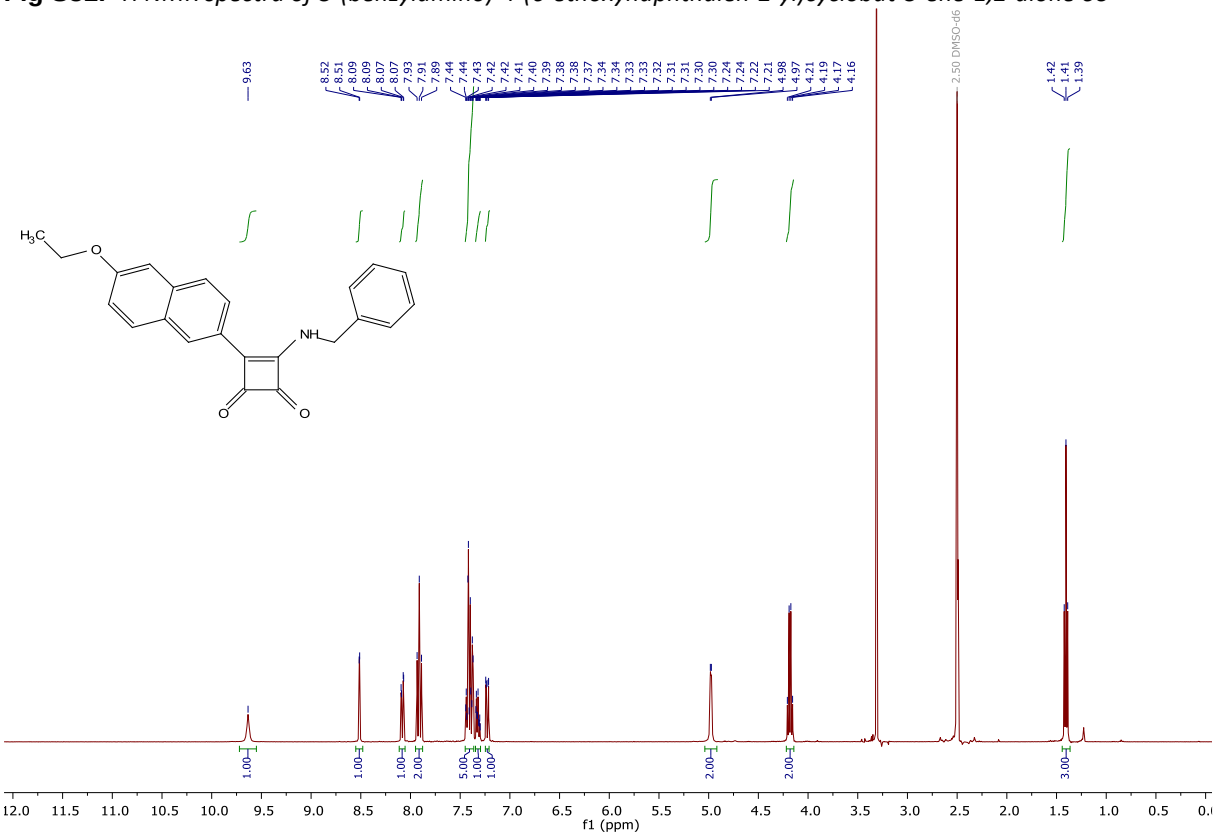

Fig S32. *^{13}C NMR spectra of 3-(benzylamino)-4-(6-ethoxynaphthalen-2-yl)cyclobut-3-ene-1,2-dione* ***6o***

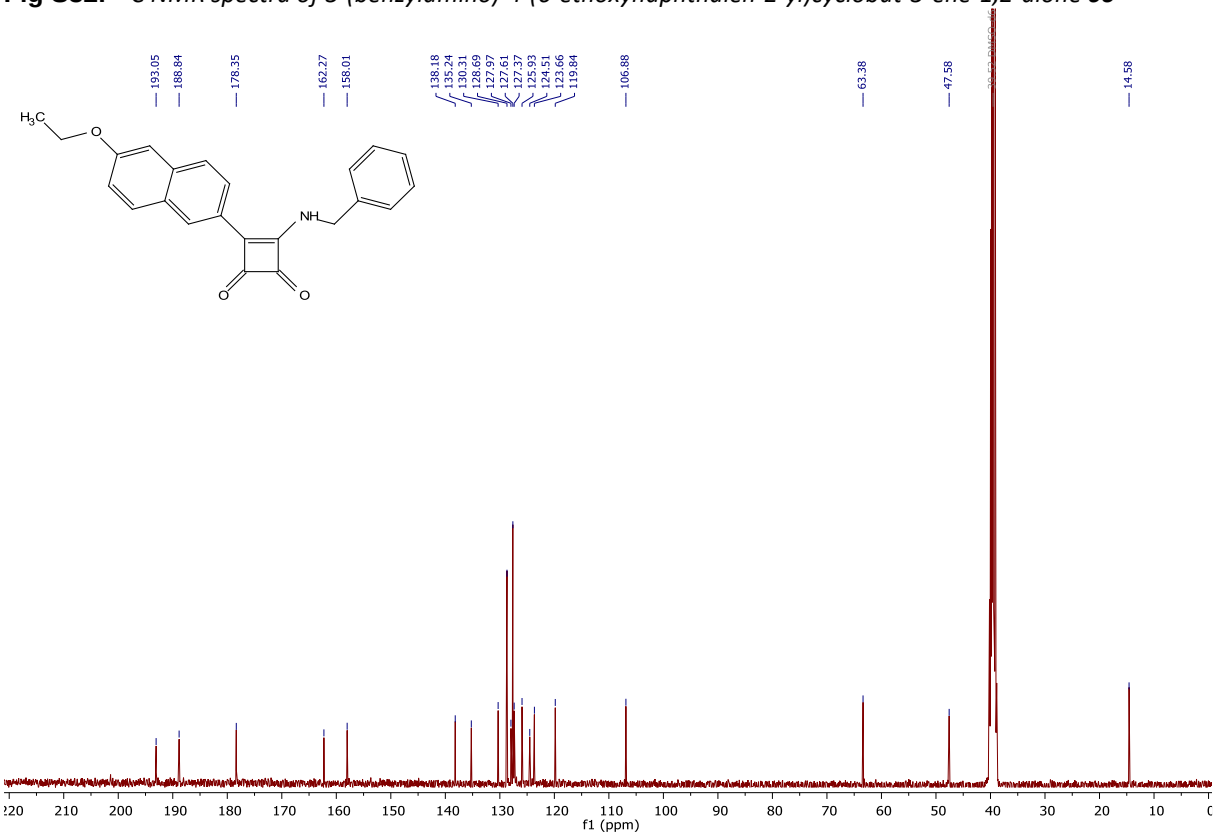

Fig S33. *^{1}H NMR spectra of 3-((pyridin-2-ylmethyl)amino)-4-(p-tolyl)cyclobut-3-ene-1,2-dione* ***6p***

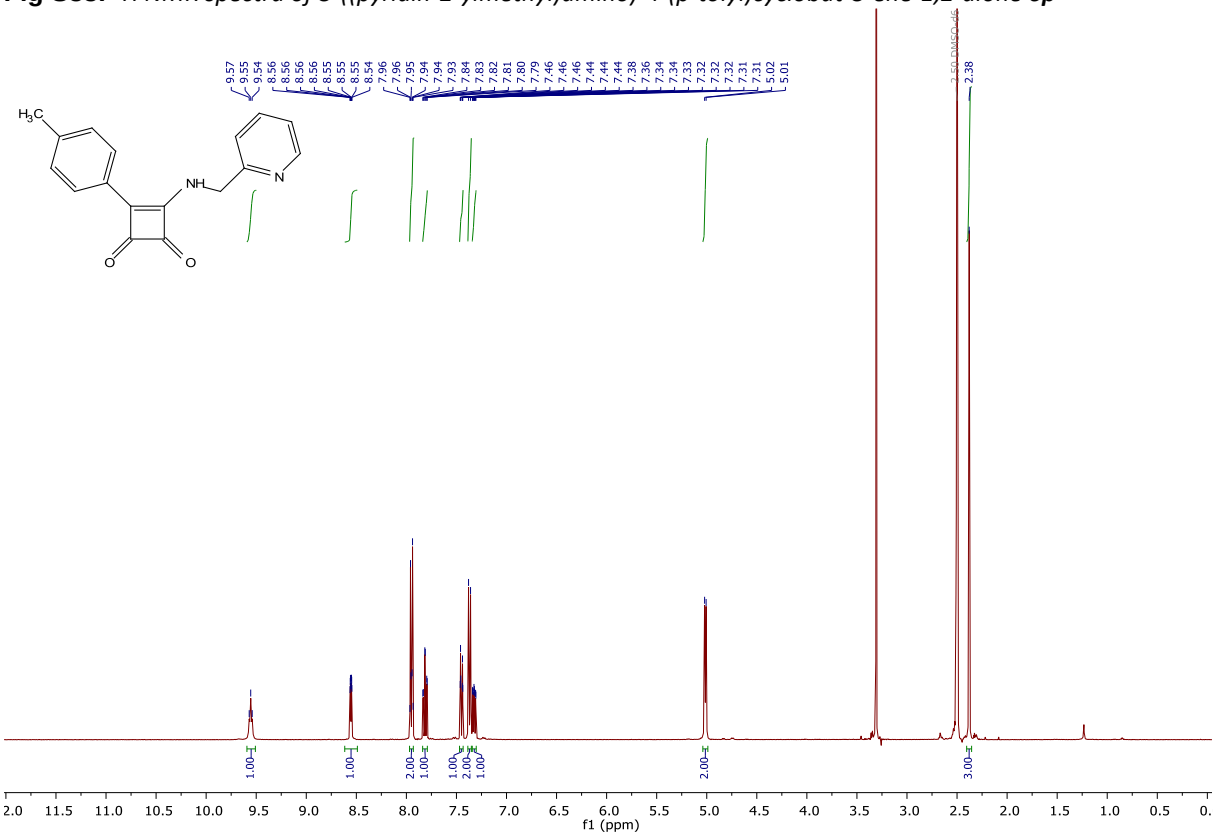

Fig S34. *^{13}C NMR spectra of 3-((pyridin-2-ylmethyl)amino)-4-(p-tolyl)cyclobut-3-ene-1,2-dione* ***6p***

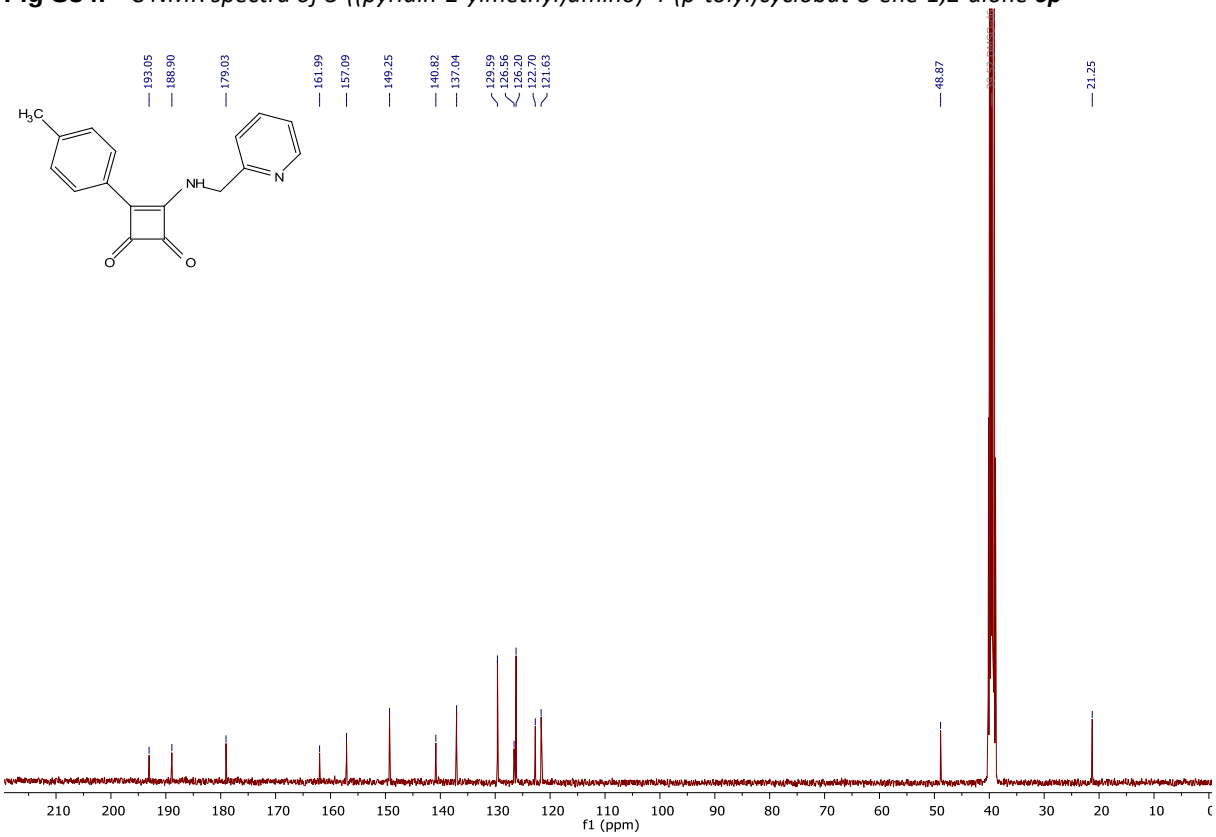

Fig S35. *^{1}H NMR spectra of 3-((4-bromobenzyl)amino)-4-(p-tolyl)cyclobut-3-ene-1,2-dione* ***6q***

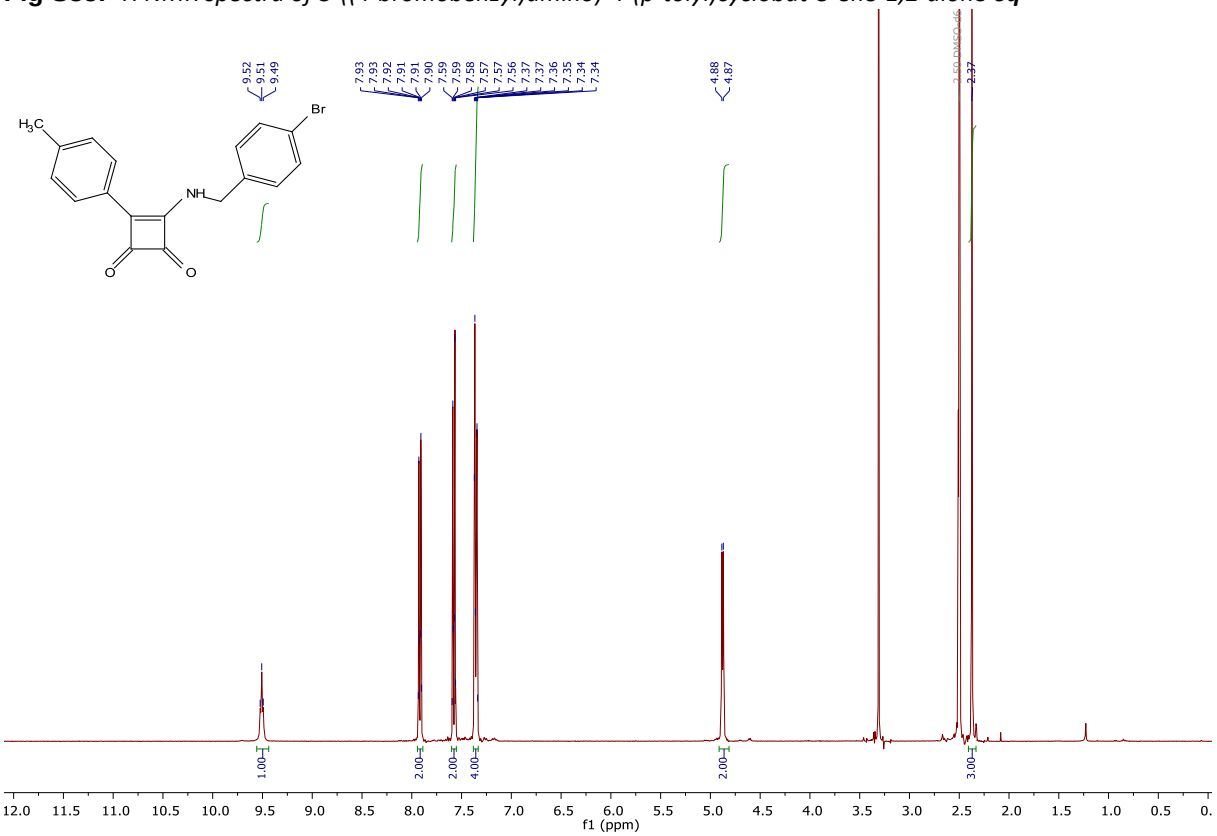

Fig S36. *^{13}C NMR spectra of 3-((4-bromobenzyl)amino)-4-(p-tolyl)cyclobut-3-ene-1,2-dione* ***6q***

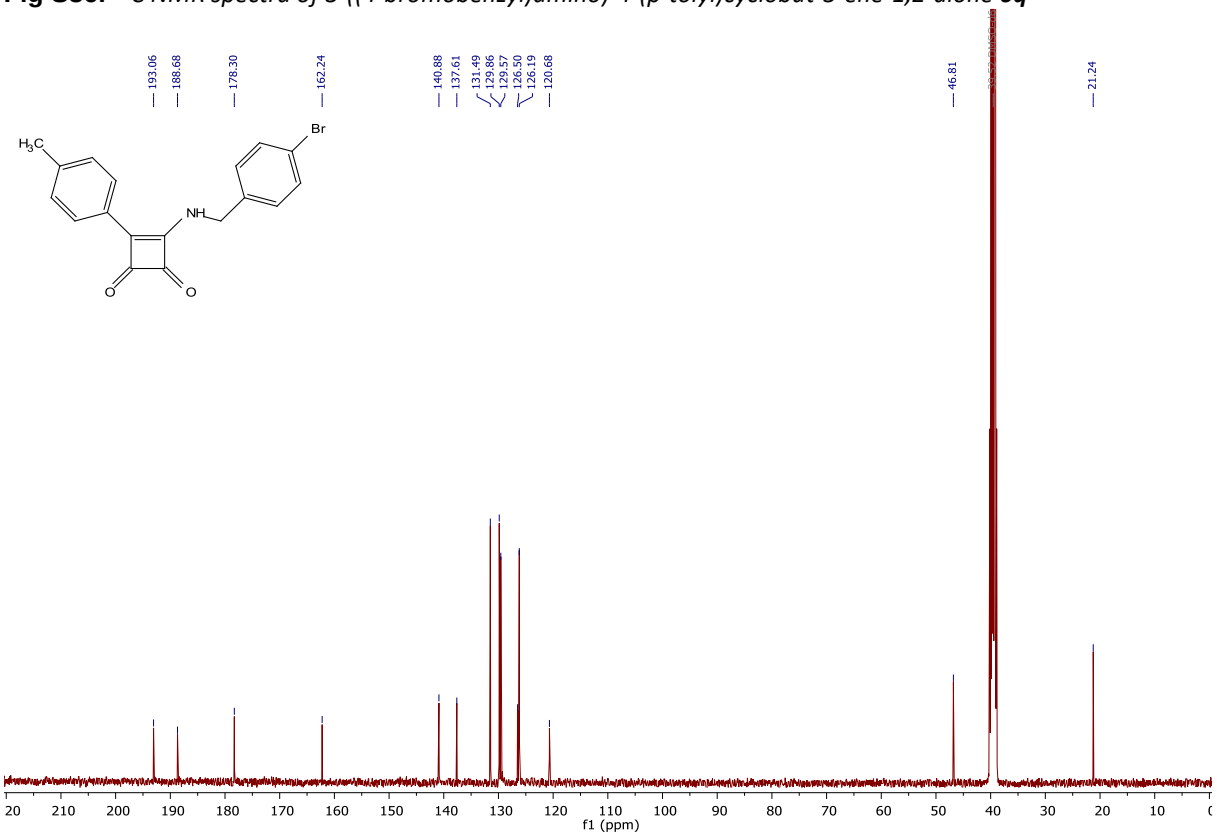

Fig S37. *^{1}H NMR spectra of 3-(propylamino)-4-(p-tolyl)cyclobut-3-ene-1,2-dione* ***6r***

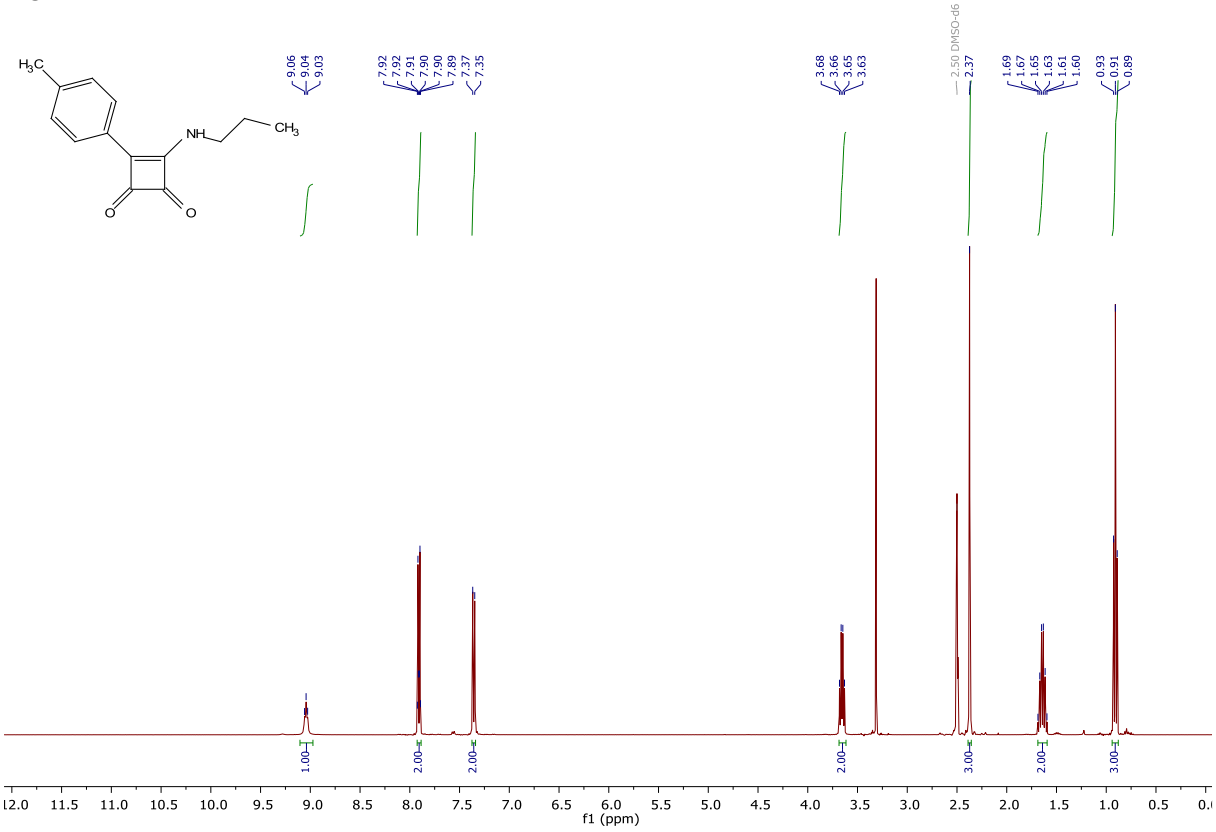

Fig S38. *^{13}C NMR spectra of 3-(propylamino)-4-(p-tolyl)cyclobut-3-ene-1,2-dione* ***6r***

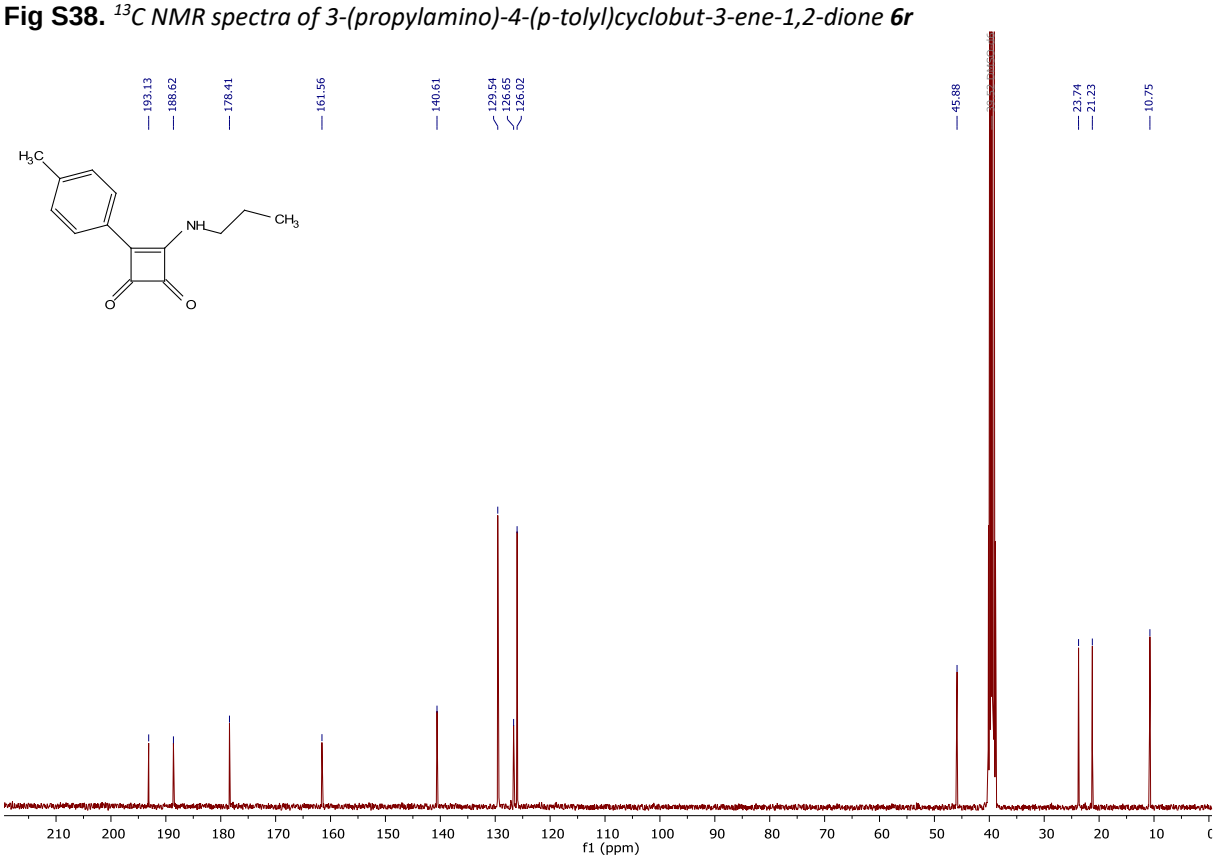

Fig S39. *^{1}H NMR spectra of 3-(cyclohexylamino)-4-(p-tolyl)cyclobut-3-ene-1,2-dione* ***6s***

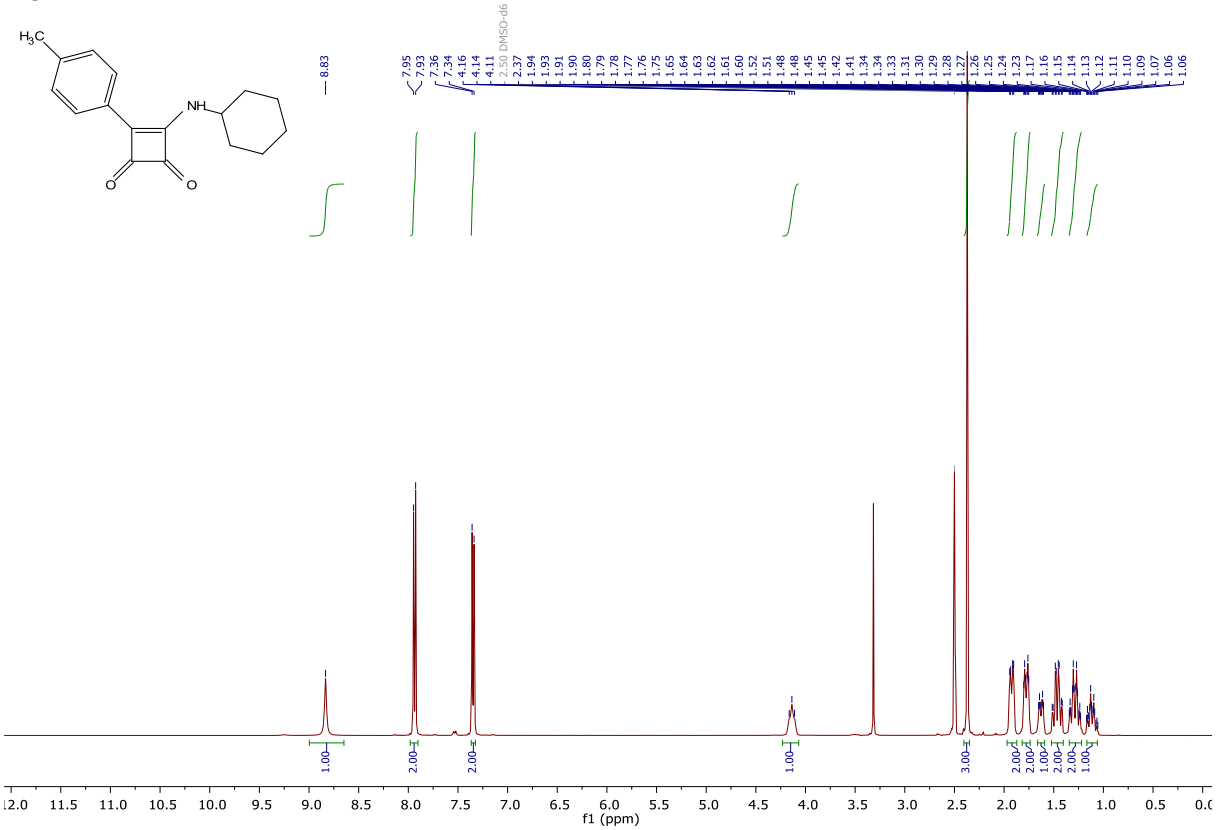

Fig S40. *^{13}C NMR spectra of 3-(cyclohexylamino)-4-(p-tolyl)cyclobut-3-ene-1,2-dione* ***6s***

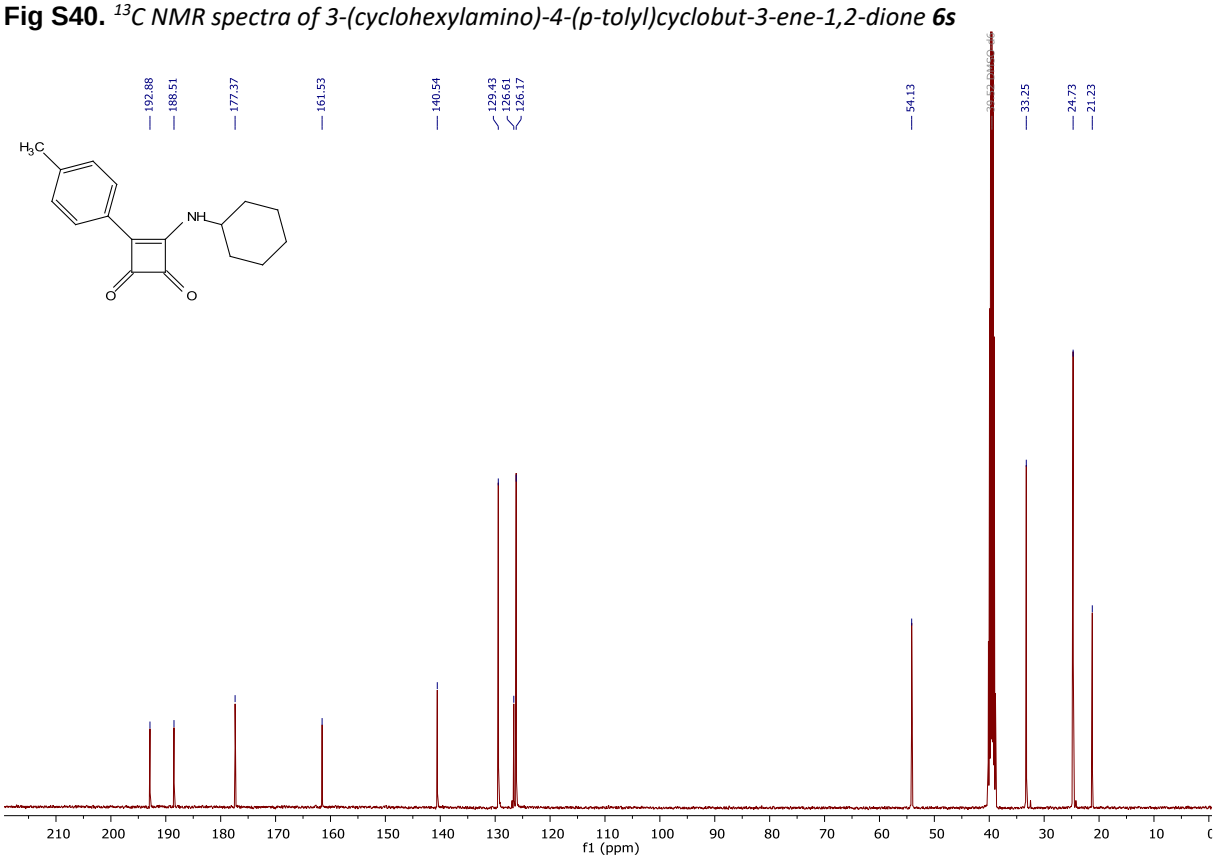

Fig S41. *^{1}H NMR spectra of 3-(phenylamino)-4-(p-tolyl)cyclobut-3-ene-1,2-dione* ***6t***

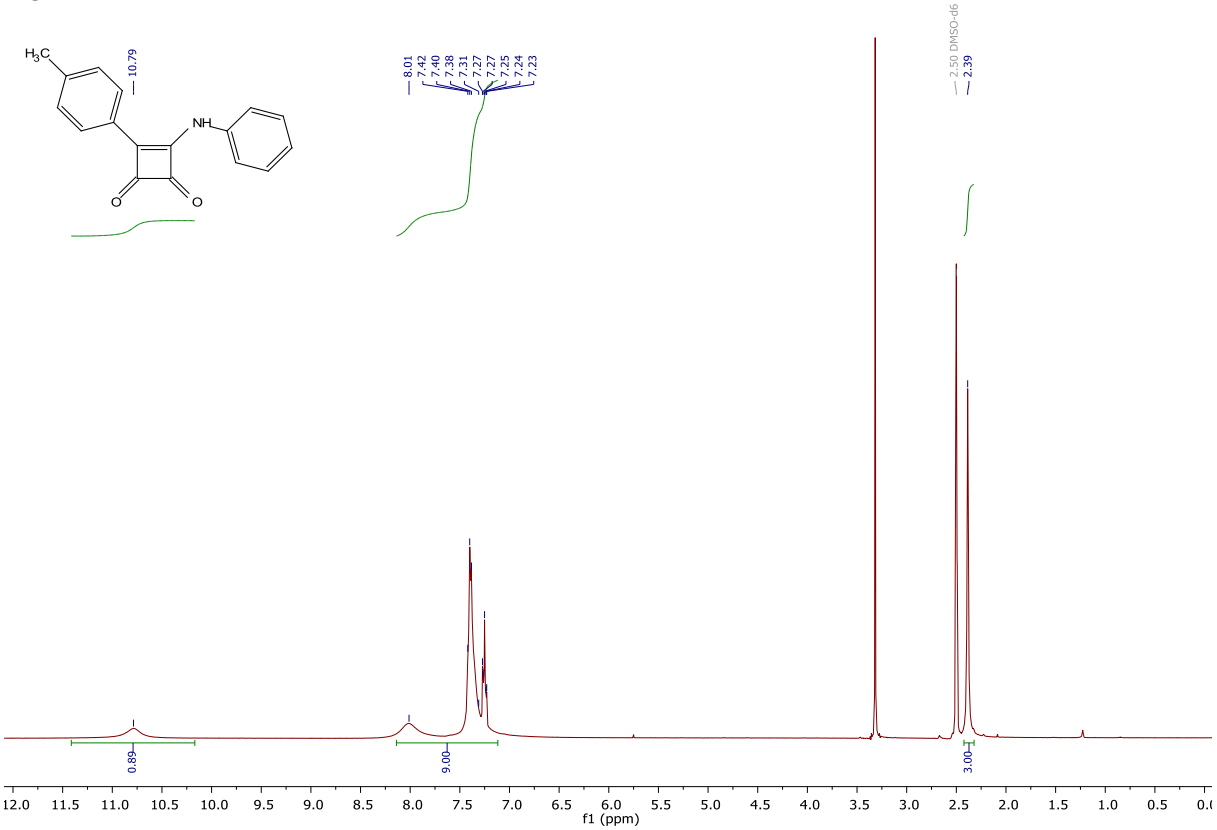

Fig S42. *^{13}C NMR spectra of 3-(phenylamino)-4-(p-tolyl)cyclobut-3-ene-1,2-dione* ***6t***

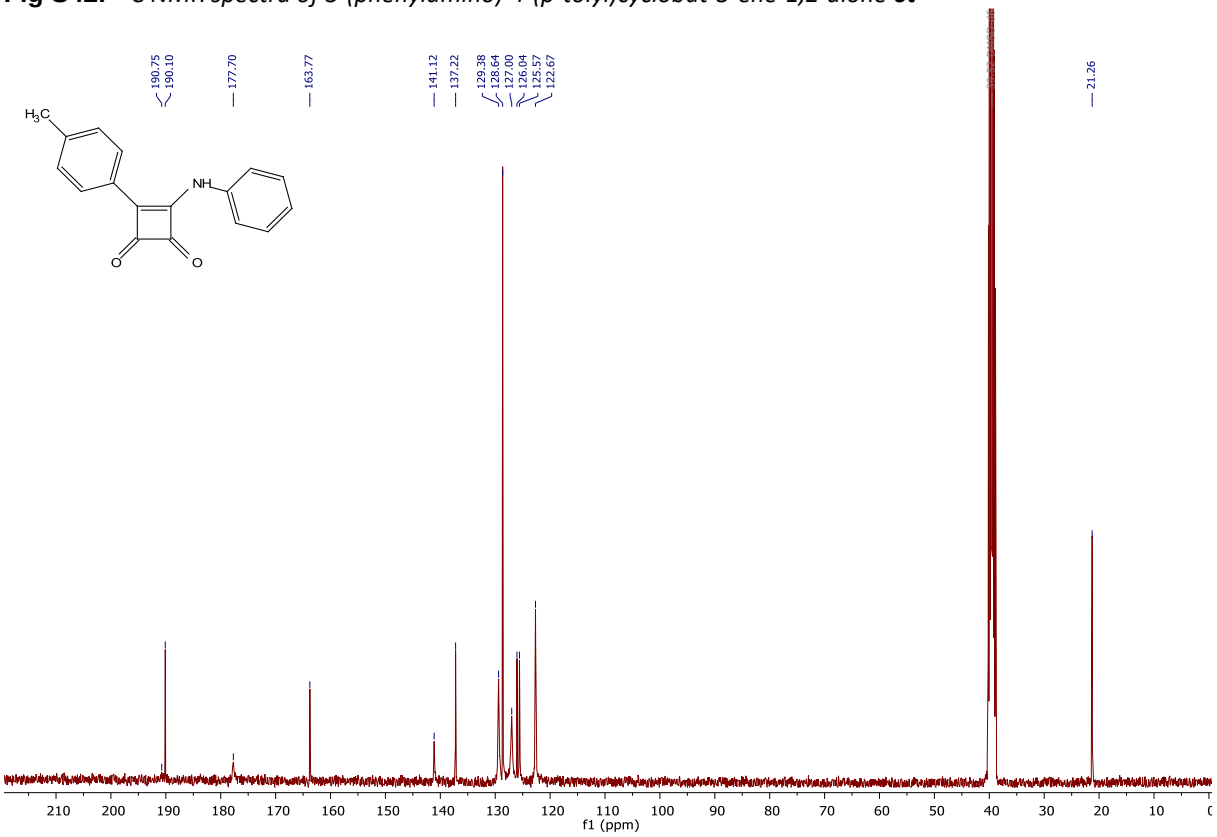

Fig S43. *^{1}H NMR spectra of 3-((4-methoxyphenyl)amino)-4-(p-tolyl)cyclobut-3-ene-1,2-dione* ***6u***

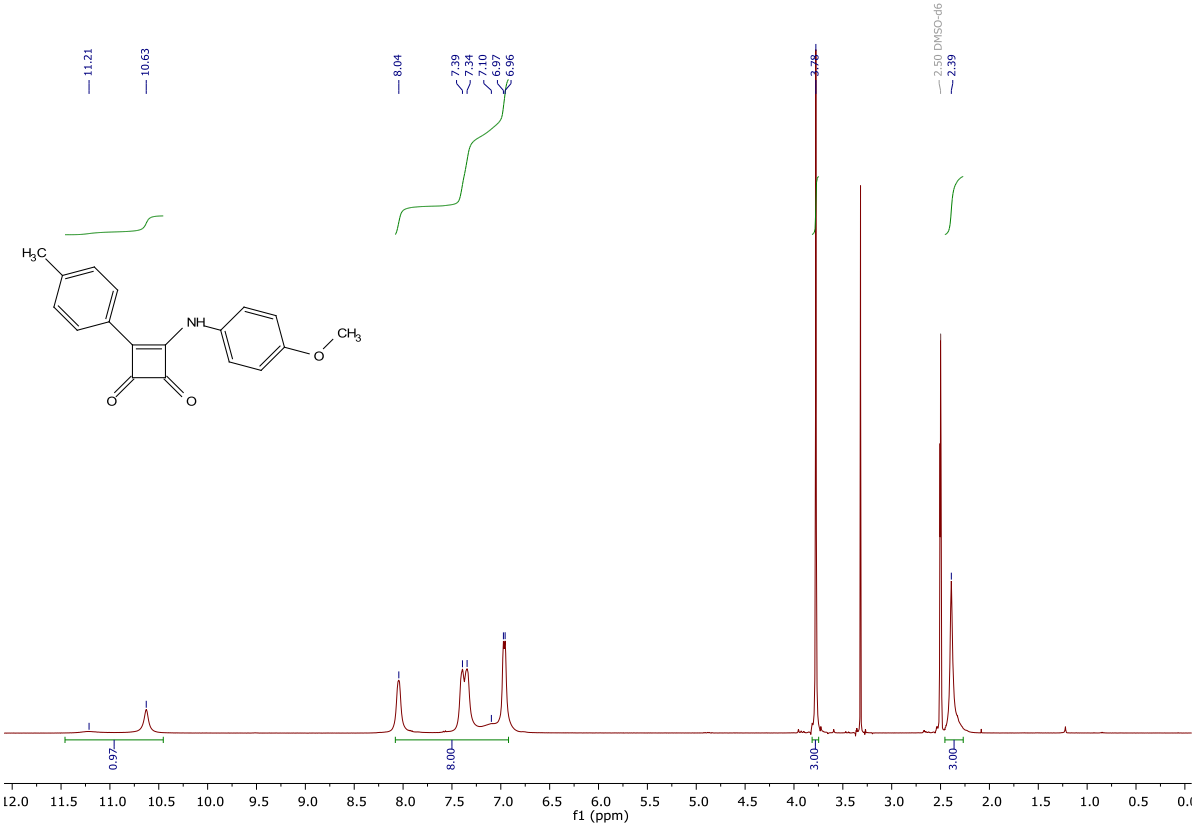

Fig S44. *^{13}C NMR spectra of 3-((4-methoxyphenyl)amino)-4-(p-tolyl)cyclobut-3-ene-1,2-dione* ***6u***

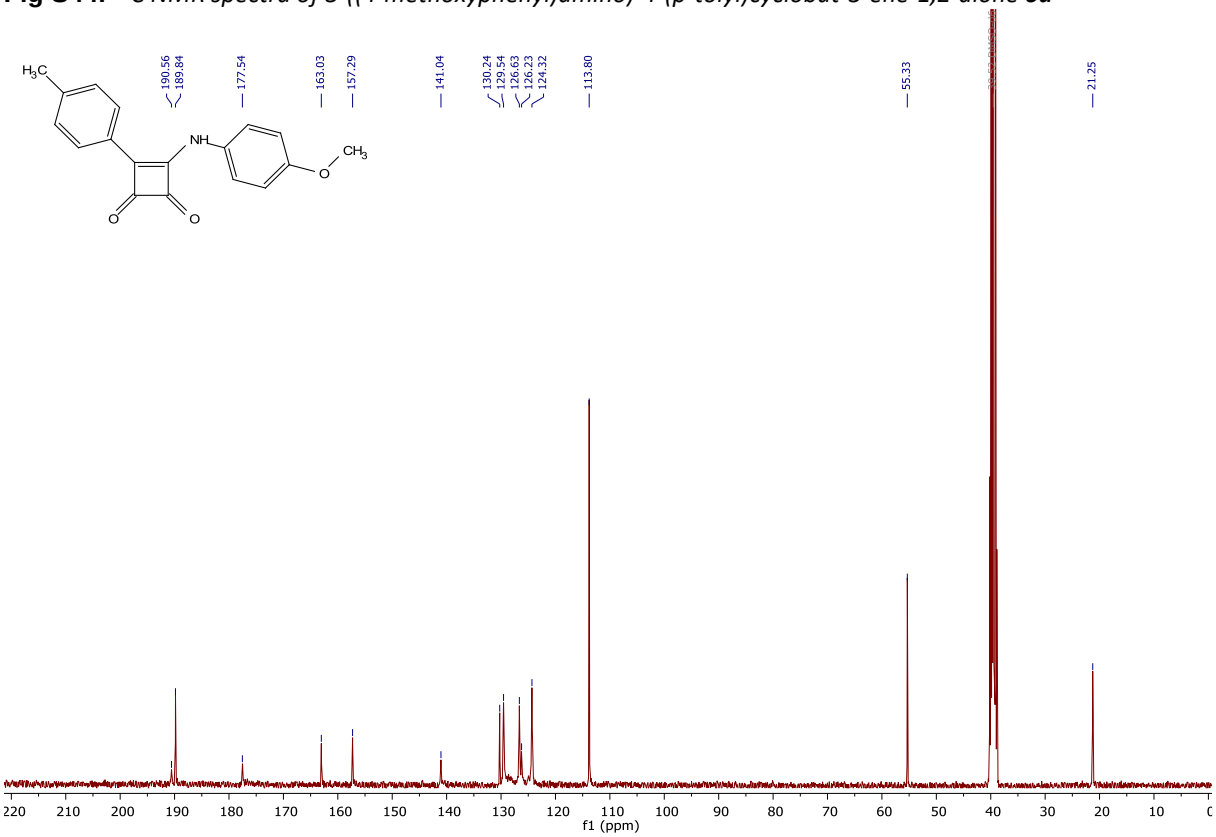

Fig S45. *^{1}H NMR spectra of methyl (3,4-dioxo-2-(p-tolyl)cyclobut-1-en-1-yl)-L-tyrosinate* ***6y***

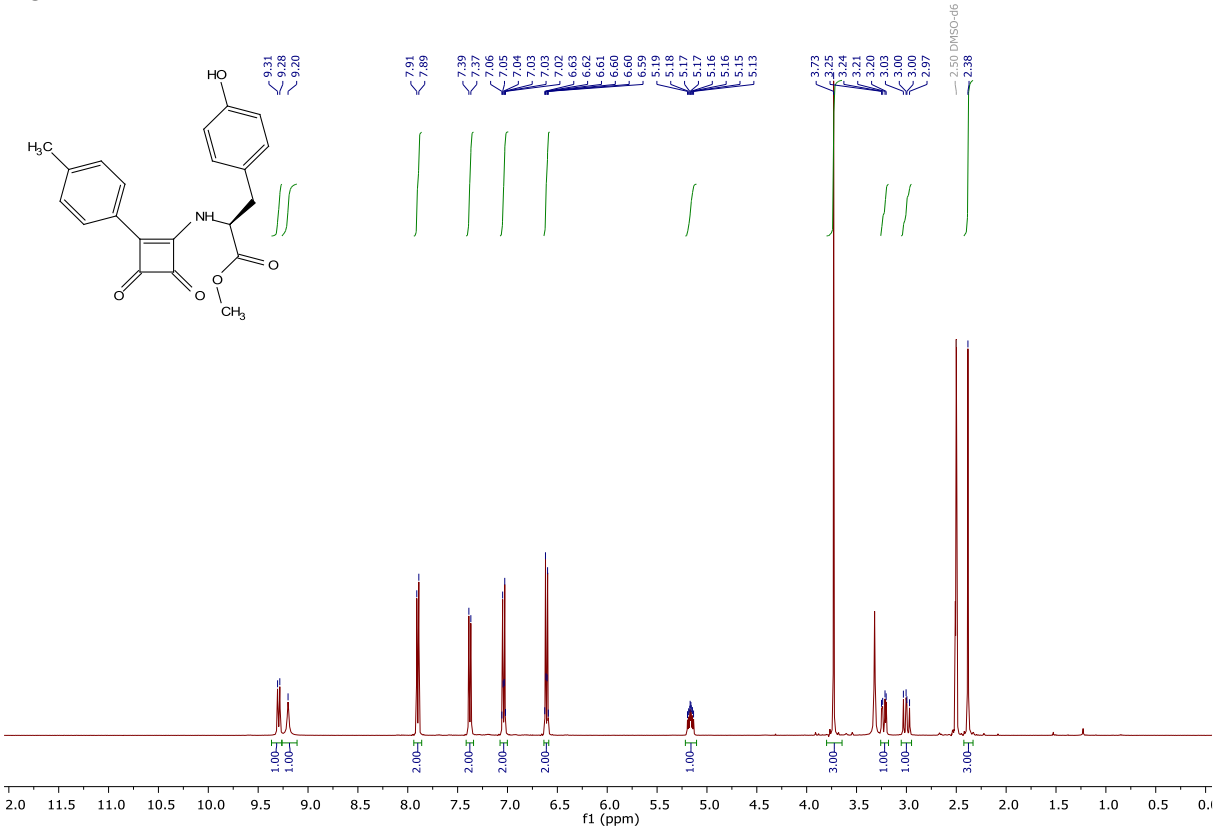

Fig S46. *^{13}C NMR spectra of methyl (3,4-dioxo-2-(p-tolyl)cyclobut-1-en-1-yl)-L-tyrosinate* ***6y***

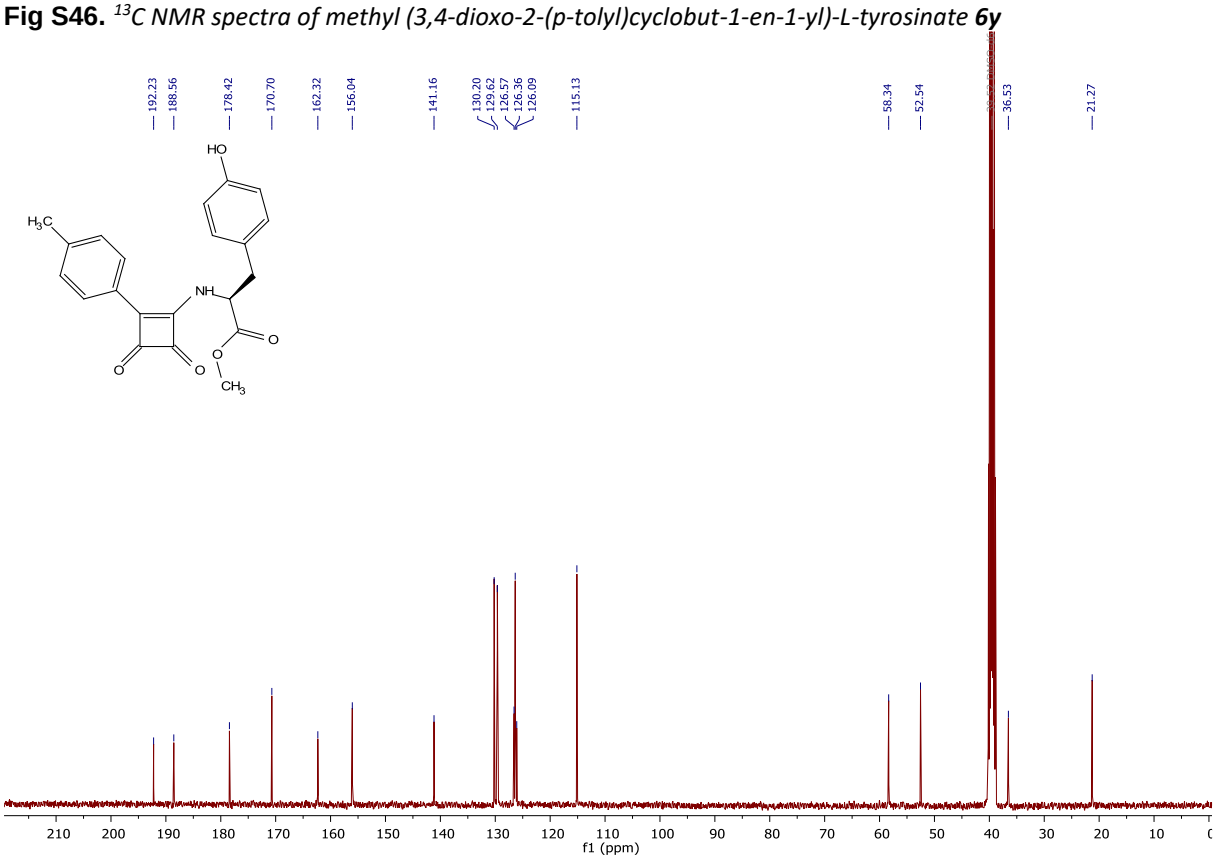

Fig S47. *^{1}H NMR spectra of 3-ethoxy-4-(p-tolyl)cyclobut-3-ene-1,2-dione* ***6aa***

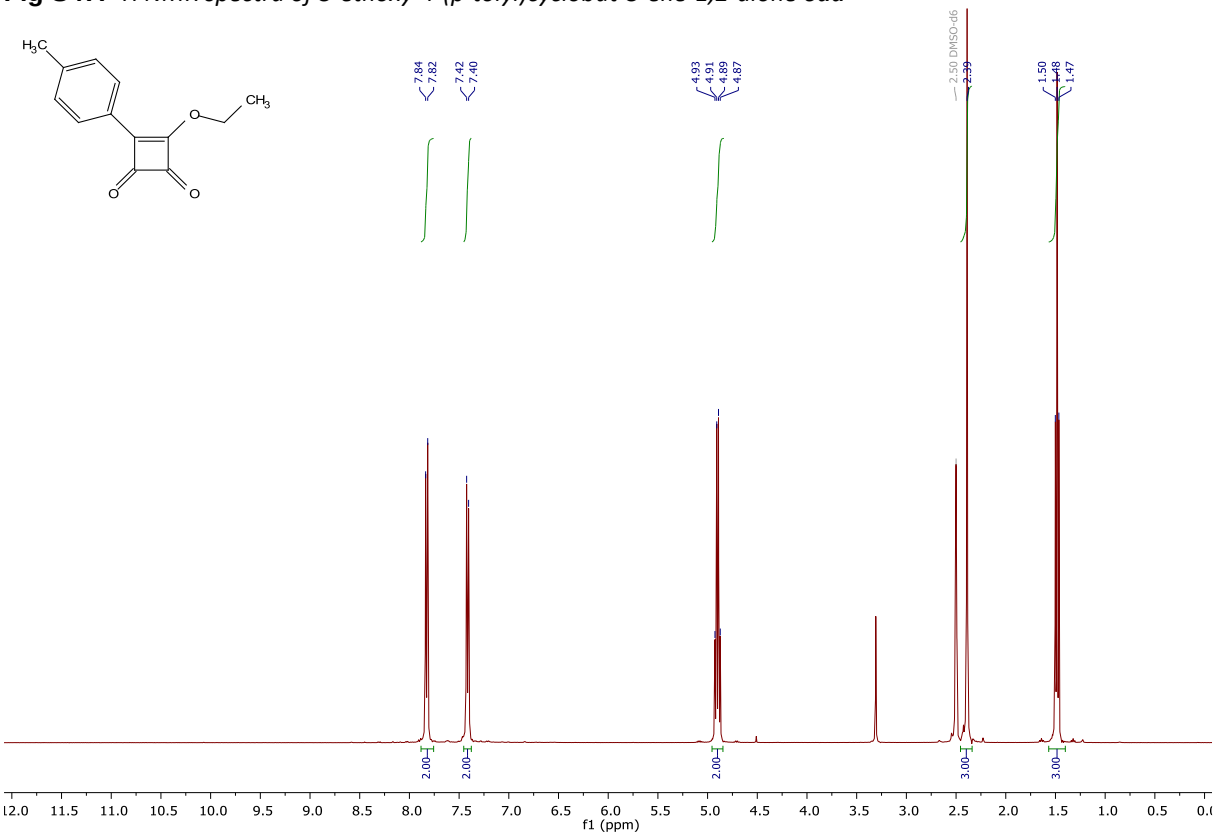

Fig S48. *^{13}C NMR spectra of 3-ethoxy-4-(p-tolyl)cyclobut-3-ene-1,2-dione* ***6aa***

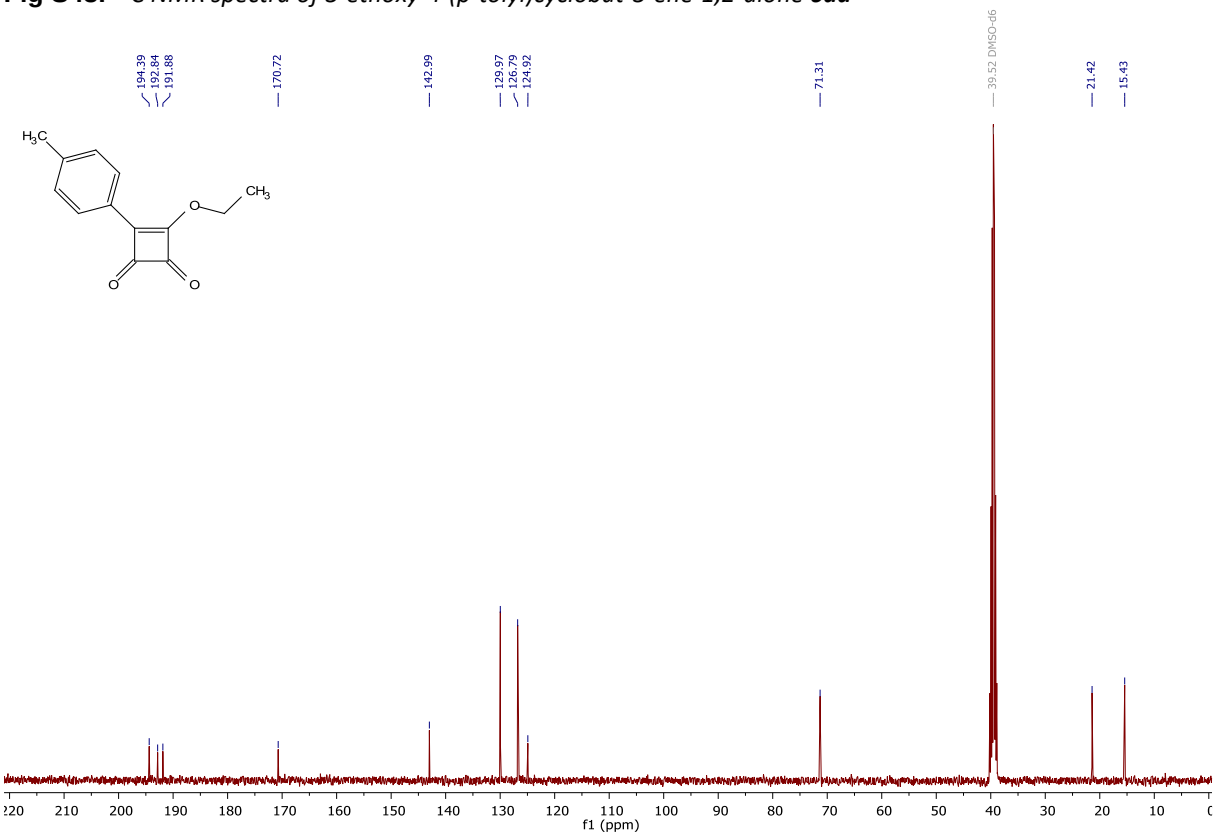

Fig S49. *^{1}H NMR spectra of 3-((4-bromophenyl)amino)-4-(p-tolyl)cyclobut-3-ene-1,2-dione* ***6ab***

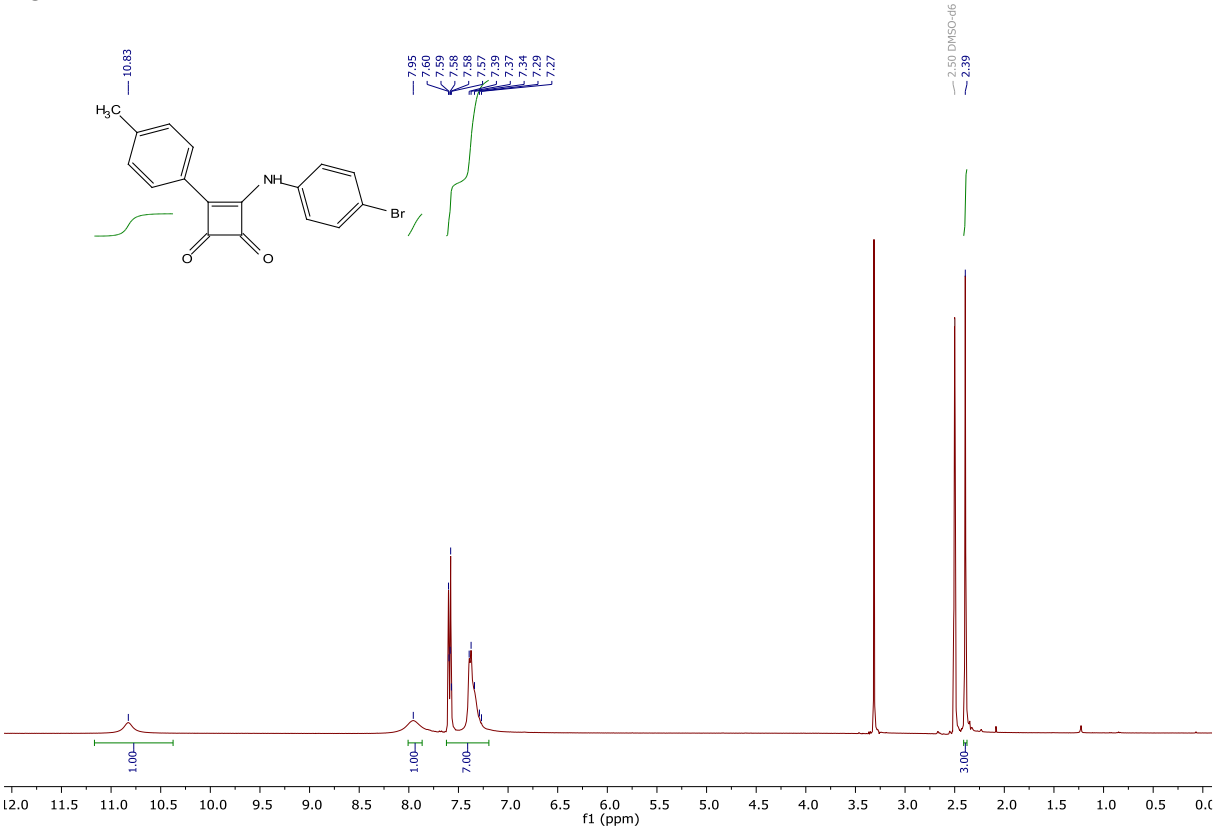

Fig S50. *^{13}C NMR spectra of 3-((4-bromophenyl)amino)-4-(p-tolyl)cyclobut-3-ene-1,2-dione* ***6ab***

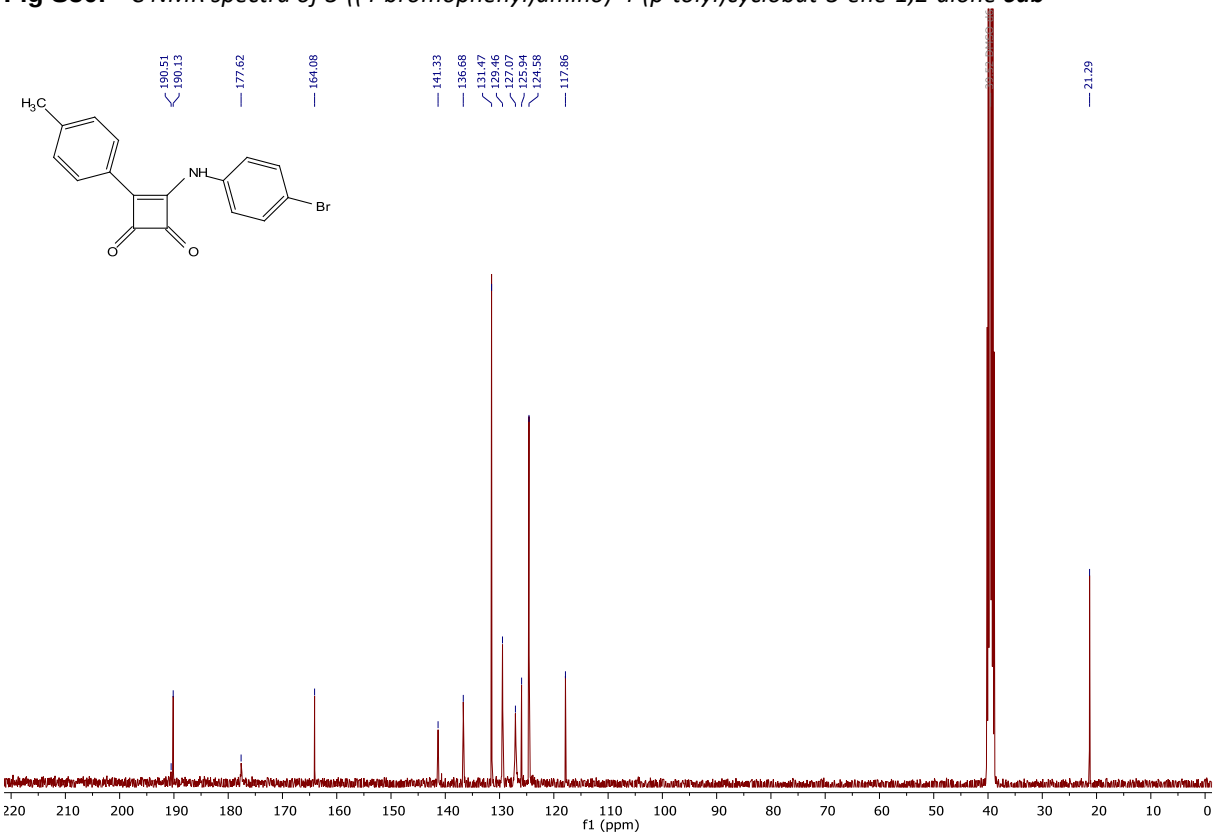

Fig S51. *^{1}H NMR spectra of 3-((4-morpholinophenyl)amino)-4-(p-tolyl)cyclobut-3-ene-1,2-dione* ***6ac***

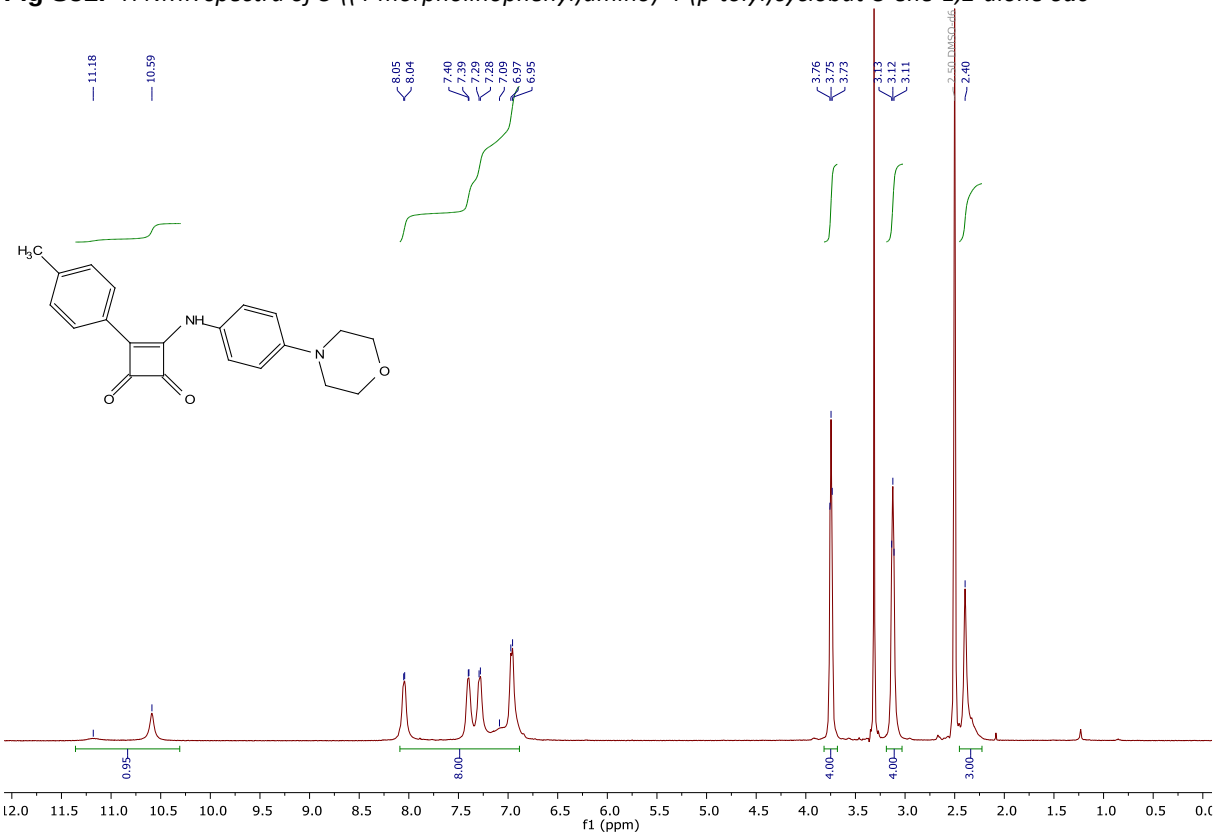

Fig S52. *^{13}C NMR spectra of 3-((4-morpholinophenyl)amino)-4-(p-tolyl)cyclobut-3-ene-1,2-dione* ***6ac***

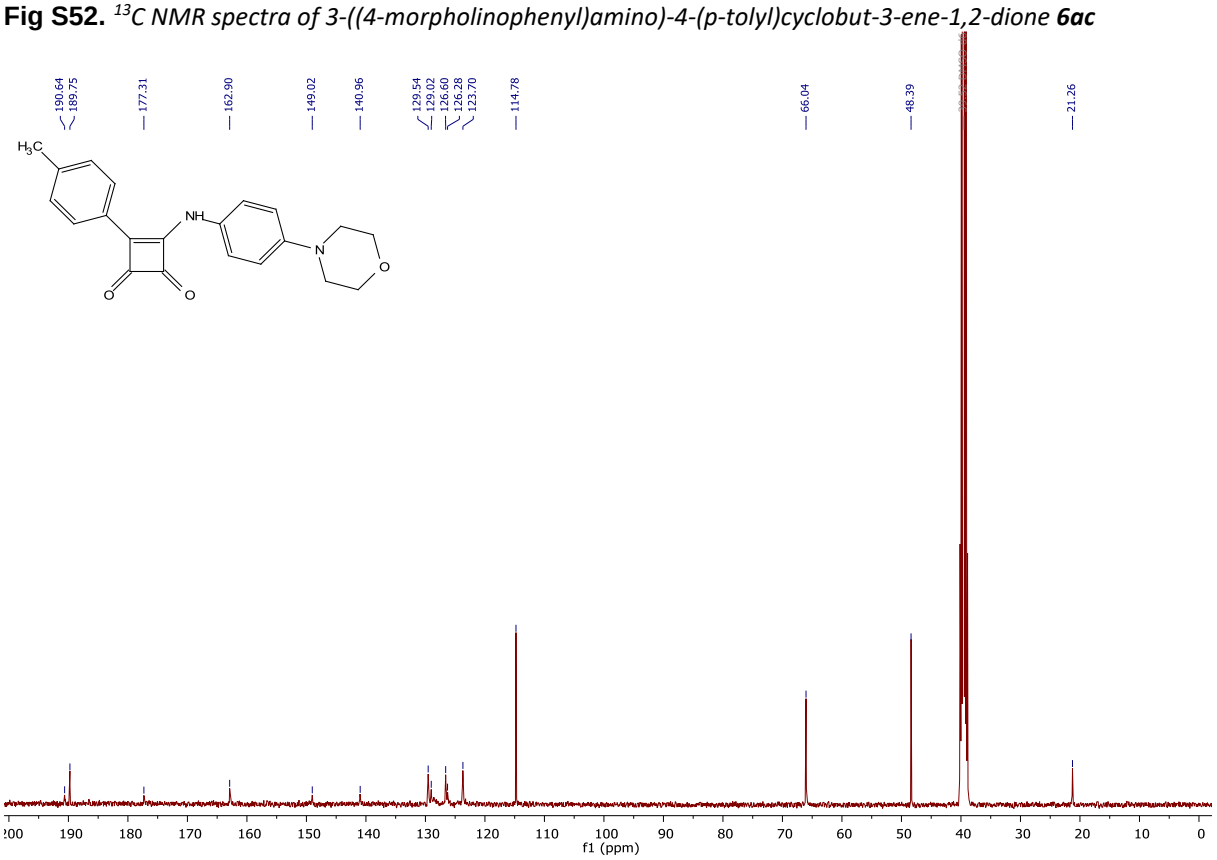

Fig S53. *^{1}H NMR spectra of ethyl 3-((3,4-dioxo-2-(p-tolyl)cyclobut-1-en-1-yl)amino)propanoate* ***6ad***

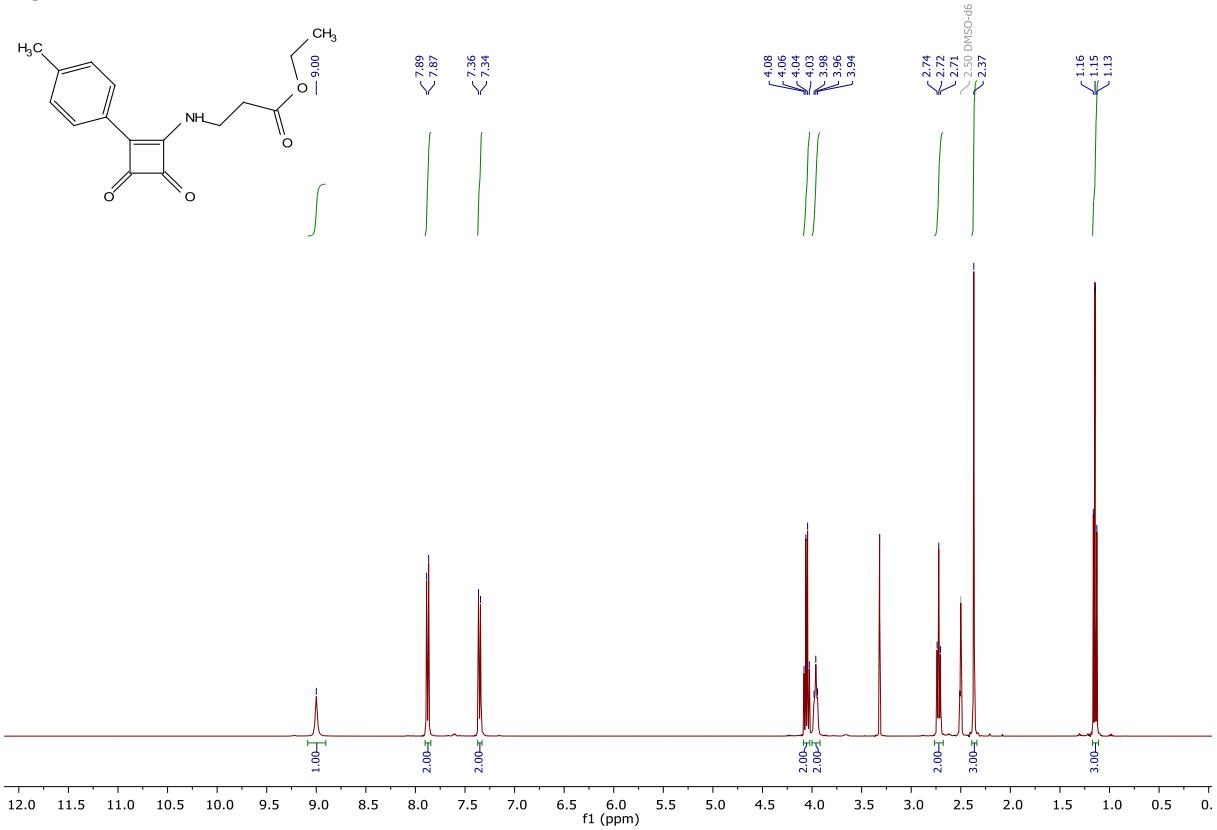

Fig S54. *^{13}C NMR spectra of ethyl 3-((3,4-dioxo-2-(p-tolyl)cyclobut-1-en-1-yl)amino)propanoate* ***6ad***

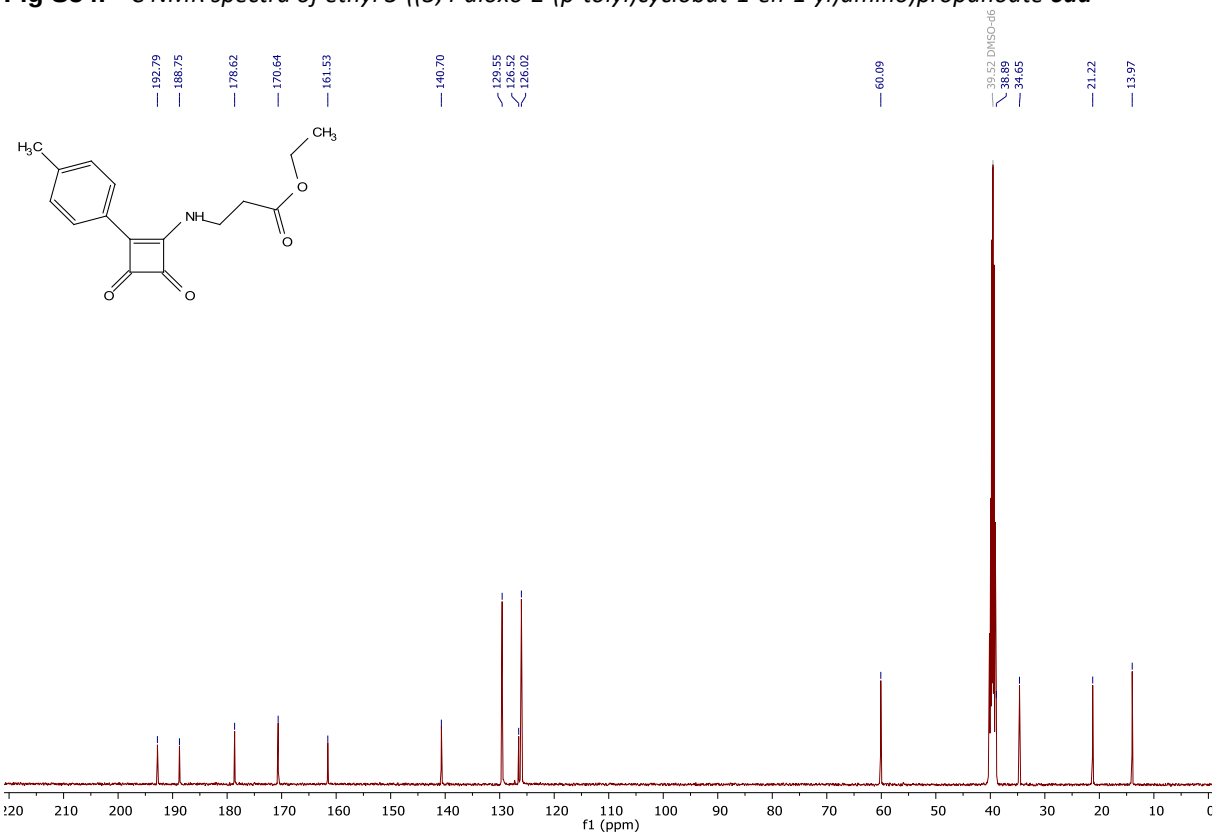

Fig S55. *^{1}H NMR spectra of 3-(benzyl(hydroxy)amino)-4-(p-tolyl)cyclobut-3-ene-1,2-dione* ***6ae***

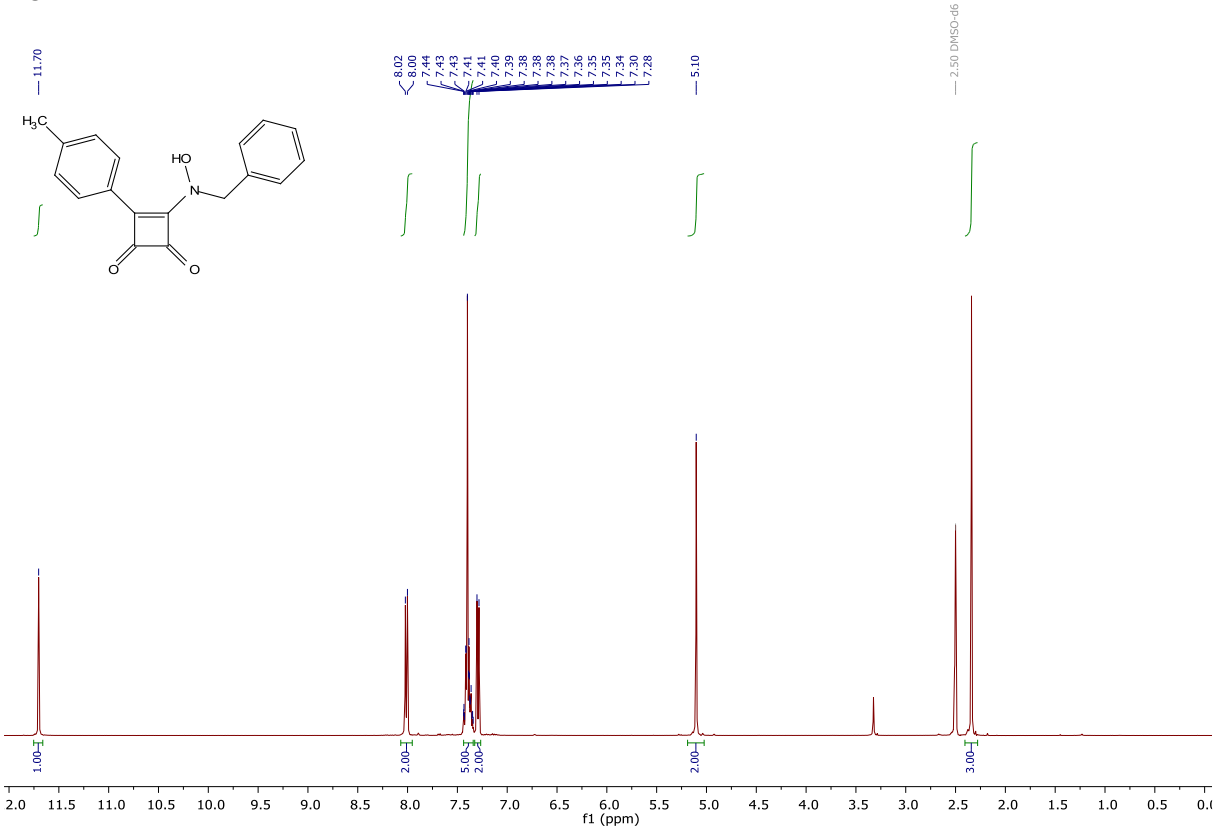

Fig S56. *^{13}C NMR spectra of 3-(benzyl(hydroxy)amino)-4-(p-tolyl)cyclobut-3-ene-1,2-dione* ***6ae***

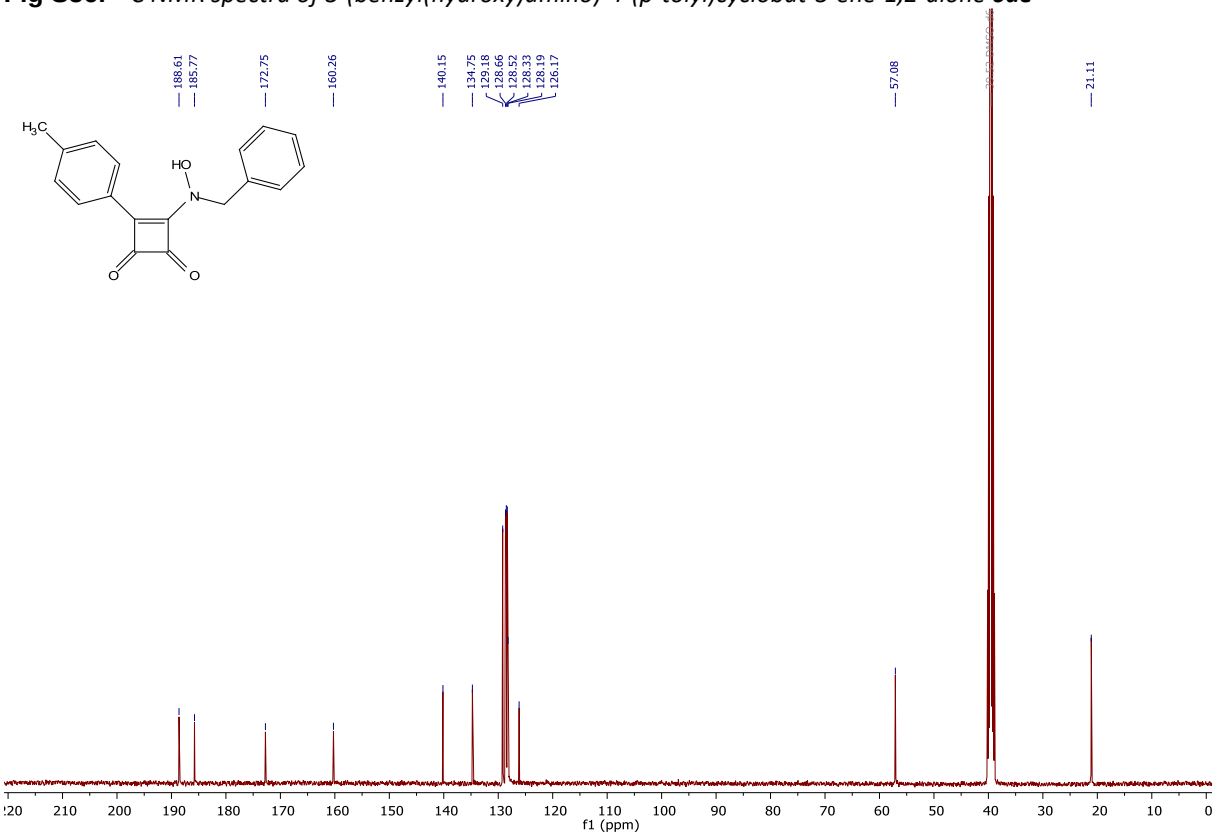

Fig S57. *^{1}H NMR spectra of 3-(methoxy(methyl)amino)-4-(p-tolyl)cyclobut-3-ene-1,2-dione* ***6af***

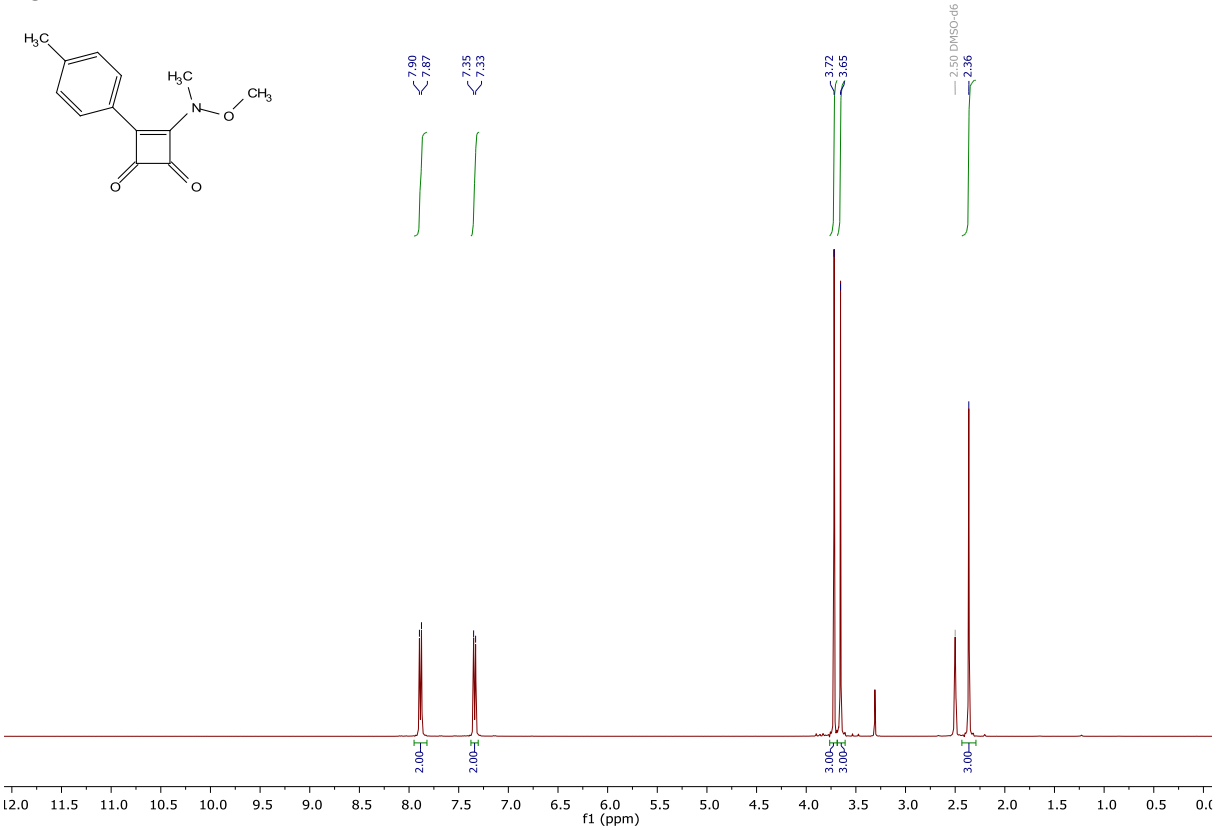

Fig S58. *^{13}C NMR spectra of 3-(methoxy(methyl)amino)-4-(p-tolyl)cyclobut-3-ene-1,2-dione* ***6af***

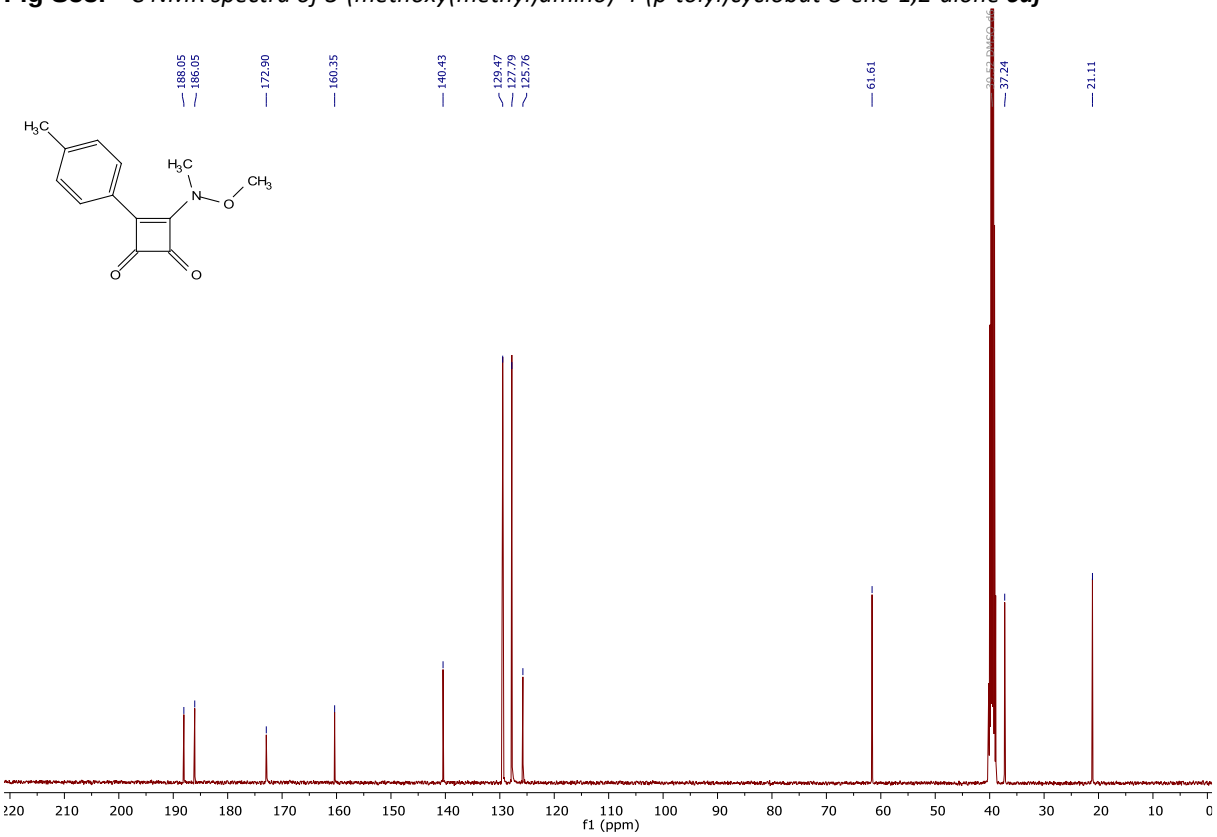

Fig S59. *^{1}H NMR spectra of 3-morpholino-4-(p-tolyl)cyclobut-3-ene-1,2-dione* ***6ag***

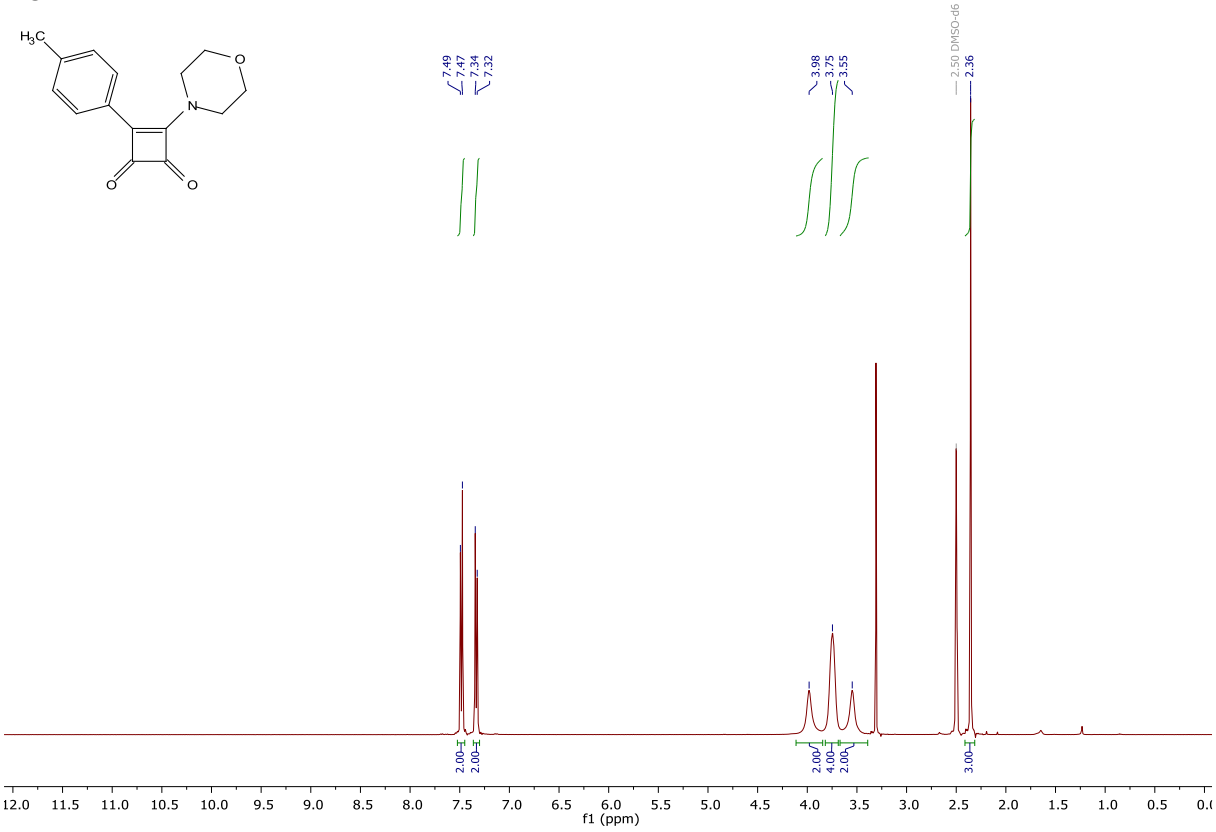

Fig S60. *^{13}C NMR spectra of 3-morpholino-4-(p-tolyl)cyclobut-3-ene-1,2-dione* ***6ag***

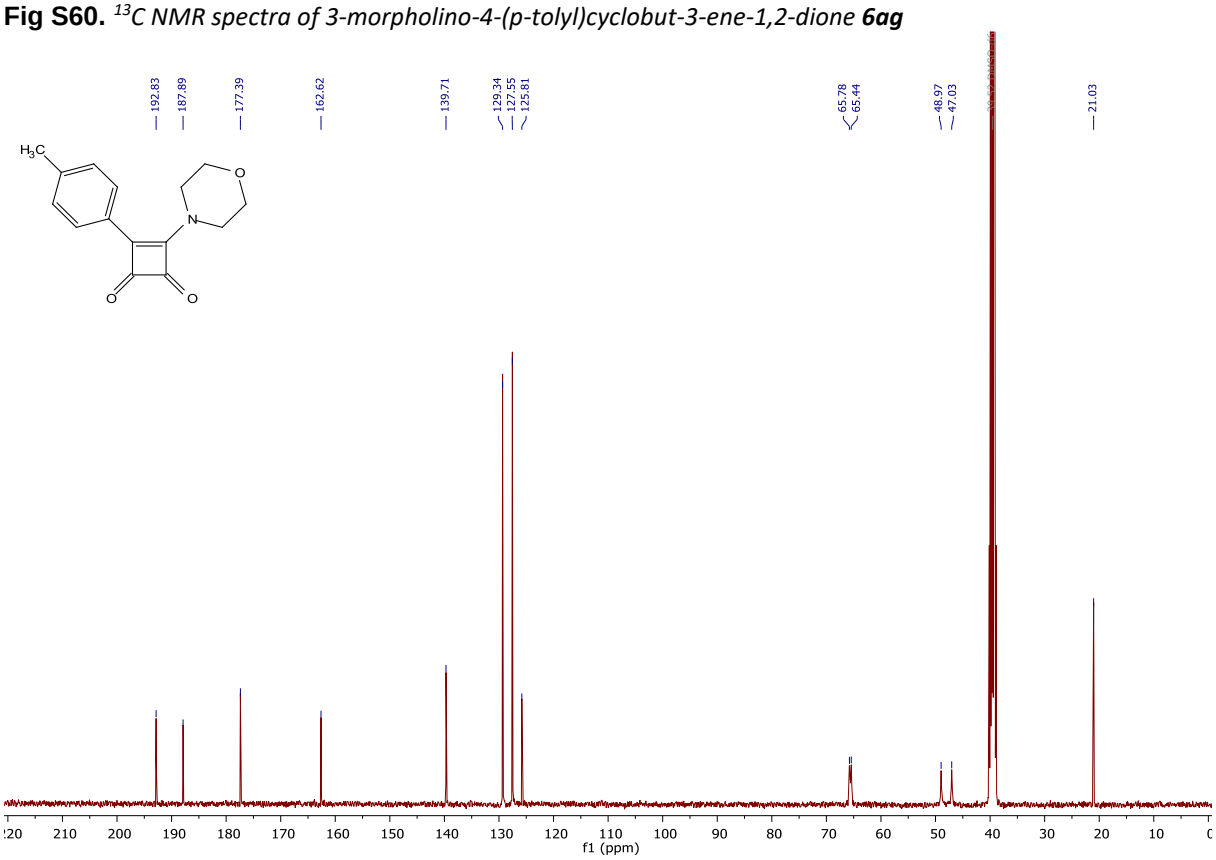

Fig S61. *^{1}H NMR spectra of tert-butyl 4-(3,4-dioxo-2-(p-tolyl)cyclobut-1-en-1-yl)piperazine-1-carboxylate* ***6ai***

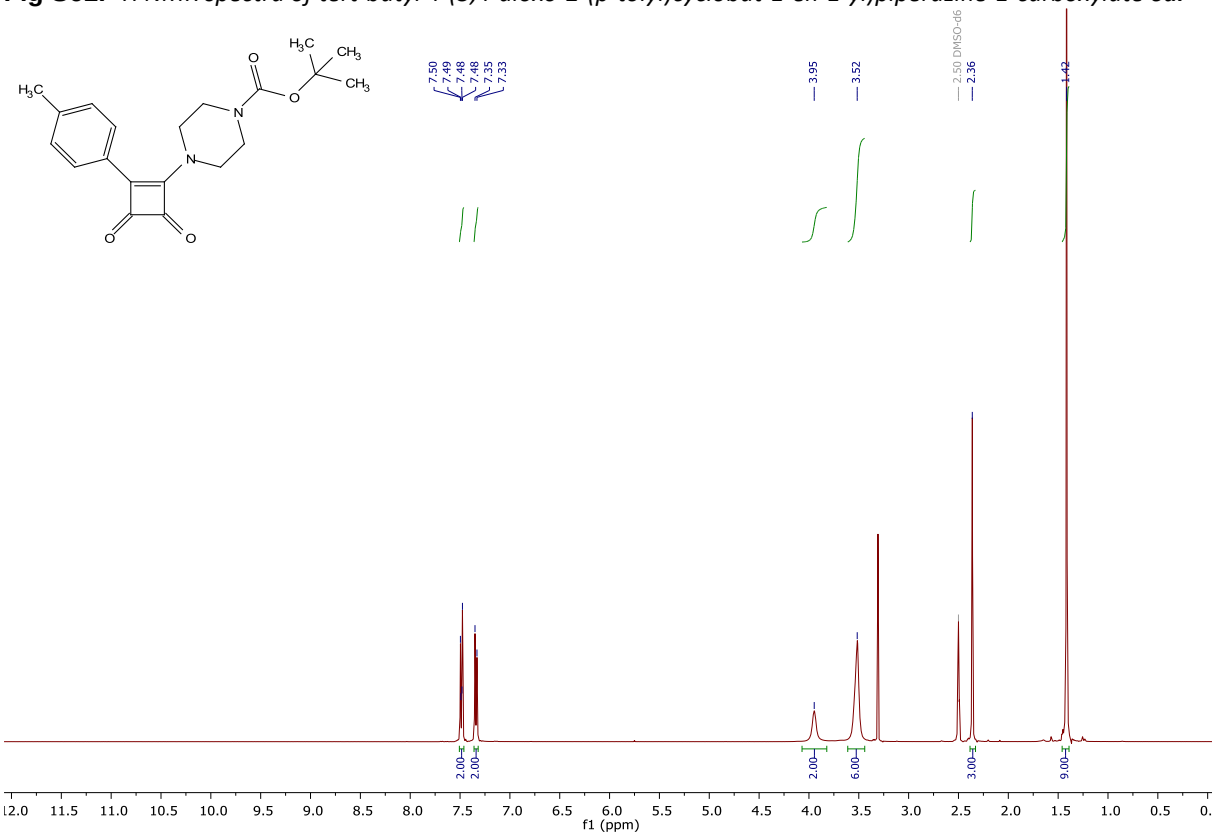

Fig S62. *^{13}C NMR spectra of tert-butyl 4-(3,4-dioxo-2-(p-tolyl)cyclobut-1-en-1-yl)piperazine-1-carboxylate* ***6ai***

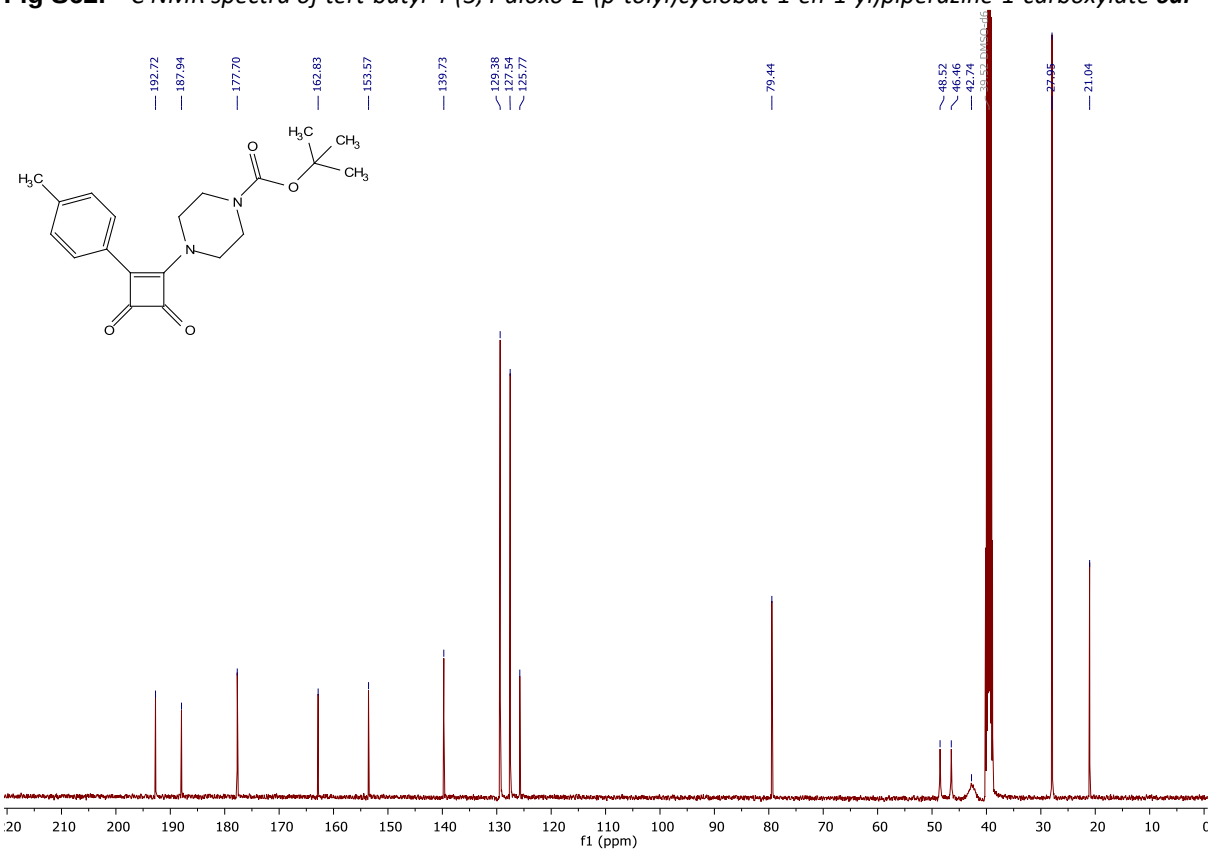

Fig S63. *^{1}H NMR spectra of 3-((furan-2-ylmethyl)amino)-4-(p-tolyl)cyclobut-3-ene-1,2-dione* ***6aj***

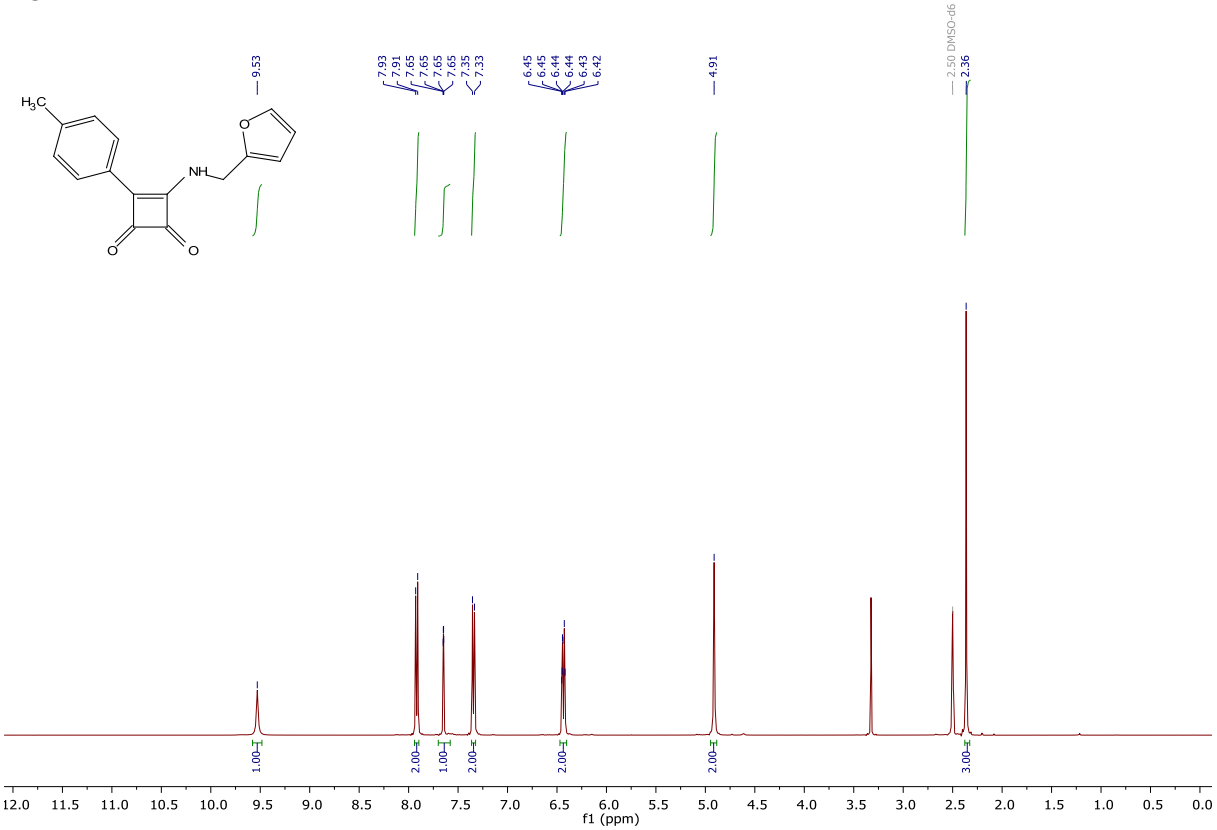

Fig S64. *^{13}C NMR spectra of 3-((furan-2-ylmethyl)amino)-4-(p-tolyl)cyclobut-3-ene-1,2-dione* ***6aj***

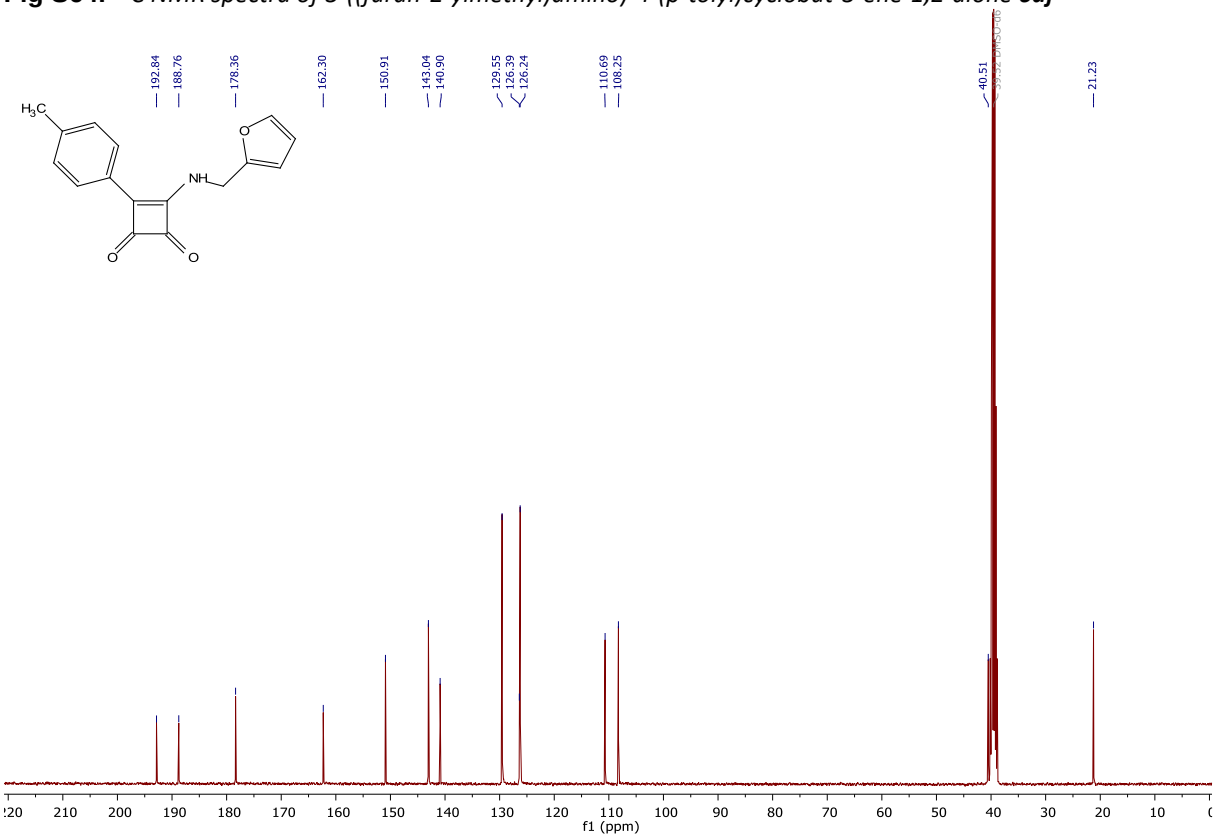

Fig S65. *^{1}H NMR spectra of 3-((4'-methoxy-[1,1'-biphenyl]-4-yl)amino)-4-(p-tolyl)cyclobut-3-ene-1,2-dione* **6am**

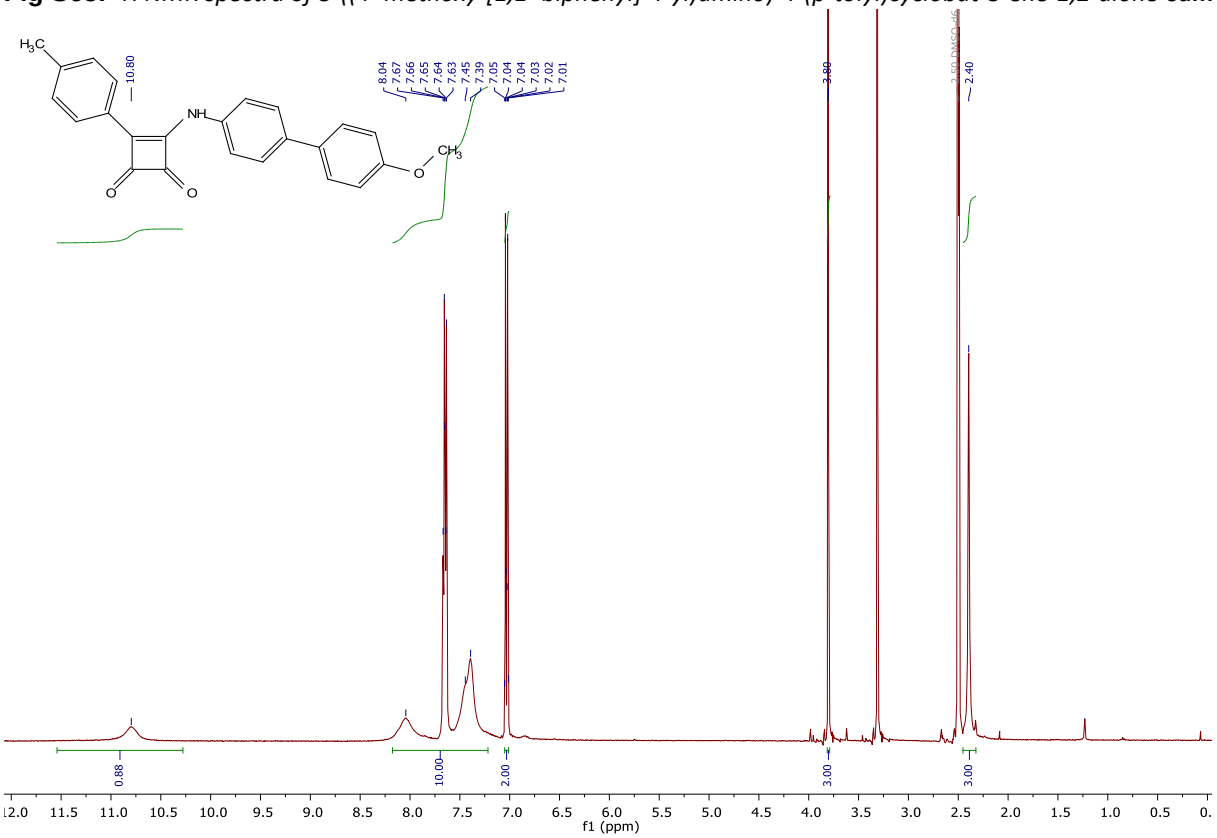
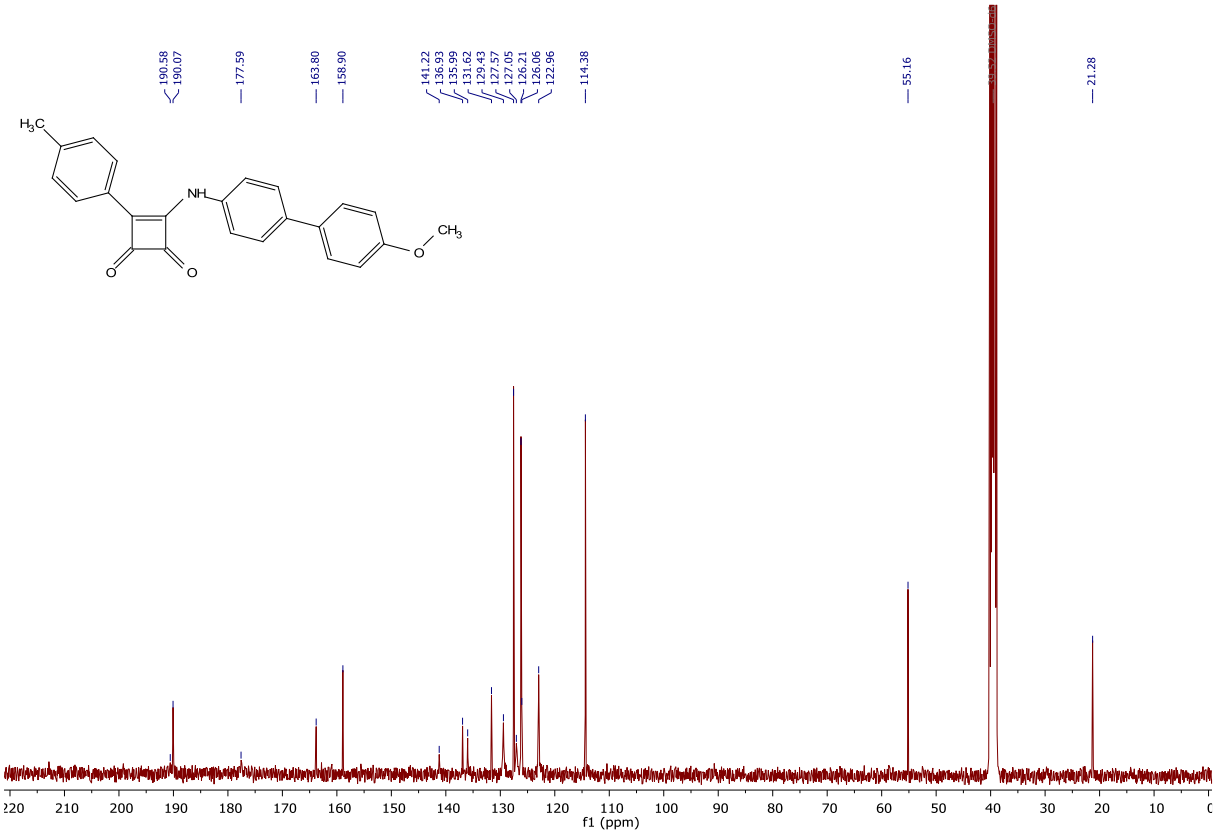
Fig S66. *^{13}C NMR spectra of 3-((4'-methoxy-[1,1'-biphenyl]-4-yl)amino)-4-(p-tolyl)cyclobut-3-ene-1,2-dione* **6am**